

Summer 8-31-2000

Autonomic activity in Gulf War veterans using heart rate and systolic blood pressure variability

Maryann S. Fam
New Jersey Institute of Technology

Follow this and additional works at: <https://digitalcommons.njit.edu/theses>



Part of the [Biomedical Engineering and Bioengineering Commons](#)

Recommended Citation

Fam, Maryann S., "Autonomic activity in Gulf War veterans using heart rate and systolic blood pressure variability" (2000). *Theses*. 782.

<https://digitalcommons.njit.edu/theses/782>

This Thesis is brought to you for free and open access by the Electronic Theses and Dissertations at Digital Commons @ NJIT. It has been accepted for inclusion in Theses by an authorized administrator of Digital Commons @ NJIT. For more information, please contact digitalcommons@njit.edu.

Copyright Warning & Restrictions

The copyright law of the United States (Title 17, United States Code) governs the making of photocopies or other reproductions of copyrighted material.

Under certain conditions specified in the law, libraries and archives are authorized to furnish a photocopy or other reproduction. One of these specified conditions is that the photocopy or reproduction is not to be “used for any purpose other than private study, scholarship, or research.” If a user makes a request for, or later uses, a photocopy or reproduction for purposes in excess of “fair use” that user may be liable for copyright infringement,

This institution reserves the right to refuse to accept a copying order if, in its judgment, fulfillment of the order would involve violation of copyright law.

Please Note: The author retains the copyright while the New Jersey Institute of Technology reserves the right to distribute this thesis or dissertation

Printing note: If you do not wish to print this page, then select “Pages from: first page # to: last page #” on the print dialog screen

The Van Houten library has removed some of the personal information and all signatures from the approval page and biographical sketches of theses and dissertations in order to protect the identity of NJIT graduates and faculty.

ABSTRACT

AUTONOMIC ACTIVITY IN GULF WAR VETERANS USING HEART RATE AND SYSTOLIC BLOOD PRESSURE VARIABILITY

by
Maryann S. Fam

Heart rate variability (HRV) describes variations of heart rate and is attributed to cyclic fluctuations in autonomic tone. The different methods of heart rate variability analysis allow for a non-invasive assessment of autonomic activity. This study analyzes the heart rate variability through both frequency domain methods and joint time-frequency domain methods which were executed through the LabVIEW graphical programming language. These algorithms were utilized to assess autonomic nervous system activity in Gulf War veterans with no health complaints versus Gulf War veterans with chronic fatigue syndrome. The heart rate variability analysis was obtained from acquired measurements of heart rate and blood pressure during periods of steady-state supine and standing positions. The subject populations as well as the physiological signals utilized in this study were obtained from the East Orange DVA Medical Center.

The results of this study indicate that there is no significant difference ($p < .05$) in autonomic nervous system activity, as assessed with low frequency/high frequency ratios, between Gulf War veterans with no health complaints versus Gulf War veterans with chronic fatigue syndrome. The results also indicate that there is no significant difference ($p < .05$) in the index of autonomic balance yielded from each of the LF/HF ratios obtained from the heart rate and blood pressure variabilities, respectively, versus the $LF_{(BP)}/HF_{(ECG)}$ ratio.

**AUTONOMIC ACTIVITY IN GULF WAR VETERANS USING HEART RATE
AND SYSTOLIC BLOOD PRESSURE VARIABILITY**

by
Maryann S. Fam

**A Thesis
Submitted to the Faculty of
New Jersey Institute of Technology
In Partial Fulfillment of the Requirements for the Degree of
Master of Science in Biomedical Engineering**

Biomedical Engineering Committee

August 2000

Blank Page

APPROVAL PAGE

**AUTONOMIC ACTIVITY IN GULF WAR VETERANS USING HEART RATE
AND SYSTOLIC BLOOD PRESSURE VARIABILITY**

Maryann S. Fam

Dr. Stanley S. Reisman, Thesis Advisor Date
Professor of Electrical Engineering, NJIT, Newark, NJ

Dr. Ronald Rockland, Committee Member Date
Assistant Professor of Engineering Technology, NJIT, Newark, NJ

Dr. Arnold Peckerman, Committee Member Date
Gulf War Research Center, VA Medical Center, East Orange, NJ

BIOGRAPHICAL SKETCH

Author: Maryann S. Fam

Degree: Master of Science

Date: August 2000

Undergraduate and Graduate Education:

- Master of Science in Biomedical Engineering
New Jersey Institute of Technology, Newark, New Jersey, 2000
- Bachelor of Science in Engineering Science
New Jersey Institute of Technology, Newark, New Jersey, 1998

Major: Biomedical Engineering

This thesis is dedicated to my parents and brothers, and foremost to the one who strengthens me, through whom all things are possible.

ACKNOWLEDGMENT

The author would like to express her sincerest gratitude to her advisor, Dr. Stanley Reisman, not only for his time and efforts in directing this research, but also for his valuable advice and guidance as a friend. His constant positive reinforcement and support were truly a source of motivation towards the achievement of this Masters' degree.

Thanks also to Dr. Ronald Rockland and Dr. Arnold Peckerman for their collaboration as members of the thesis committee.

Special thanks to all the engineers at the East Orange DVA Medical Center, East Orange, NJ, and to Douglas Newandee for providing much needed assistance with the computer resources necessary for this research.

Last, but not least, the author is greatly indebted most of all to her parents, her brothers, family and friends for their strength, inspiration, support and divine intervention throughout the Masters' program. They are all very much appreciated and esteemed.

TABLE OF CONTENTS

Chapter	Page
1 PHYSIOLOGICAL BACKGROUND.....	1
1.1 Introduction.....	1
1.2 Cardiovascular System.....	1
1.2.1 Heart.....	2
1.2.2 Nerve Supply of the Heart.....	5
1.2.3 Conduction System of the Heart.....	6
1.2.4 Electrical Events of Contraction.....	8
1.2.5 The Electrocardiogram.....	12
1.2.6 Cardiac Cycle.....	15
1.2.7 Circulation and Blood Pressure.....	16
1.2.8 Photoplethysmogram: A Measurement of Blood Volume.....	20
1.3 Respiratory System.....	22
1.3.1 Mechanism of Pulmonary Ventilation.....	23
1.3.2 Thoracic Plethysmography.....	25
1.4 Definition of Heart Rate Variability.....	26
1.5 Statement of Objective.....	29
1.6 Factor that Influences Breathing.....	31
1.7 Factors that Affect Aspects of the Cardiovascular System.....	31
1.7.1 Respiration.....	31
1.7.2 Gravity and Posture.....	33
1.7.3 Emotional Stress.....	34

TABLE OF CONTENTS
(continued)

Chapter	Page
1.8 Chronic Fatigue Syndrome.....	35
1.8.1 Definition of Chronic Fatigue Syndrome.....	35
1.8.2 Methods and Criteria for Diagnosis.....	37
1.8.3 Possible Causes of CFS.....	40
2 HEART RATE VARIABILITY.....	42
2.1 Introduction.....	42
2.2 Methods of HRV Analysis.....	42
2.2.1 Frequency Domain (Power Spectrum) Analysis.....	42
2.2.2 Time-Frequency Analysis.....	46
3 EXPERIMENTAL METHODS AND PROCEDURES.....	52
3.1 Introduction.....	52
3.2 Subject Selection.....	52
3.3 Protocol.....	55
3.3.1 The Forehead Cold Pressor Test.....	56
3.3.2 The Speech Task.....	56
3.3.3 The Arithmetic Stressor.....	57
3.4 Data Acquisition of Physiological Measurements.....	57
3.5 Data Files.....	58
4 ANALYSIS METHODS AND PROCEDURES.....	60
4.1 Introduction.....	60
4.2 LabVIEW.....	60

TABLE OF CONTENT
(continued)

Chapter	Page
4.3 Wigner Time-Frequency Analysis.....	62
4.4 Power Spectrum Analysis of Heart Rate.....	63
4.5 Power Spectrum Analysis of Blood Pressure.....	64
4.6 Preliminary Study.....	67
4.6.1 Introduction.....	67
4.6.2 Findings of Preliminary Study.....	68
4.6.3 Conclusions of Preliminary Study.....	73
4.7 Limitations of Data Analysis.....	73
4.8 Statistical Analysis of Data.....	75
5 RESULTS AND DISCUSSION OF ANALYSIS.....	80
5.1 Introduction.....	80
5.2 Observations and Results of Time-Frequency Analysis.....	80
5.3 Observations and Results of Power Spectrum Analysis.....	81
5.4 Discussion of Results.....	88
6 CONCLUSIONS.....	93
6.1 Introduction.....	93
6.2 Summary of Results.....	93
6.3 Future Research.....	94
6.3.1 Suggestions for Future Work on this Study.....	94
6.3.2 Clinical Relevance of HRV.....	96

TABLE OF CONTENTS
(continued)

Chapter	Page
APPENDIX A EXPLANATION OF SIGNIFICANCE OF THE USE OF NORMALIZED UNITS.....	98
APPENDIX B LABVIEW DIAGRAM.....	99
APPENDIX C RESULTS OF HEART RATE VARIABILITY ANALYSIS OF PRELIMINARY STUDY.....	115
APPENDIX D RESULTS OF HEART RATE VARIABILITY ANALYSIS OF TIME-FREQUENCY CURVES UTILIZING ECG SIGNAL.....	125
APPENDIX E RESULTS OF HEART RATE VARIABILITY ANALYSIS POWER SPECTRUM CURVES UTILIZING ECG SIGNAL.....	131
APPENDIX F RESULTS OF HEART RATE VARIABILITY ANALYSIS POWER SPECTRUM CURVES UTILIZING BP SIGNAL.....	137
REFERENCES.....	143

LIST OF TABLES

Table	Page
4.1 A comparison of calculated heart rate variability generated from the two analysis methods utilized in the preliminary study.....	71
5.1 Summary of data obtained from power spectrum analysis.....	81
5.2 Comparison of average percent difference between GHC subjects vs. GCF subjects based on data obtained from power spectrum analyses.....	85
5.3 Summary of <i>t</i> tests comparing equivalence of means of the ratios between the two sample groups.....	86

LIST OF FIGURES

Figure	Page
1.1 Structure of cardiac bundles and valves.....	4
1.2 Conduction system of heart and sequence of action potentials.....	8
1.3 Leads of ECG.....	13
1.4 ECG tracing of three recognizable deflection waves.....	15
1.5 Flow of blood through circulatory system.....	17
1.6 Primary principle of circulation.....	19
1.7 Events that take place during measurement of blood pressure.....	21
1.8 Major respiratory organs shown in relation to surrounding structures.....	23
1.9 Mechanics of ventilation.....	25
1.10 Steps in construction of an interbeat interval (IBI) signal.....	28
1.11 Venous pumping mechanism.....	32
1.12 Effects of moving from lying to standing position.....	34
2.1 Frequency spectrum of an interbeat interval signal.....	44
2.2 How time-frequency analysis allows for dynamic display of spectral characteristics as opposed to a static display provided by power spectrum analysis.....	48
2.3 Flow chart of time-frequency analysis methods.....	49
4.1 HRV power spectrum using BP signal, acquired in supine position (Subject GHC-AR).....	69
4.2 HRV power spectrum using ECG signal, acquired in supine position (Subject GHC-AR).....	69
4.3 HRV power spectrum using BP signal, acquired in supine position (Subject GHC-DU).....	69
4.4 HRV power spectrum using ECG signal, acquired in supine position (Subject GHC-DU).....	70

LIST OF FIGURES
(continued)

Figure	Page
4.5 Blood pressure waveform as displayed in LabVIEW graphical programming language.....	71
4.6 Blood pressure waveform as displayed in LabVIEW graphical programming language.....	72
4.7 ECG waveform as displayed in LabVIEW graphical programming language.....	72
5.1 Graphical comparison between the three different ratios within each group.....	83
5.2 Graphical displays of the three different calculated ratios showing comparison between the GHC group vs. GCF group.....	84

CHAPTER 1

PHYSIOLOGICAL BACKGROUND

1.1 Introduction

Electrical signals and waveforms obtained from the physiological systems of the body can yield information of clinical significance. Therefore, it is important to understand both the physiological system serving as source of each of these signals or waveforms, as well as the mechanisms for acquiring signal or waveform data. This chapter provides the background information on the physiological systems and their respective data acquisition methods pertinent to the research in this study. The understanding of this background information is critical to the analysis and interpretation of the results from the data obtained experimentally in this study.

1.2 Cardiovascular System

The cardiovascular system is sometimes called, simply, the circulatory system [1]. It consists of the heart, which is a muscular pumping device, and a closed system of vessels called arteries, veins, and capillaries. Blood contained in the circulatory system is pumped by the heart around a closed circle or circuit of vessels as it repeatedly passes through the various “circulations” of the body. The vital role of the cardiovascular system in maintaining homeostasis is dependent upon the continuous and controlled movement of blood to reach every cell in the body. Regulation of blood pressure and flow must change in response to cellular activity. Consequently, numerous control

mechanisms help to regulate and integrate the diverse functions and component parts of the cardiovascular system to supply blood to specific body areas according to need.

1.2.1 Heart

The human heart is a four-chambered muscular organ, shaped and sized roughly like a person's closed fist. It lies in the middle region of the thorax, just behind the body of the sternum between the points of attachment of the second through sixth ribs [1].

The heart is divided into left and right halves, each half operating as a separate pump. The right half receives blood from the systemic circulation (all of the organs except the lungs) and pumps blood to the lungs. The left half receives blood from the pulmonary circulation (lungs) and pumps it into the systemic circulation [2]. Each half of the heart has two chambers, an atrium and a ventricle. The left and right atria are separated by the interatrial septum; similarly, the left and right ventricles are separated by the interventricular septum. Three distinct layers of tissue make up the heart wall in both the atria and ventricles: a superficial epicardium, a middle myocardium, and a deep endocardium. The myocardium, composed mainly of cardiac muscle, forms the bulk of the heart.

The minute structure of joined cardiac muscle cells allows large areas of cardiac muscle to be electrically coupled into a single functional unit called a syncytium [1]. Because they form a syncytium, muscle cells can pass an action potential along a large area of the heart wall, stimulating contraction in each muscle fiber of the syncytium. Another advantage of the syncytium structure is that the cardiac fibers form a continuous sheet of muscle that wraps entirely around the cavities within the heart. Thus, the

encircling myocardium can compress the heart cavities, and the blood within them, with great force. Also, the cardiac muscles are autorhythmic, meaning that they can contract on their own in a slow, steady rhythm. Because the muscular myocardium can contract powerfully and rhythmically, the heart is an efficient pump for blood. In addition to allowing for powerful contraction the myocardial layer provides structural support. Within this layer, the branching cardiac muscle cells are tethered to each other by crisscrossing connective tissue fibers and arranged in spiral or circular bundles. These interlacing bundles effectively link all parts of the heart together. The connective tissue fibers form a dense network that reinforces the myocardium internally and anchors the cardiac muscle fibers. Often called the skeleton of the heart, this set of connected rings not only serves as a semirigid support for the heart valves but also serves as an electrical barrier between the myocardium of the ventricles and the myocardium of the atria (Figure 1.1).

Blood flows through the heart in one direction: from the atria to the ventricles and out the great arteries, leaving the superior aspect of the heart [3]. This uni-directional flow of blood is permitted by the four heart valves: the paired atrioventricular and semilunar valves, which open and close in response to differences in blood pressure on their two sides. The two atrioventricular (AV) valves, located at the junctions of the atria and their respective ventricles, prevent backflow into the atria when the ventricles are contracting. The two other valves, the semilunar valves, determine the direction of flow of blood from the ventricles to the arteries [2]. These mechanical devices are of importance to the normal functioning of the heart.

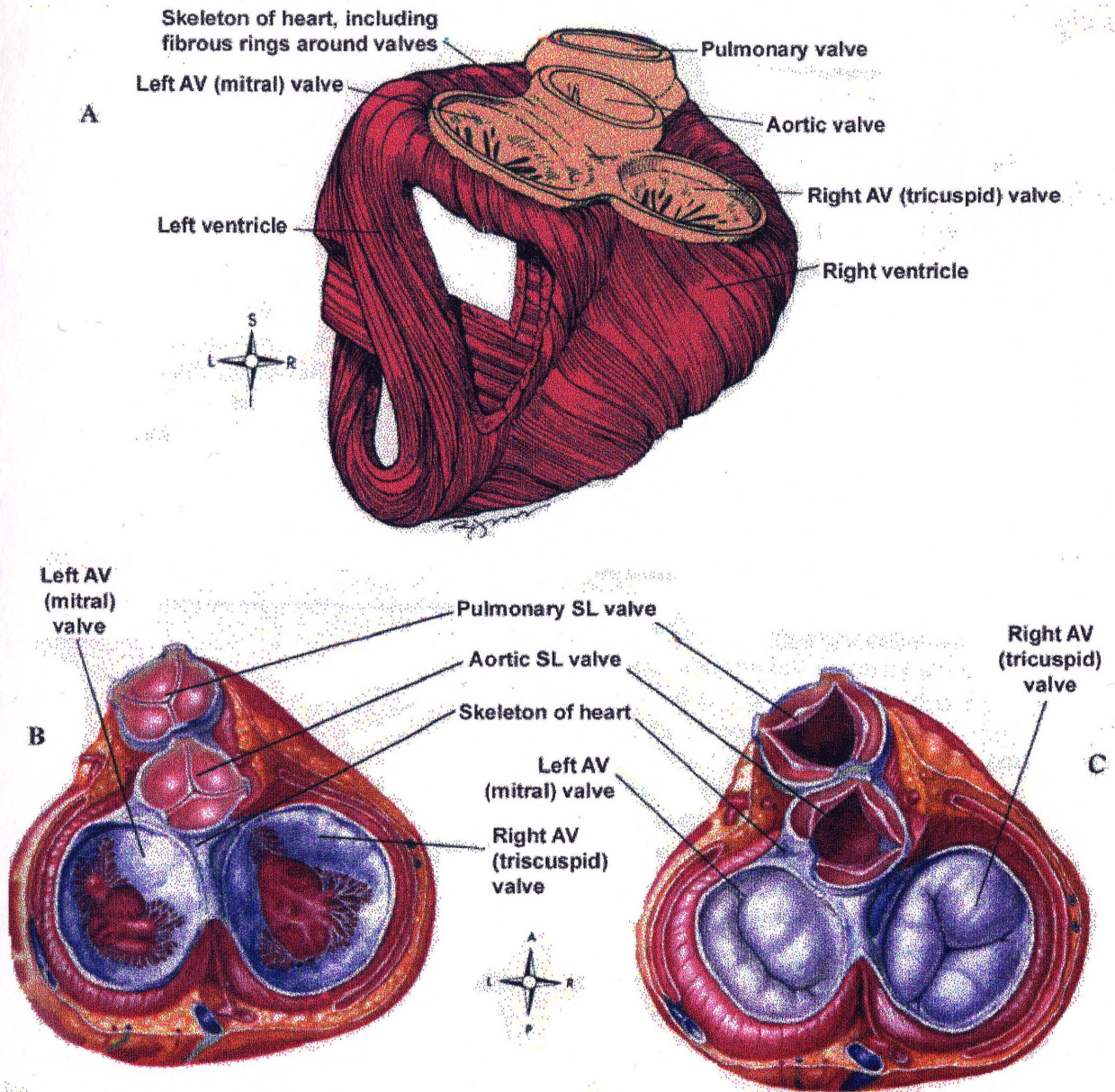


Figure 1.1 Structure of cardiac bundles and valves. **A**, This posterior view shows part of the ventricular myocardium with the heart valves still attached. **B**, This figure shows the heart valves viewed from above. The semilunar (SL) valves are closed and the atrioventricular (AV) valves are open, as when the atria are contracting. **C**, This figure shows the heart valves viewed from above. The semilunar valves are open and the atrioventricular valves are closed, as when the ventricles are contracting. (From G. A. Thibodeau and K. T. Patton, *Anthony's Textbook of Anatomy & Physiology*, 14th ed. St. Louis, MO: Mosby-Year Book, Inc., 1994.)

The two atrioventricular (AV) valves, located at the junctions of the atria and their respective ventricles, prevent backflow into the atria when the ventricles are contracting. The two other valves, the semilunar valves, determine the direction of flow of blood from the ventricles to the arteries [2]. These mechanical devices are of importance to the normal functioning of the heart.

1.2.2 Nerve Supply of the Heart

Both divisions of the autonomic nervous system send fibers to the heart. The autonomic nervous system is primarily responsible for maintaining a nearly constant internal environment in the body, regardless of changes occurring in the external environment. Pathways of the autonomic nervous system (ANS) carry information to the smooth muscles, cardiac muscle and glands. As its name implies, the autonomic nervous system is autonomous of voluntary control--it seems to govern itself without conscious knowledge.

The pathways of the ANS can be divided into the sympathetic division and the parasympathetic division. The sympathetic division, comprised of pathways that exit the middle portions of the spinal cord, is involved in preparing the body to deal with immediate threats to the internal environment. It produces the "fight or flight" response. The general functions of the sympathetic division are to increase heart rate and respiratory rate, dilate bronchioles (small passages in the lungs), stimulate sweating, increase the glucose level in the blood, and decrease activities of the digestive tract. On the contrary, the parasympathetic pathways exit at the brain or lower portions of the spinal cord and coordinate the body's normal resting activities. The parasympathetic division is thus sometimes called the "rest and repair" division. The general functions of

the parasympathetic division are often opposite of those of the sympathetic: to decrease heart rate and respiratory rate, increase digestive activities, and stimulate the storage of glucose in the liver. The alternate stimulation of an organ, for example, by the sympathetic and parasympathetic divisions keeps the organ functioning within a narrow range of functional levels. This alternation contributes to the ability of the ANS to maintain homeostasis, or a state of dynamic equilibrium of the body's internal environment.

Sympathetic fibers (contained in the middle, superior, and inferior cardiac nerves) and parasympathetic fibers (in branches of the vagus nerve) combine to form cardiac plexuses located close to the arch of the aorta [1]. From the cardiac plexuses, fibers accompany the right and left coronary arteries to enter the heart. At this point, most of the fibers terminate in the sinoatrial node (SA node), but some end in the atrioventricular node (AV node) and in the atrial myocardium. Sympathetic nerves to the heart are also called accelerator nerves. Vagus fibers to the heart serve as inhibitory or depressor nerves.

1.2.3 Conduction System of the Heart

Normally, the parts of the heart beat in an orderly sequence: first the atria contract, then the ventricles contract [2]. This orderly sequence is maintained by a conduction system, consisting of heart muscle cells that are specialized to initiate and conduct action potentials. Other heart muscle cells, the contractile cells, are normally stimulated to contract in the proper sequence by action potentials delivered to them by cells of the

conduction system. However, cardiac muscle cells have an inherent ability to contract in the absence of stimulation.

The conduction system of the heart (Figure 1.2) consists of the SA node; the AV node; the atrioventricular bundle (or the bundle of His); and the Purkinje fibers. Each of these structures consists of cardiac muscle modified enough in structure to differ in function from ordinary cardiac muscle. Although the main specialty of cardiac muscle is contraction, ordinary cardiac muscle can also conduct impulses. However, conduction alone is the specialty of this modified cardiac muscle. Therefore, the conduction system of the heart is composed of noncontractile cardiac cells specialized to initiate and distribute impulses throughout the heart, so that it contracts in an orderly, sequential manner from atria to ventricles [2]:

- (1) The SA node consists of hundreds of cells located in the right atrial wall near the opening of the superior vena cava.
- (2) The AV node is a small mass of special cardiac muscle tissue that lies in the right atrium along the lower part of the interatrial septum, just superior to the ventricles.
- (3) The bundle of His is a bundle of special cardiac muscle fibers that originate in the AV node and extend by two branches down the two sides of the interventricular septum. From there, they continue as the Purkinje fibers. The latter extend out to the lateral walls of the ventricles and papillary muscles.

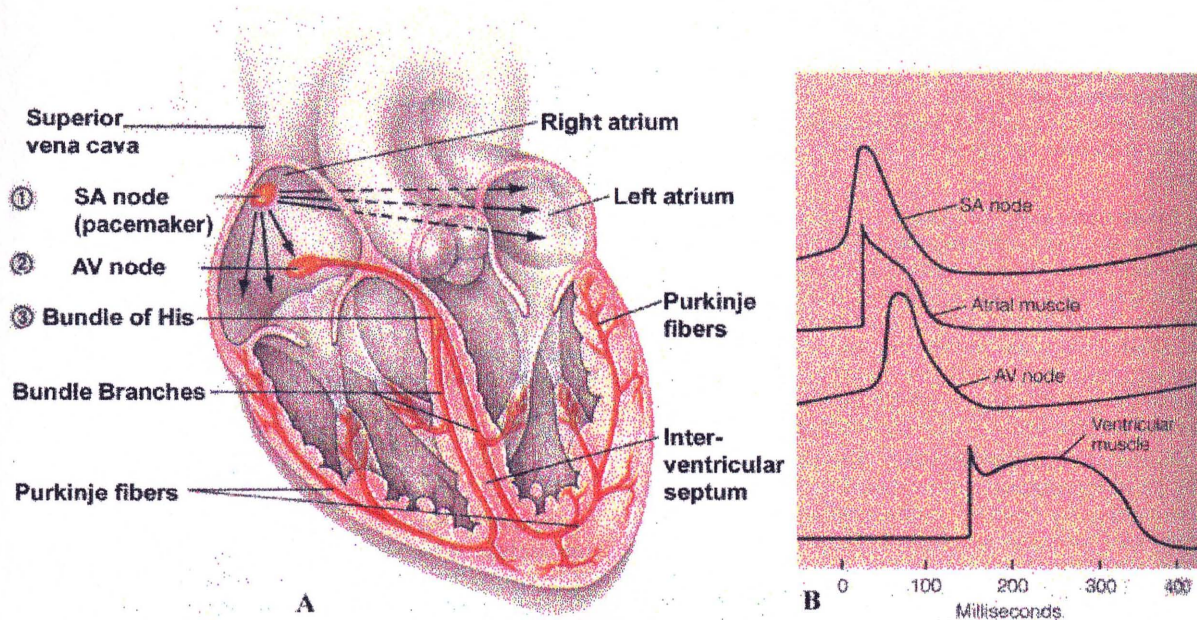


Figure 1.2 A, The intrinsic conduction system of the heart and succession of the action potential through selected areas of the heart during one heart beat. **B**, The sequence of potentials generated across the heart is shown from top to bottom beginning with the pacemaker potential generated by the SA node and ending with an action potential. (From E. N. Marieb, *Human Anatomy and Physiology*, 3rd ed. New York: The Benjamin/Cummings Publishing Company, Inc., 1995.)

1.2.4 Electrical Events of Contraction

The ability of the cardiac muscle to contract is intrinsic, i.e. it is a property of the heart muscle itself and not dependent upon the nervous system. Although the heart is adequately supplied with nerve fibers which can alter the basic rhythm of heart activity, the systematic mechanical pumping action of the heart is a result of a complex sequence of electrical events which are controlled by the conduction system.

These electrical events are possible due to the electrical nature of the plasma membrane. All living cells, including neurons, maintain a difference in the concentration of ions across their membrane [1]. There is a slight excess of positive ions on the outside of the membrane and a slight excess of negative ions on the inside of the membrane.

This, of course, results in a difference in electrical charge across their plasma membranes

called the membrane potential. This difference in electrical charges is called a “potential” because it is a type of stored energy, i.e. potential energy. Whenever opposite electrical charges (in this case, ions) are thus separated by a membrane, they have the potential to move toward one another if they are allowed to cross the membrane. A membrane that exhibits a membrane potential is said to be polarized because it possesses a negative and positive pole, respectively. This imbalance of ion concentrations is produced primarily by ion transport mechanisms in the neuron’s plasma membrane. The sodium-potassium pump, for example, is an active transport mechanism in the plasma membrane that transports sodium ions (Na^+) and potassium ions (K^+) in opposite directions and at different rates. When a stimulus reaches the membrane of a muscle cell, the permeability of the membrane to sodium and potassium ions is altered. The voltage that exists across the plasma membrane that has not been stimulated is the resting membrane potential.

Excitation occurs when an adequate stimulus triggers the opening of additional sodium channels, which permits more Na^+ to enter the cell. As the excess of positive ions outside the plasma membrane decreases, the magnitude of the membrane potential is reduced. Such movement of the membrane potential toward zero is called depolarization. As suddenly as the cell membrane became more permeable to sodium, it again becomes less permeable to sodium ions while the permeability to potassium increases. The potassium ions move out of the cell, again making the membrane negative on the inside. This process is called repolarization. This change in the balance of electrical charges during the rapid sequence of depolarization and repolarization creates an electrical potential known as an action potential, or impulse [2]. An action potential is produced

only if the local depolarization surpasses a limit called the threshold potential, after which point even more Na^+ channels are stimulated to open.

The normal cardiac impulse that initiates mechanical contraction of the heart arises in the SA node. Specialized “pacemaker” cells in the node possess an intrinsic rhythm; i.e., they have an inherent ability to depolarize spontaneously and rhythmically. These cells have a resting potential of -55 to -60 millivolts instead of the -80 to -90 millivolts found in most other heart cells [2]. SA node cells have a low potential because their membranes naturally allow large numbers of sodium ions to leak into the cells. This resting potential is unstable and gradually undergoes depolarization caused by a slow decrease in membrane permeability to potassium. This slow depolarization is called the pacemaker potential, or diastolic depolarization. It causes the membrane potential to reach a threshold level for an action potential.

Once this threshold of -45 to -50 millivolts is reached, an action potential is generated. When this occurs, sodium ions rush into the cells, and total depolarization of the membranes occurs rapidly. The membranes remain depolarized for about 0.1 second, after which the permeability of the membranes to potassium increases and their permeability to sodium decreases. Return to the resting potential occurs as potassium ions move out of the cells. When the resting potential is regenerated, the membranes' permeability to potassium again decreases, causing a gradual membrane depolarization. Another cycle in the automatic rhythmicity of the SA node cells is initiated. The process is repeated continuously throughout life, establishing the resting heart rate. When the heart rate is above or below this rate, the SA node is being influenced by neural or

chemical factors. However, its ability to continuously depolarize and repolarize is inherent in the properties of the membranes of the cells of the SA node (Figure 1.2).

The action potential generated by the depolarizing cells of the SA node spreads through the muscle cells of the atria. The action potential causes the atria to contract in a wave that passes from the area of the SA node toward the ventricles, but not to them, because of the connective tissue rings between the atria and ventricles. Blood is thus pushed from the atria into the ventricles on each side of the heart at the same time. Because the action potentials from the SA node are generated at a greater frequency than in any other part of the heart's conducting system, the SA node determines the frequency of the heart beat and is thus known as the pacemaker. As the pacemaker, the SA node sets the rate of contraction of the entire heart and synchronizes the action of the atria and ventricles.

The AV node receives impulses from the SA node. These impulses cause the AV node to depolarize. After a short delay due to its own slow conductivity, the AV node relays impulses to the specialized cells of the bundle of His in the interventricular septum. These cells carry the action potential across the nonconductive connective tissue of the septum. The bundle of His divides into left and right bundle branches and ultimately into Purkinje fibers. Impulses from the many branches of the Purkinje fibers stimulate the muscle cells of the ventricles to depolarize and contract. The ventricles contract in a sudden wave that begins at the apex of the heart and travels through the ventricles, forcing blood out of the heart.

Each portion of the conduction system has its own inherent rate of depolarization [2]. For example, if no pacesetting stimuli are received from the SA node, the AV node

generates impulses at a rate of forty to sixty times per minute; and in the absence of other stimuli the Purkinje fibers generate impulses at a rate of fifteen to forty times per minute. Of course, these values may vary with each individual.

All muscle cells have a refractory period, a period during an action potential when a second stimulus will not normally generate a second action potential [2]. The refractory period is divided into the absolute refractory period, during which no stimulus can affect the muscle, and a later relative refractory period, during which only a suprathreshold (unusually strong) stimulus can stimulate the muscle. In cardiac muscle the absolute refractory period is extremely long (about 300 milliseconds) relative to that of skeletal muscle (1 to 2 milliseconds). The long refractory period prevents cardiac muscle from being stimulated repeatedly without undergoing relaxation between contractions. This allows time for the heart chambers and the blood vessels of the heart wall to refill between contractions; it also allows the heart muscle to relax between contractions.

1.2.5 The Electrocardiogram

The smooth, rhythmic contraction of the atria and ventricles has an underlying electrical precursor in the form of a well-coordinated series of electrical events that takes place within the heart [4]. The coordinated contraction of the atria and ventricles is set up by a specific pattern of electrical activation in the musculature of these structures. The electrical potentials in the heart generated from impulse conduction spread through surrounding tissues to the surface of the body. This is of great clinical significance because from the skin, visible records of the pattern of the heart's electrical activity can

be graphically displayed by an instrument called an electrocardiogram (ECG or EKG). Potential differences are determined by positioning recording electrodes (leads) at various sites on the body surface and measuring the voltage between them (being careful to draw little current.) If the two electrodes are located on different equal-potential lines of the electric field of the heart, a nonzero potential difference, or voltage, is measured [4]. Different pairs of electrodes at different locations generally yield different voltages because of the spatial dependence of the electric field of the heart. Thus, it is important to have certain standard positions for clinical evaluation of the ECG. Typically, twelve standard leads are used to record an ECG [3]. Three of which are bipolar leads that measure the voltage between the arms, or an arm and a leg, and nine are unipolar leads (Figure 1.3).

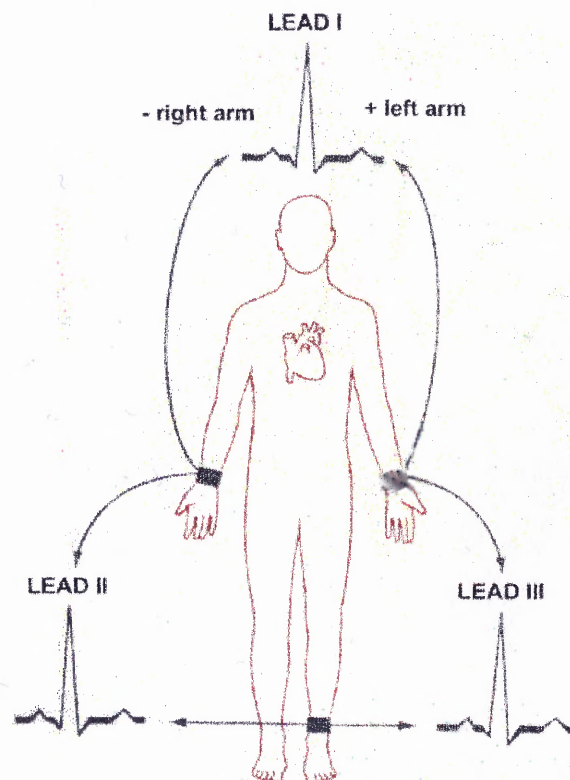


Figure 1.3 The placement of the positive and negative electrodes for three commonly used leads, as shown. (From J. G. Creager, *Human Anatomy and Physiology*. Belmont, CA: Wadsworth Inc., 1983.)

A typical ECG consists of a series of three distinguishable waves called deflection waves (Figure 1.4). The first wave, the small P-wave, lasting about 0.08 s, results from movement of the depolarization wave from the SA node through the atria. Approximately 0.1 s after the P-wave begins, the atria contract. The large QRS complex results from ventricular depolarization and precedes ventricular contraction. Its complicated shape reveals the different size of the two ventricles and the time required for each to depolarize. Average duration of the QRS complex is 0.08 s. The T-wave is caused by ventricular repolarization and typically lasts about 0.16 s. Repolarization is slower than depolarization, so the T-wave is more spread out and has a lower amplitude than the QRS wave. Because atrial repolarization takes place during the period of ventricular excitation, its occurrence is normally obscured by the large QRS complex being recorded at the same time.

The P-R (or P-Q) interval is the time (about 0.16 s) from the beginning of atrial excitation to the beginning of ventricular excitation. It includes atrial depolarization (and contraction) as well as the passage of the depolarization wave through the rest of the conduction system. The Q-T interval, lasting about 0.36 s, is the period from the beginning of ventricular depolarization through their repolarization and includes the time of ventricular contraction.

In a healthy heart, the size, duration and timing of the deflection waves tend to be consistent. Such records are useful in assessing the manner in which impulses from the conduction system pass through the heart and in detecting electrical abnormalities. Thus, changes in the pattern or timing of the ECG may reveal a diseased or damaged heart or problems with the heart's conduction system.

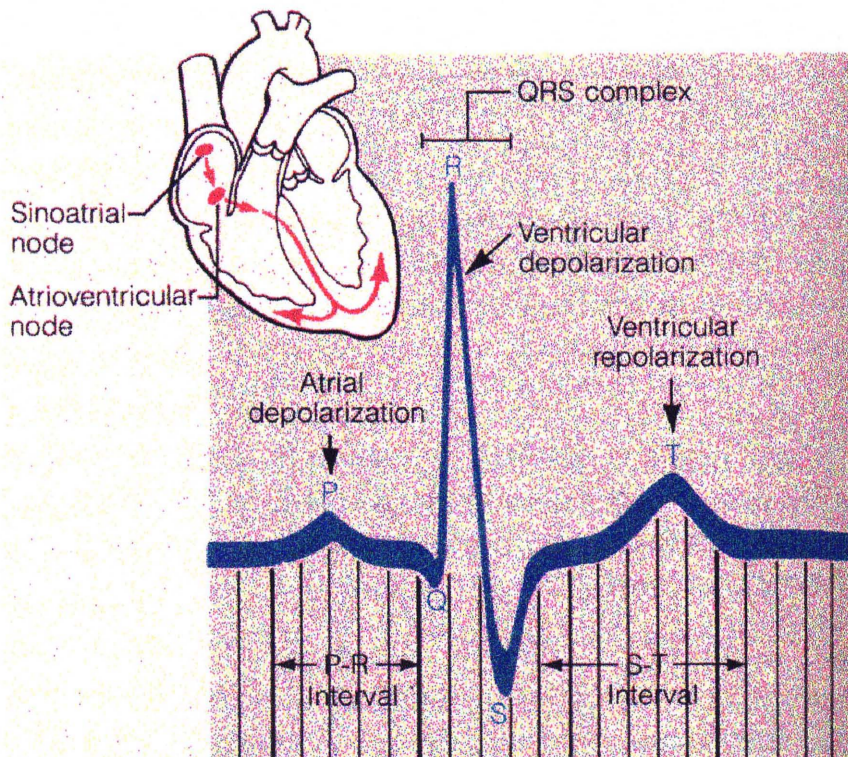


Figure 1.4 An electrocardiogram tracing (lead I) illustrating the three normally recognizable deflection waves and the important intervals. (From E. N. Marieb, *Human Anatomy and Physiology*, 3rd ed. New York: The Benjamin/Cummings Publishing Company, Inc., 1995.)

1.2.6 Cardiac Cycle

The cardiac cycle consists of one heart beat, or one cycle of contraction and relaxation of the cardiac muscle—both atria and both ventricles. The two atria contract simultaneously. Then, as the atria relax, the two ventricles contract and relax, instead of the entire heart contracting as a unit [1, 2]. These movements of the heart create a pumping phase and a filling phase. Pumping occurs when the blood is forced out of its chambers during contraction; filling occurs when the chambers are allowed to refill with blood during relaxation. The terms systole and diastole refer, respectively, to these contraction and relaxation periods of heart activity.

1.2.7 Circulation and Blood Pressure

The heart is divided into two pumping systems, the right side of the heart and the left side of the heart [4]. These two pumps and their associated valves are separated by the pulmonary circulation and the systemic circulation. (The function of the blood circulation is to transport oxygen and other nutrients to the tissues of the body and to carry metabolic waste products away from the cells.) Each pump has a filling chamber, the atrium, which in turn helps to fill the ventricle, the stronger pump.

The left ventricle ejects blood through the aortic valve into the aorta, and the blood is then distributed through the branching network of arteries, arterioles and capillaries. The resistance to blood flow is regulated by the arterioles, which are under local, neural, and endocrine control. The blood then returns to the right side of the heart via the venous system. Blood fills the right atrium, the filling chamber of the right heart, and flows through the tricuspid valve into the right ventricle. The blood is pumped from the right ventricle into the pulmonary artery through the pulmonary valve. It next flows through the pulmonary arteries, arterioles, capillaries, and veins to the left atrium. The blood flows from the left atrium, the filling chamber of the left heart, through the mitral valve into the left ventricle (Figure 1.5). When the left ventricle contracts in response to the electric stimulation of the myocardium, blood is pumped through the aortic valve into the aorta.

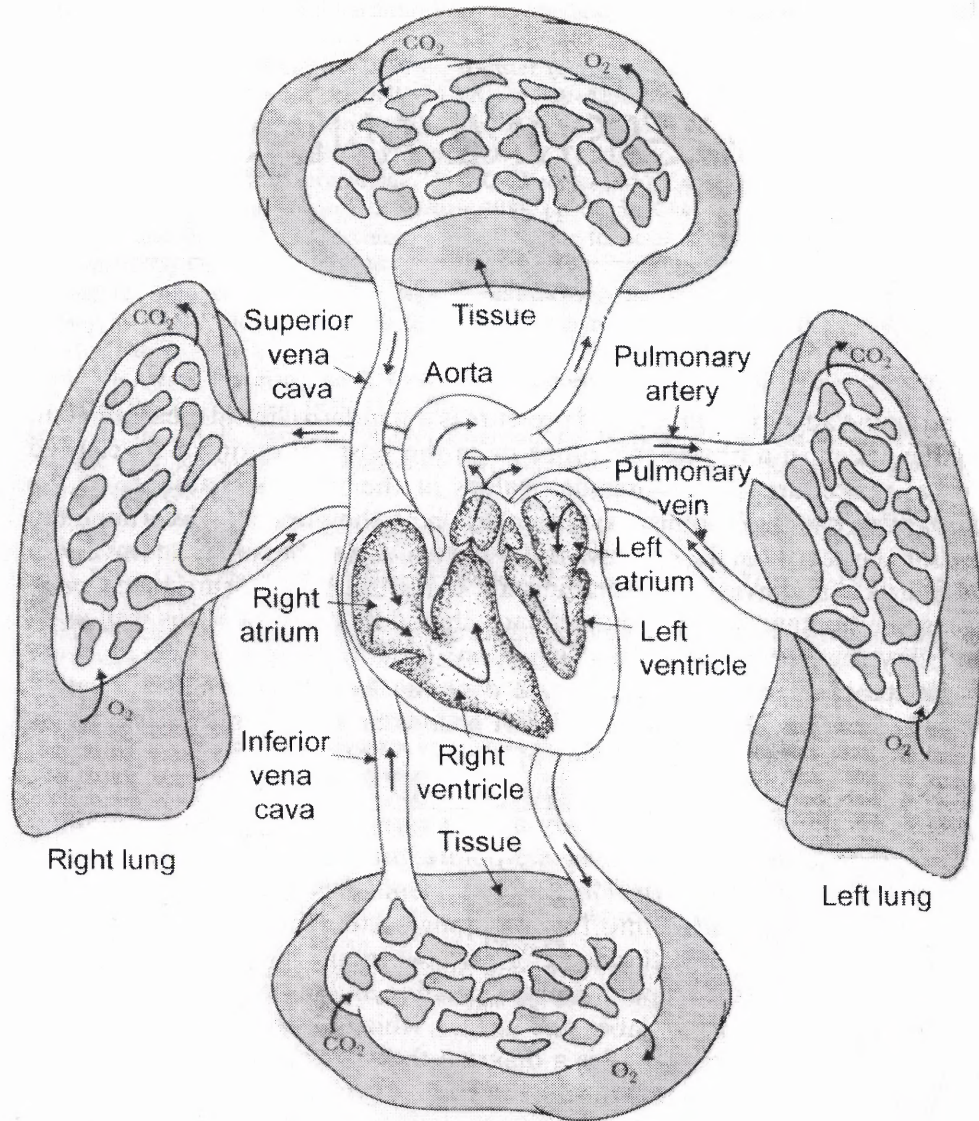


Figure 1.5 The left ventricle ejects blood into the systemic circulatory system. The right ventricle ejects blood into the pulmonary circulatory system. (From J. G. Webster, *Medical Instrumentation: Application and Design*, 3rd ed. New York: John Wiley & Sons, Inc., 1998.)

The pressures generated by the right and left sides of the heart differ somewhat in shape and amplitude. Mechanical contraction of the ventricular muscle generates ventricular pressures that force blood through the pulmonary and aortic valves into the pulmonary circulation and the systemic circulation, causing pressures in each.

The mechanisms of circulation are based upon basic principles of fluid mechanics. Blood circulates for the same reason that any fluid flows—whether it is water in a river or blood in a vessel. A fluid flows because a pressure gradient exists between different parts of its volume (Figure 1.6). This primary fluid flow principle derives from Newton's first and second laws of motion. In essence, these laws state the following principles: (1) A fluid does not flow when the pressure is uniform throughout. (2) A fluid flows only when its pressure is higher in one area than in another, and it flows always from its higher pressure area to its lower pressure area.

Therefore, applying these basic principles to circulation shows that: (1) Blood flow through the heart is controlled entirely by pressure changes, and (2) Blood flows along a pressure gradient, always from higher to lower pressure through any available opening. The pressure changes, in turn, reflect the alternating contraction and relaxation of the myocardium and cause the opening of the heart valves, which keeps blood flowing in the forward direction.

Any fluid driven by a pump through a circuit of closed channels operates under pressure, and the nearer the fluid is to the pump, the greater the pressure it is under [3]. The dynamics of blood flow in blood vessels is no exception, and blood flows through the blood vessels along a pressure gradient, always moving from higher-to lower-pressure areas. Fundamentally, the pumping action of the heart generates blood flow. Pressure results when flow is opposed by resistance.

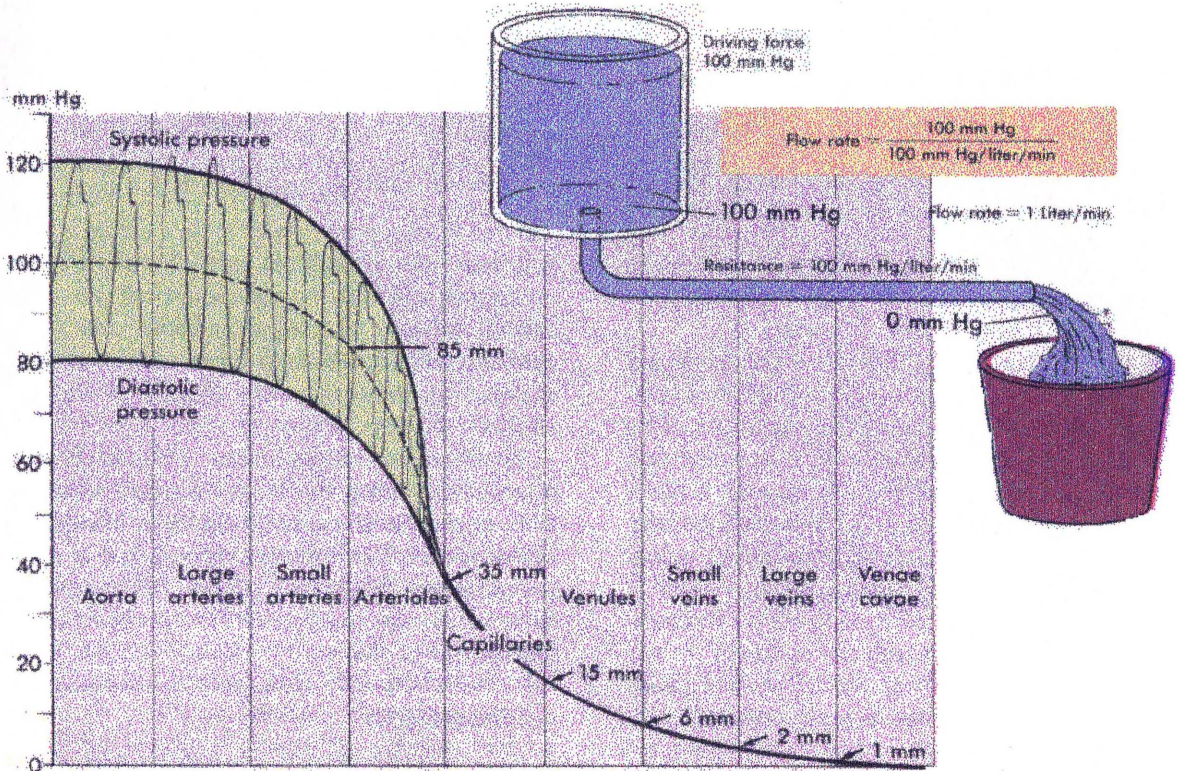


Figure 1.6 The primary principle of circulation. Fluid always travels from an area of high pressure to an area of low pressure. (From G. A. Thibodeau and K. T. Patton, *Anthony's Textbook of Anatomy & Physiology*, 14th ed. St. Louis, MO: Mosby-Year Book, Inc., 1994.)

The steepest change (drop) in blood pressure occurs in the arterioles, which offer the greatest resistance to blood flow. However, so long as a pressure gradient exists, blood continues to flow from higher to lower pressure areas until it completes the circuit back to the heart. Because of basic principles, pressure varies in the different types of blood vessels. When speaking of blood pressure, it is in reference to arterial pressure—or more precisely, to two arterial pressures, the systolic pressure and the diastolic pressure [2]. These pressures reflect changes in pressure as the heart goes through the cardiac cycle. The systolic pressure is the maximum pressure developed in the arteries during the systolic phase of the cardiac cycle; the diastolic pressure is the minimum pressure in the

ventricle contracts with greater force than the right ventricle, the pressures in the aorta are greater than the pressures in the pulmonary trunk.

Blood pressures are measured as the height of a column of mercury that the pressure will support, expressed in millimeters of mercury (mm Hg). Normal adult male systemic pressures are a systolic pressure in the range of 120 mm Hg and a diastolic pressure in the range of 80 mm Hg.

The primary determinant of arterial blood pressure is the arterioles [1]. Arterial blood volume is directly proportional to arterial pressure through their influence on arterial volume. Essentially, arterial blood pressure reflects two of the most important factors that are directly proportional to blood volume: (1) how much the elastic arteries close to the heart can be stretched, i.e. their compliance or distensibility, and (2) the volume of blood forced into them at any instant, i.e. cardiac output.

1.2.8 Photoplethysmogram: A Measurement of Blood Volume

The measurement of human systemic blood pressure can be obtained both invasively and noninvasively. Although more accurate measurements are obtained invasively, noninvasive methods are preferred and more often utilized.

A method of noninvasively measuring the complete arterial waveform was developed by Dr. Jan Penaz of Czechoslovakia and presented at the 10th International Conference on Medical and Biological Engineering in 1973 at Dresden (2300 Operation & Maintenance Manual, 2-3). The technique is based on the concept that if an externally applied pressure (via the bladder in the cuff) is equal to the arterial pressure at all times (instantaneously), the arterial walls will be unloaded (zero transmural pressure) and the

arteries will not change in size, the blood volume, which is only contained in the arteries at these pressures, will not change so the photoplethysmogram will be constant at some value, i.e. a set point value. The pressure in the cuff will be driven to equal the arterial pressure throughout each pressure cycle. This cuff pressure can be measured with an electronic pressure transducer and the resulting signal displayed as the arterial pressure (Figure 1.7).

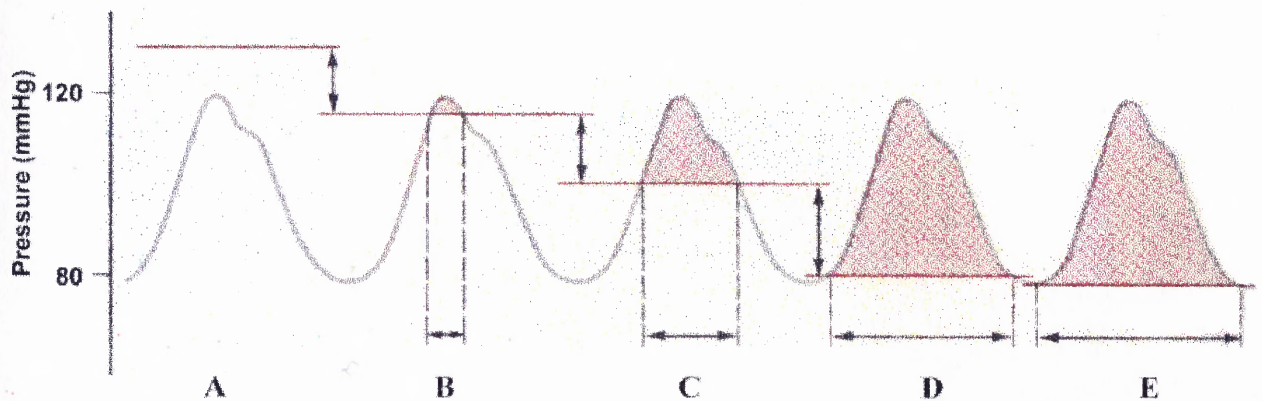


Figure 1.7 The events that take place during the measurement of blood pressure. **A**, Cuff pressure above systolic pressure; artery completely occluded. **B**, Cuff pressure just below systolic pressure. **C**, Flow turbulent. **D**, Cuff pressure equals diastolic pressure. **E**, Smooth flow is resumed. Systolic pressure, normally 110 to 120 mm Hg, is recorded at B, and diastolic pressure, normally 70 to 80 mm Hg, is recorded at D. (From J. G. Creager, *Human Anatomy and Physiology*. Belmont, CA: Wadsworth Inc., 1983.)

The technique was further developed and clinically evaluated for over a decade by researchers at TNO in the Netherlands and engineers at Ohmeda, resulting in the 2300 Finapres monitor. The Finapres generally consists of a finger cuff, a pressure transducer that feeds pressure to the computer and a monitor to display the instantaneous pressure. The 2300 Finapres monitor uses two methods to determine the set point. The first method, which is referred to as the servo-start up adjustment, is an automated process and

is used to establish an initial approximate set point. The second method, referred to as the servo self-adjust, provides fine-tuning of the set point and corrects for slow moving physiologic changes occurring in the finger and arteries under the cuff. This second method, otherwise known as the calibration feature of the Finapres, results in a loss in data for the period of correction for physiologic changes, thus, yielding a non-continuous signal.

1.3 Respiratory System

The main function of the respiratory system is to move oxygen from the atmosphere to the blood and to remove carbon dioxide from the blood to the atmosphere [2]. This involves two processes—breathing and external respiration. Breathing, or pulmonary ventilation, is the mechanical process by which air is moved into and out of the lungs. External respiration is the process by which gases are exchanged between the blood and the air.

The respiratory system consists of a set of passageways through which air enters and leaves the system. From the surface of the body inward, they include the nasal cavity, pharynx, larynx, trachea, bronchi, bronchioles, and alveoli (Figure 1.8). At the lower end of the trachea the passageway branches to form two primary bronchi; each primary bronchus branches to form secondary bronchi, which in turn branch many times, forming bronchioles and alveoli. One primary bronchus enters each of the two lungs, and all the subsequent branches form the tissues of the lungs. The lung as an organ is thus a mass of tubes and thin-walled sacs, along with some connective tissues that support the other tissues.

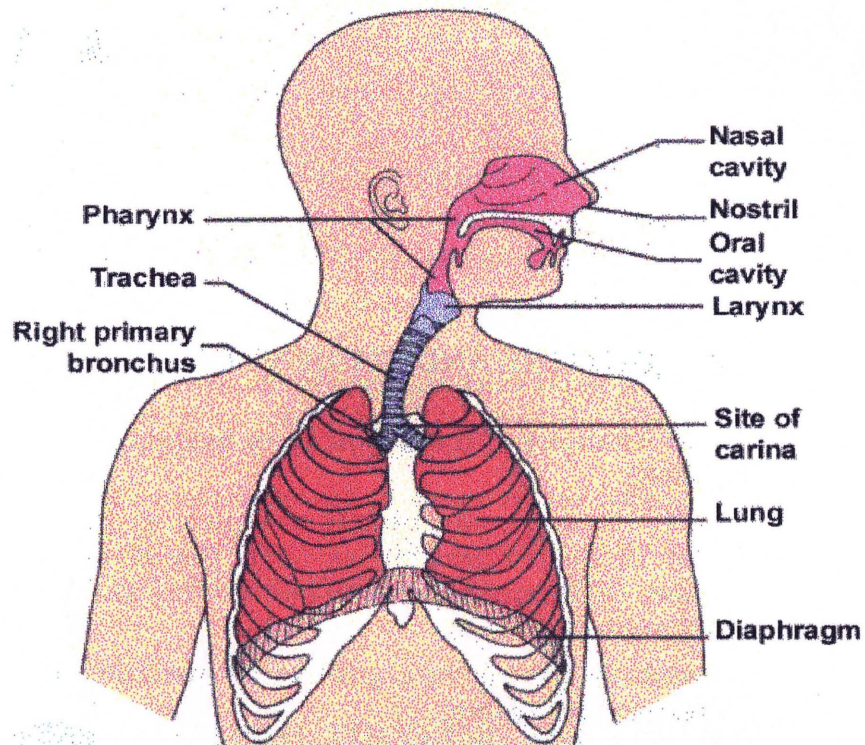


Figure 1.8 The major respiratory organs shown in relation to surrounding structures. (From E. N. Marieb, *Human Anatomy and Physiology*, 3rd ed. New York: The Benjamin/Cummings Publishing Company, Inc., 1995.)

To properly understand the respiratory system and respiration, the relationship between the respiratory and circulatory systems must be kept in mind. Gases are exchanged between the air and the blood in the lungs. The blood vessels then transport the blood to all other tissues, where gases are exchanged between the blood and the cells. Therefore, the role of the circulation of blood in internal respiration is similar to the role of breathing in external respiration.

1.3.1 Mechanism of Pulmonary Ventilation

Air moves in and out of lungs for the same basic reason that any fluid, i.e. a liquid or a

always moves down its pressure gradient. Under standard conditions, air in the atmosphere exerts a pressure of 760 mm Hg. Air in the alveoli at the end of one expiration and before the beginning of another inspiration also exerts a pressure of 760 mm Hg. This fact explains the reason why, at that instant, air is neither entering nor leaving the lungs. The mechanism that produces pulmonary ventilation is that which establishes a gas pressure gradient between the atmosphere and the alveolar air.

When atmospheric pressure is greater than pressure within the lung, air flows down this gas pressure gradient. Then air moves from the atmosphere into the lungs, and inspiration occurs. When pressure in the lungs becomes greater than atmospheric pressure, air again moves down a gas pressure gradient. However, it is moving in the opposite direction from the lungs into the atmosphere. The pulmonary ventilation mechanism, therefore, must establish these two gas pressure gradients to produce inspiration, where intraalveolar pressure is lower than atmospheric pressure, and expiration, where intraalveolar pressure is higher than atmospheric pressure.

These pressure gradients are established via changes in the size of the thoracic cavity, which, in turn, are produced by contraction and relaxation of respiratory muscles. In order to understand the pressure changes that occur in the lungs and thorax during the breathing cycle, it is important to have an understanding of Boyle's Law. This principle states that given a constant temperature, the volume of a gas varies inversely with the pressure. Therefore application of this principle shows that expansion of the thorax, i.e. an increase in volume, results in a decreased intrapleural (intrathoracic) pressure. This leads to a decreased intraalveolar pressure that causes air to move from the outside into the lungs (Figure 1.9).

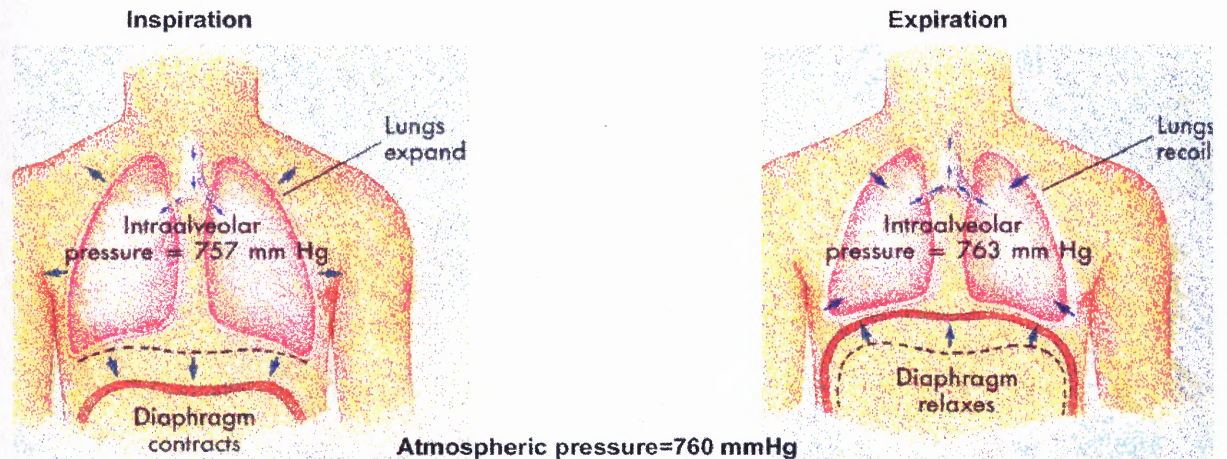


Figure 1.9 Mechanics of ventilation. (From G. A. Thibodeau and K. T. Patton, *Anthony's Textbook of Anatomy & Physiology*, 14th ed. St. Louis, MO: Mosby-Year Book, Inc., 1994.)

During inspiration, the diaphragm contracts, increasing the volume of the thoracic cavity. This increase in volume results in a decrease in pressure, which causes air to rush into the lungs. During expiration, the diaphragm returns to an upward position, reducing the volume in the thoracic cavity. Air pressure increases then, forcing air out of the lungs.

1.3.2 Thoracic Plethysmography

The term plethysmography refers, in general, to measurement of the volume or change in volume of a portion of the body [4]. In respiratory applications involved in this study, plethysmography has been approached by inferring changes in thoracic cavity volume from geometrical changes at discrete location on the torso.

Several devices have been used to measure continuously the kinematics of the chest wall that are associated with changes in thoracic volume. The electrical impedance

of the thoracic cavity changes with breathing movements and can be sensed in order to monitor ventilatory activity. Impedance pneumographs are used for studies in which the presence or absence (relative magnitude and frequency) of breathing movements rather than their actual volume changes are important. The application of magnetometers, strain gages, and variable-inductance sensors requires the simultaneous measurement of motion at two locations on the chest wall. During most breathing patterns, the chest wall behaves as though it has two predominant degrees of freedom corresponding to movements of the ribcage and diaphragm. The weighted sum of the displacements of these two structures, with the movement of the abdomen taken as a measure of diaphragmatic motion, can yield an estimate of the volume change of the thoracic cavity.

1.4 Definition of Heart Rate Variability

Cyclical changes in heart rate and hemodynamic parameters, such as arterial blood pressure and stroke volume, have been known since ancient times and systematically examined at least since the eighteenth century [5]. Heart rate is principally influenced by two factors: (1) the intrinsic firing rate of the “pacemaker” cells of the sinoatrial node, and (2) the modulating influences of the autonomic nervous system [5]. In turn, the sinoatrial node has dual innervation: (1) the sympathetic system, which enhances spontaneous firing rate, and (2) the parasympathetic system, which exerts a counterinhibitory action, depressing spontaneous firing. The balance between the opposing innervations may be the principal determinant of normal heart rate.

Given the known association between a variety of physiologic and pathophysiologic processes and autonomic function, researchers and clinicians have long

sought noninvasive methods for assessing sympathetic and parasympathetic activity [5]. Heart rate variability (HRV) has been developed as a semiquantitative method of assessing this autonomic activity [6, 7]. "Heart rate variability" has become the conventionally accepted term to "describe variations of both instantaneous heart rate and RR intervals" [6], and is attributed to cyclic fluctuations in autonomic tone [6].

To observe oscillations in consecutive cardiac cycles, a continuous ECG signal may be used. The R wave serves as a marker of each beat position and because of its distinctive shape and prominent amplitude, it becomes the easiest part of the beat for computer detection [8]. The basic measurement is the time interval between heart beats as calculated from consecutive R waves obtained in the ECG (Figure 1.10). The construction of this interbeat interval (IBI) involves several steps. Each R wave is detected and a pulse is produced at the position of each R wave. The height of each pulse is adjusted to be the length of the previous RR interval. For example, two successive pulses occur at T_1 and T_2 seconds, respectively, where the distance between the two is Y . Therefore, the interval of Y seconds becomes the height of the pulse that occurs at time T_2 . The consecutive pulses that follow form a pulse wave. This pulse wave is interpolated to produce a wave with equally spaced samples. This type of interpolation is called backward step interpolation where the height of the wave in a time interval is kept constant at the value of the length of the time interval. This IBI signal will become the basis from which information on HRV will be obtained.

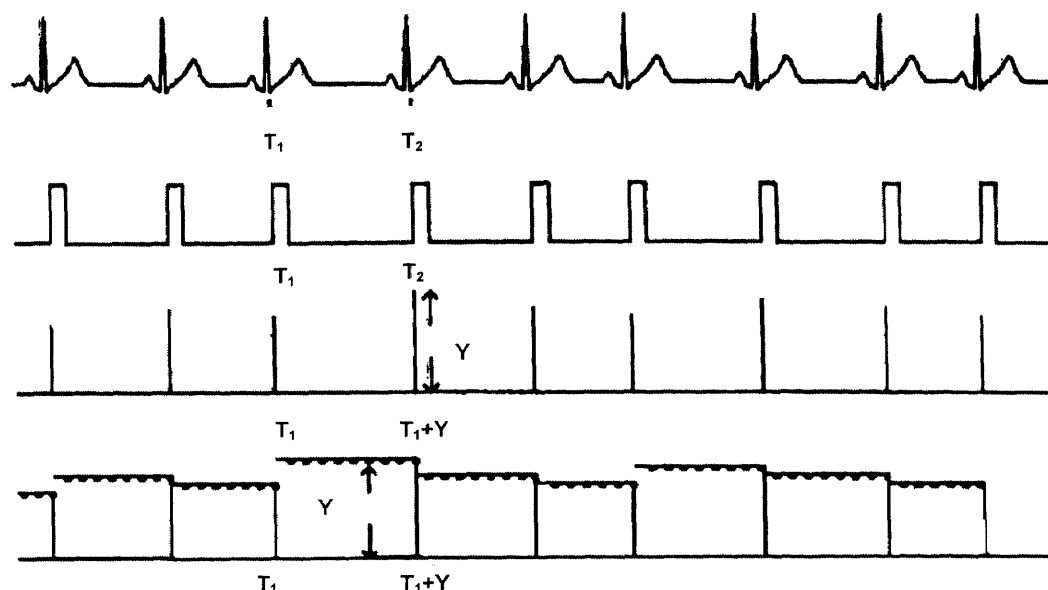


Figure 1.10 Steps in the construction of an interbeat interval (IBI) signal. (From S. Shin, W. N. Tapp, S. Reisman, and B. H. Natelson, "Assessment of Autonomic Regulation by the Method of Complex Demodulation," *IEEE Transactions in Biomedical Engineering*, vol. 36, pp. 274-283, 1983.)

Each consecutive heart beat may also be detected using a continuous arterial blood pressure signal. The method of heart rate detection using the blood pressure signal is similar to that of the ECG signal; however, the systolic pressure peak is detected as opposed to the R wave. The method of interpolation performed on the detected blood pressure signal, however, varies from that of the ECG. Rather than detect the position at which each peak occurs, as with the ECG, the amplitude of each successive systolic peak is detected. The value of the amplitude is then interpolated over the time period between each consecutive systolic pressure peak.

The various analysis methods of heart rate variability utilized in this study, such as frequency domain analysis and joint time-frequency domain analysis, will be described in further detail in Chapter 2. Each method offers a different window of information on

HRV. The different power frequency regions obtained from the analyses, i.e. the very low frequency, low frequency and high frequency regions, correspond to activity in the sympathetic and/or parasympathetic nervous systems, respectively.

1.5 Statement of Objective

The original objective of this research was to assess autonomic nervous system activity, specifically sympathetic activity, in Gulf War veterans with no health complaints versus Gulf War veterans with chronic fatigue syndrome (CFS), through the examination of three pertinent physiological measurements (heart rate, blood pressure, and respiration) acquired during the application of a cardiovascular stressor. In conjunction with a power spectrum analysis, a time-frequency analysis was originally to be carried out with the support of respiratory data to determine if observed activity was purely sympathetic or if it was influenced by vagal activity. Studies have indicated that the respiratory component of the HF band could be readily identified by comparison with the respiratory power spectrum. In this way it would be possible to be certain that the HF component at a lower breathing rate does not extend into the preset LF band of the heart rate variability spectrum. Therefore, the availability of the respiratory signal, in addition to the ECG and blood pressure signals, would have provided greater insight into autonomic activity. However, the scope of this research was limited by the lack of data analysis tools for the respiratory signal, a factor which will be addressed in Chapter 6.

Consequently, the goal of this study was to examine the heart rate variability obtained from the ECG signal in conjunction with that obtained from the blood pressure signal. The physiological signals consist of 2 minutes of measurements acquired in the

supine position, and 5 minutes of measurements acquired in the standing position, including measurements obtained during the transition period from the supine to the standing position. Heart rate variability has long been studied as a noninvasive method to extract information on the autonomic nervous system. In the time-frequency domain and by power spectral analysis, heart rate variability analysis has been suggested to be a valid method of assessing sympathetic activity, measured as the ratio of the power of the low frequency (LF) and the high frequency (HF) components. This ratio was evaluated through a power spectrum analysis of both the ECG and the blood pressure signals, respectively. A time-frequency analysis was carried out to investigate autonomic activity during the transition period from the supine to the standing position. All signal analyses were performed with algorithms implemented in LabVIEW (National Instruments).

Furthermore, in an attempt to find a more sensitive index of sympathetic activity, recent studies have shown that the ratio of the LF component of the systolic blood pressure signal to the HF component of the ECG signal, i.e. $LF_{(BP)}/HF_{(ECG)}$, is significantly more sensitive than the conventional LF/HF ratio [27, 28]. This new index was shown to be much more sensitive in detecting sympathovagal imbalance in subjects with postural tachycardia syndrome (POTS). Because chronic fatigue syndrome bears strong resemblance to features of POTS, the new index may thus prove to be more sensitive in this study as well.

As a result, the scope of this research also included further investigation of this new index as a marker of sympathetic activity in comparison to the conventional ratio obtained via ECG and blood pressure, respectively. Ultimately, the different indices of autonomic activity were compared between the two sample populations in order to

determine the more accurate indicator of sympathetic activity, as well as to determine the possible effect of chronic fatigue syndrome on the autonomic nervous system.

1.6 Factor that Influences Breathing

Arterial blood pressure helps control breathing through the respiratory pressoreflex mechanism [1]. A sudden rise in arterial pressure, by acting on aortic and carotid baroreceptors, results in reflex slowing of respirations. A sudden drop in arterial pressure brings about a reflex increase in rate and depth of respirations. The pressoreflex mechanism is probably not of great importance in the control of respirations. It is, however, of major importance in the control of circulation.

1.7 Factors that Affect Aspects of the Cardiovascular System

There are many factors that affect the normal resting function of the cardiovascular system. These affects may be manifested in changes in heart rate, blood flow, blood volume, etc. However, only those that are applicable to this study will be addressed in the following section.

1.7.1 Respiration

One important factor that promotes the return of venous blood to the heart is the blood-pumping action of respiration and skeletal muscle contractions [1]. Both actions produce their facilitating effect on venous return by increasing the pressure gradient between the peripheral veins and the venae cavae (central veins).

The process of inspiration increases the pressure gradient between peripheral and central veins by decreasing central venous pressure and also by increasing peripheral venous pressure. Each time the diaphragm contracts, the thoracic cavity necessarily becomes larger and the abdominal cavity smaller. Therefore the pressures in the thoracic cavity, in the thoracic portion of the vena cava, and in the atria decrease, and those in the abdominal cavity and the abdominal veins increase. This change in pressure between expiration and inspiration acts as a “respiratory pump” that moves blood along the venous route (Figure 1.11).

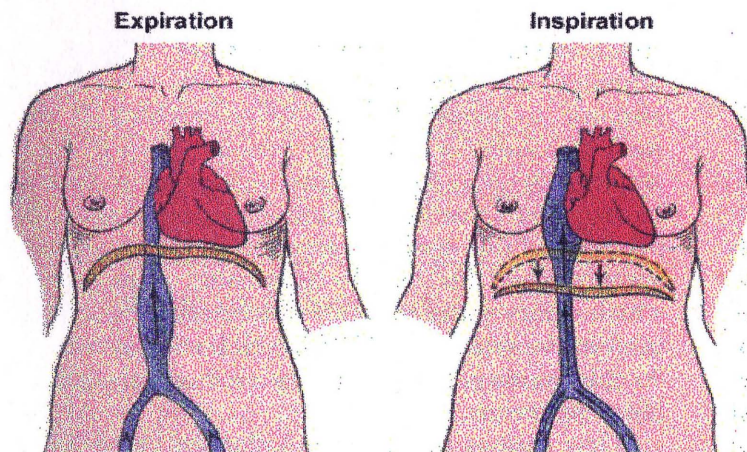


Figure 1.11 Venous pumping mechanism. The respiratory pump operates by alternately decreasing thoracic pressure during inspiration (thus pulling venous blood into the central veins) and increasing pressure in the thorax during expiration (thus pushing central venous blood into the heart). (From G. A. Thibodeau and K. T. Patton, *Anthony's Textbook of Anatomy & Physiology*, 14th ed. St. Louis, MO: Mosby-Year Book, Inc. 1994.)

Deeper respirations intensify these effects and therefore tend to increase venous return to the heart more than normal respirations. This characteristic contributes to the principle that increased respirations and increased circulation tend to go hand in hand.

1.7.2 Gravity and Posture

Gravity affects the pressure in both arteries and veins [2]. Compared to the pressure at the level of the heart, the pressure in any vessel above the heart is lower, and the pressure in any vessel below the heart is higher. Similar but smaller pressure differences occur in veins. In contrast, in a human lying down, most of the blood vessels are nearly level with the heart, and gravity has little effect on pressures. When a person changes from a lying to a standing position, the force of gravity causes blood to collect in the veins below the heart. This causes a decrease in the venous return and a concurrent decrease in stroke volume. When the stroke volume decreases, the blood pressure also drops.

The compensatory mechanisms that overcome the drop in blood pressure begin with the decrease in the rate at which baroreceptors send inhibitory impulses to the cardiovascular center. With the removal of this inhibition the heart rate accelerates. In addition, the veins constrict and cause an increase in venous return. Together, these effects increase the heart rate and stroke volume and therefore the cardiac output. The decrease in baroreceptor inhibition also results in vasoconstriction and an increase in total peripheral resistance. When the cardiac output and the total peripheral resistance increase, the mean arterial pressure will increase toward normal. If these compensatory mechanisms fail to respond quickly enough, the blood flow to the brain decreases suddenly, and fainting occurs (Figure 1.12). Such a condition is called postural hypotension.

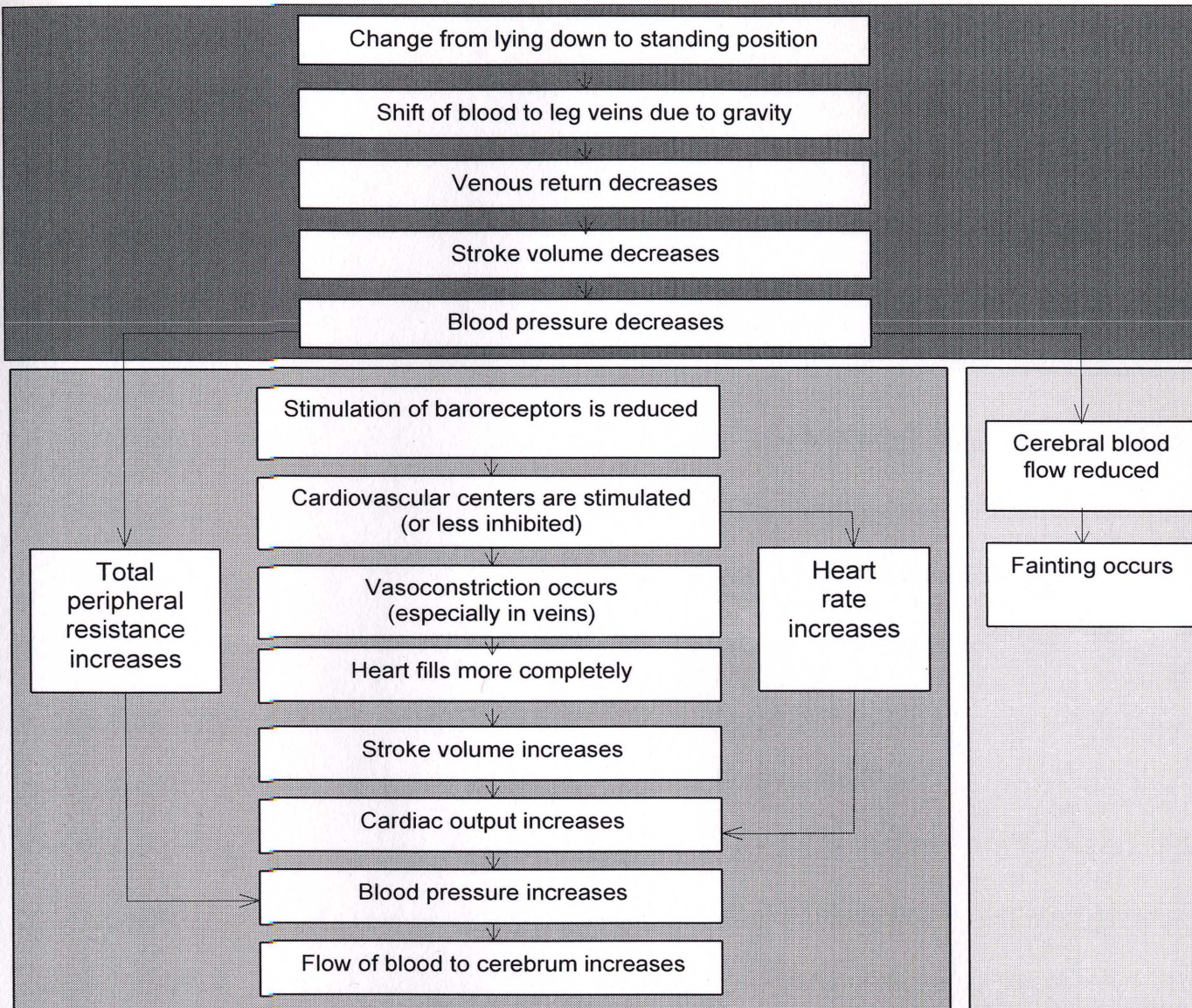


Figure 1.12 Effects of moving from a lying to a standing position, and how these effects are compensated by the cardiovascular system. (From J. G. Creager, *Human Anatomy and Physiology*. Belmont, CA: Wadsworth Inc., 1983.)

1.7.3 Emotional Stress

Emotional stress usually affects the higher brain centers and may stimulate sympathetic nerve impulses. These impulses cause constriction of arterioles and increase arterial blood pressure [2]. Thus, emotional stress contributes to hypertension. Such impulses also cause constriction of veins, increased venous pressure, and increased venous return,

thereby increasing heart rate, stroke volume, and thus cardiac output. This sequence of results is those of the fight-or-flight effects of sympathetic stimulation.

However, depending on the response of the higher brain centers, a sudden emotional stimulus can cause effects opposite to those described above. The activity of the sympathetic nervous system is suddenly suppressed, and the blood vessels lose their tone. The arterial pressure decreases, the veins fail to constrict, and venous return is reduced. Heart rate and stroke volume decrease, and therefore so does cardiac output. Insufficient cardiac output is called shock. If the person is standing, the flow of blood to the brain is decreased, and fainting occurs. Since fainting places the person in a lying-down position, the act of fainting initiates the compensatory mechanisms of increasing blood flow to the brain.

1.8 Chronic Fatigue Syndrome

This study made use of data collected from Gulf War veterans with a healthy diagnosis, as well as from veterans diagnosed with chronic fatigue syndrome or idiopathic chronic fatigue. In order to provide a further understanding of this study, this section describes chronic fatigue syndrome, in terms of its definition, methods and criteria for diagnosis, and possible causes.

1.8.1 Definition of Chronic Fatigue Syndrome

According to the Centers for Disease Control and Prevention (CDC) (www.cdc.gov/ncidod/diseases/cfs), chronic fatigue syndrome, or CFS, is a debilitating and complex disorder characterized by profound fatigue that is not improved by bed rest

and that may be worsened by physical or mental activity, where fatigue is defined as “weariness from labor or exertion” [10]. Persons with CFS must often function at a substantially lower level of activity than they were capable of before the onset of illness. In addition to these key defining characteristics, patients report various nonspecific symptoms, including weakness, muscle pain, impaired memory and/or mental concentration, insomnia, and post-exertional fatigue lasting more than 24 hours. In some cases CFS can persist for years. The cause or causes of CFS have not been identified and no specific diagnostic tests are available. Moreover, since many illnesses have incapacitating fatigue as a symptom, care must be taken to exclude other known and often treatable conditions before a diagnosis of CFS is made.

Because the complexities of the chronic fatigue syndrome and the methodologic problems associated with its study, there was a need for a comprehensive, systematic, integrated approach to the evaluation, classification, and study of persons with this condition and other fatiguing illnesses [11]. In an effort to resolve the issues associated with CFS, an international panel of CFS research experts convened in 1994 to draft a definition of CFS that would be useful both to researchers studying the illness and to clinicians diagnosing it. Fukuda, et al., proposed a conceptual framework and a set of guidelines that provided a comprehensive approach to its definition and study [11]. Their guidelines include recommendations for the clinical evaluation of fatigued persons, a revised case definition of the chronic fatigue syndrome, and a strategy for subgrouping fatigued persons in formal investigations.

Prolonged fatigue is defined as a self-reported, persistent fatigue of 1 month or longer [11]. Chronic fatigue is defined as self-reported persistent or relapsing fatigue of

6 or more consecutive months. The presence of prolonged or chronic fatigue requires clinical evaluation to identify underlying or contributing conditions that require treatment. Further diagnosis or classification of chronic fatigue cases cannot be made without such an evaluation. If a patient has had 6 or more consecutive months of severe fatigue that is reported to be unrelieved by sufficient bed rest and that is accompanied by nonspecific symptoms, including flu-like symptoms, generalized pain, and memory problems, the physician should further investigate the possibility that the patient may have CFS.

1.8.2 Methods and Criteria for Diagnosis

According to the CDC method for diagnosis of CFS, the first step in this investigation is obtaining a detailed medical history and performing a thorough physical examination of the patient. This history should cover medical and psychosocial circumstances at the onset of fatigue, such as depression or other psychiatric disorders, episodes of medically unexplained symptoms, alcohol or other substance abuse, and current use of prescription and over-the-counter medications and food supplements [11]. Initial testing should include a mental status examination, which ordinarily will involve a short discussion in the office or a brief oral test. This mental status examination is meant to identify abnormalities in mood, intellectual function, memory, and personality. Particular attention should be directed toward current symptoms of depressive or anxiety, self-destructive thoughts, and observable signs such as psychomotor retardation. Evidence of psychiatric or neurologic disorder requires that an appropriate psychiatric, psychological, or neurologic evaluation be done. Finally, a standard series of laboratory tests of the

patient's blood and urine should be performed to help the physician identify other possible causes of illness. While the number and type of tests performed may vary from physician to physician, the following tests constitute a typical standard battery to exclude other causes of fatiguing illness: alanine aminotransferase (ALT), albumin, alkaline phosphatase (ALP), blood urea nitrogen (BUN), calcium, complete blood count, creatinine, electrolytes, erythrocyte sedimentation rate (ESR), globulin, glucose, phosphorus, thyroid stimulating hormone (TSH), total protein, transferrin saturation, and urinalysis. If test results suggest an alternative explanation for the patient's symptoms, further testing may be required to confirm a diagnosis for illness other than CFS. If no cause for the symptoms is identified, the physician may render a diagnosis of CFS if the other conditions of the case definition are met.

Conditions that exclude a patient from the diagnosis of unexplained chronic fatigue, and thus from CFS, include the following: (1) any active medical condition that may explain the presence of chronic fatigue, such as untreated hypothyroidism, sleep apnea and narcolepsy, and the side effects of medication, (2) any previously diagnosed medical condition whose resolution has not been documented beyond reasonable clinical doubt and whose continued activity may explain the chronic fatiguing illness, such as previously treated malignancies and unresolved cases of hepatitis B or C virus infection, (3) any past or current diagnosis of a major depressive disorder with psychotic or melancholic features, such as bipolar affective disorders, schizophrenia of any subtype, delusional disorders of any subtype, dementias of any subtype, anorexia nervosa, or bulimia nervosa, (4) alcohol or other substance abuse within 2 years prior to the onset of the chronic fatigue and any time afterward, (5) severe obesity as defined by a body mass

index equal to or greater than 45, where body mass index=(weight in kilograms)/(2 x height in meters) [11]. Any unexplained physical examination finding or laboratory imaging test abnormality that strongly suggests the presence of an exclusionary condition must be resolved before further classification.

On the contrary, the following conditions do not exclude a patient from the diagnosis of unexplained chronic fatigue: (1) any condition defined primarily by symptoms that cannot be confirmed by diagnostic laboratory tests, including fibromyalgia, anxiety disorders, somatoform disorders, nonpsychotic or nonmelancholic depression, neurasthenia, and multiple chemical sensitivity disorder, (2) any condition under specific treatment sufficient to alleviate all symptoms related to that condition for which the adequacy of treatment has been documented, such as asthma in which the adequacy of treatment has been determined by pulmonary function and other testing, (3) any condition, such as lyme disease or syphilis, that was treated with definitive therapy before development of chronic symptomatic sequelae, (4) any isolated and unexplained physical examination finding, or laboratory or imaging test abnormality that is insufficient to strongly suggest the existence of an exclusionary condition [11].

After thorough clinical evaluation based on the methods of diagnosis and the conditions above, unexplained chronic fatigue cases can be separated into either the chronic fatigue syndrome or idiopathic chronic fatigue. A diagnosis of chronic fatigue syndrome is defined by satisfaction of the following CDC-established criteria: (1) the presence of severe chronic fatigue of 6 months or longer duration with other known medical conditions excluded by clinical diagnosis; and (2) the concurrent existence of four or more of the following symptoms, all of which must have persisted or recurred

during 6 or more consecutive months of illness and must not have predated the fatigue: substantial impairment in short-term memory or concentration; sore throat; tender lymph nodes; muscle or severity; unrefreshing sleep; and post-exertional malaise lasting more than 24 hours. However, a diagnosis of idiopathic chronic fatigue is defined as clinically evaluated, unexplained chronic fatigue that fails to meet criteria for the chronic fatigue syndrome [11], "idiopathic" denoting a disease of unknown cause.

1.8.3 Possible Causes of CFS

Despite the many studies performed, the cause or causes of CFS remain unknown. While a single cause for CFS may yet be identified, another possibility is that CFS represents a common endpoint of disease resulting from multiple precipitating causes. However, there is no evidence to support the view that CFS is a contagious disease. Conditions that have been proposed to trigger the development of CFS include virus infection or other transient traumatic conditions, stress, and toxins. Several studies have shown that Persian Gulf War veterans report more symptoms of chronic fatigue than nonveterans. In a study performed by Reeves, et al., an illness that closely resembles CFS and to a lesser extent post-traumatic stress disorder (PTSD) was identified and was 4-16 times more common among Gulf War veterans. Illness rates for nonveterans were similar to those for civilian populations. Other than deployment to the Persian Gulf, there were no unique risk factors. According to Haley, the popular view that general life stress plays an important causal role in chronic illnesses, such as chronic fatigue syndrome, is a theoretical and popular concept but is not supported by the preponderance of scientific evidence [13].

PTSD is officially recognized as a condition caused by a specific traumatic experience [13]. A definitive diagnosis of chronic PTSD requires that all six of the following features be present: (1) occurrence of a specific, severely stressful event beyond ordinary life experiences, (2) intrusive thoughts of re-experiencing the event, i.e. "flashbacks", (3) persistent avoidance of reminder stimuli, (4) symptoms of increased arousal which may interfere with cognition and other mental and physical functions, (5) persistence for more than one month, and (6) impairment of general functioning [13]. The definitive diagnosis of PTSD is made from a psychiatrist's or psychologist's clinical interview, usually following a structured interview technique such as the Structured Clinical Interview for DSM-IV or the Clinician-Administered PTSD Scale. Various psychometric scales, calculated from symptom questionnaires filled out by patients, are used in conjunction with definitive clinical interviews, but these are not considered diagnostic per se. Rational scales (i.e., those calculated from questions that ask directly about the symptoms of PTSD) include the Mississippi Scale for Combat-Related PTSD, the Impact of Event Scale, and the PTSD questionnaire for DSM-IV criteria.

CHAPTER 2

HEART RATE VARIABILITY

2.1 Introduction

Assessment of the autonomic system has been researched for over a decade. This chapter will serve to introduce the different methods of analysis of heart rate variability as a means to assess autonomic activity.

2.2 Methods of HRV Analysis

The autonomic nervous system activity may be extracted from the variations in heart rate by a number of methods; however, the two major approaches to HRV analysis utilized in this study include: (1) Frequency Domain (Power Spectrum) Analysis, and (2) Time-Frequency Analysis.

2.2.1 Frequency Domain (Power Spectrum) Analysis

Power spectrum analysis decomposes the heart rate variability signal into its frequency components and quantifies them in terms of their relative intensity, or power [5]. This analysis provides the basic information of how power (variance) distributes as a function of frequency [6]. Independent of the method used, only an estimate of the true power spectral density of the signal can be obtained by proper mathematical algorithms; i.e. each mathematical algorithm does not yield an actual value of the power spectral density of a signal, but only an estimate.

The heart rate power spectrum can be analyzed in two major ways: (1) Fast Fourier transformation and (2) autoregressive model estimation, which are generally classified as nonparametric and parametric methods, respectively [5, 6]. As was utilized in this study, Fast Fourier transformation (FFT) spectra are characterized by discrete peaks for the several frequency components. The advantages of such nonparametric methods include the simplicity of the algorithm used (i.e. FFT), and the high processing speed [6]. On the other hand, the autoregressive (AR) method results in a continuous smooth spectrum of activity [5]. The advantages of this parametric method are smoother spectral components that can be distinguished independent of preselected frequency bands, easy postprocessing of the spectrum with an automatic calculation of low and high frequency power components with an easy identification of the central frequency of each component, and an accurate estimation of the power spectral density, even on a small number of samples on which the signal is supposed to maintain stationarity [6].

The Fourier transform is a signal processing technique that is used to represent a function in the time domain as a function within the frequency domain [15]. It does this by representing the components of a non-periodic signal as a sum of complex exponentials or sinusoids. The following is the equation for the Fourier transform:

$$X(\omega) = \int_{-\infty}^{\infty} x(t)e^{-j\omega t} dt \quad (2.1)$$

where $X(\omega)$ represents the Fourier transform time function of $x(t)$, and $e^{-j\omega t}$ represents the complex exponentials or sinusoids that make up the signal. Essentially the Fast Fourier transform is a computer algorithm used to efficiently compute the discrete time equivalent of the continuous time Fourier transform [8]. Once the frequency domain

analysis is completed using the Fast Fourier transform, the frequency content of the power spectrum can be analyzed.

Three major frequency bands can be distinguished in a power spectrum, where each is generally associated with different systems that control heart rate and calculated from short-term recording of approximately 5 minutes (Figure 2.1).

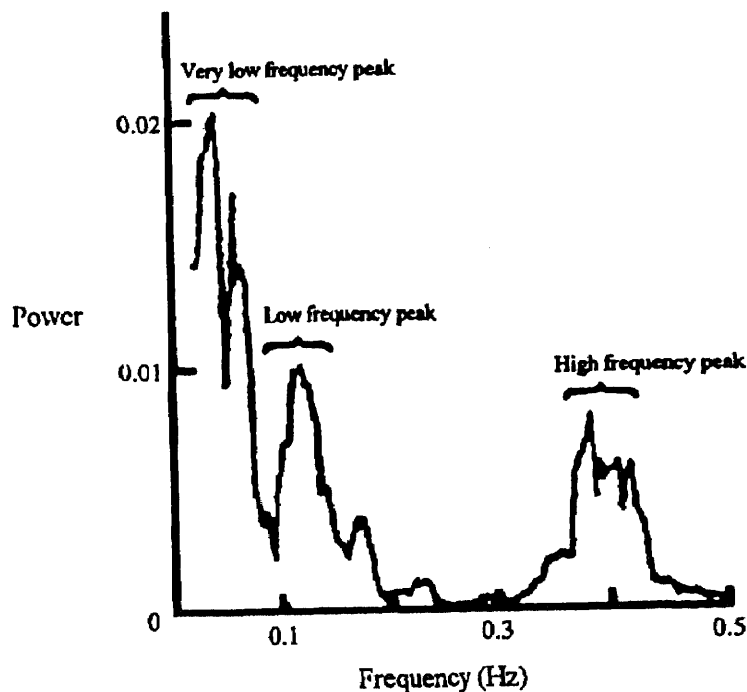


Figure 2.1 Frequency spectrum of an interbeat interval signal. (From M. V. Kamath and E. L. Fallen, "Power Spectral Analysis of Heart Rate Variability: A Noninvasive Signature of Cardiac Autonomic Function." *Clinical Reviews in Biomedical Engineering*, vol. 21, pp. 245-311, 1993.)

The high frequency (HF) band, ranging between 0.15 Hz and 0.4 Hz, is associated with parasympathetic activity [5, 7, 8] and is influenced by respiratory sinus arrhythmia [5, 7, 16, 17]. A predominant peak usually occurs at the respiration frequency [8]; therefore, depending on respiratory rate, the HF peak may not be within this HF range. For

example, the respiration peak may reside below 0.15 Hz for respiratory rates below 9 breaths per minute or above 0.4 Hz for rates above 24 breaths per minute [18]. Consequently, the HF range is not limited to 0.15-0.4 Hz because for respiration rates below 9 breaths per minute, the HF peak begins to move into the low frequency region.

The low frequency (LF) band ranges between 0.05 Hz and 0.15 Hz. According to Hojgaard, et al., this LF component is, to some extent, generated by baroreceptor modulation of sympathetic and vagal nervous tone [7]. It has been widely accepted that the low frequency band can serve as an indicator of both parasympathetic and sympathetic nervous system activity [5, 7, 8].

The third major frequency band that can be distinguished is the band of frequencies lying between 0.02 Hz and 0.05 Hz known as the very low frequency (VLF) band. The physiological origin of these very slow fluctuations is still to be determined; however, it has been suggested that variations in the activity of the renin-angiotensin system and thermoregulation are of importance [7, 8]. Because the physiological explanation of the VLF component is much less defined, the assessment of VLF from short-term recordings (i.e. approximately 5 minutes) is a precarious measure and should be avoided when power spectral analysis of short-term ECGs is interpreted [6].

Since the LF band is modulated by both parasympathetic and sympathetic activity, there is no frequency band in the power spectrum analysis of heart rate variability that yields a direct assessment of the sympathetic nervous system. As a result, an indirect measure has been established. The ratio of LF to HF power (LF/HF power ratio) may be considered to be a measure of sympathovagal balance, a conclusion supported by many experimental and clinical studies [5]. However, as is the case with

many other indirect physiological measures, there are limitations to the use of LF/HF as marker of autonomic balance [7]. Considering that the rationale for using LF/HF is that LF fluctuations are caused by the combined action of the sympathetic and the vagal nerves, whereas the HF fluctuations are caused mainly by vagal activity, it logically follows that the LF/HF ratio also depends on respiratory pattern [5].

The measurement of VLF, LF, and HF power components is usually made in absolute values of power (milliseconds squared) [6]. LF and HF may also be measured in normalized units, which represent the relative value of each power component in proportion to the total power minus the VLF component. The representation of LF and HF in normalized units emphasizes the controlled and balanced behavior of the two branches of the autonomic nervous system. Moreover, the normalization tends to minimize the effect of the changes in total power on the values of LF and HF components (Appendix A). Nevertheless, normalized units should always be quoted with absolute values of the LF and HF power in order to describe completely the distribution of power in spectral components.

2.2.2 Time-Frequency Analysis

Time-frequency analysis methods estimate the frequency content of a signal as a function of time and provide even more information for improved heart rate variability analysis [19]. Power spectral analyses assume that the signal to be analyzed is stationary over the entire period of the analysis, i.e. where the mean and autocorrelation do not change with time [8]. However, in many cases, the signal is not stationary; some researchers have even noted that the frequency content of the ECG waveform varies with time [19].

Sometimes it is the non-stationary nature of the signal during certain time periods that is of interest during a protocol. Time-frequency analysis provides a means for exhibiting the spectrum for non-stationary signals without distorting the resulting spectrum. It allows for a dynamic display of the spectral characteristics as opposed to a static display.

For example, consider a sine wave whose frequency varies with time (Figure 2.2A). By simply taking the FFT of the wave, the spectrum will clearly show that three frequencies are present (Figure 2.2B); however, it will not indicate any information on when the components were present, the duration of time for which the components were present, the sequence in which the components occurred, or whether they occurred simultaneously or individually. Notice that the waves shown in the figure contain the same frequencies, but each occurs at a different time. This time difference cannot be distinguished because both waves result in the same power spectrum. However, by analyzing through a time-frequency domain, the plots are quite different (Figure 2.2C), illustrating the contrast in signals both in time and frequency.

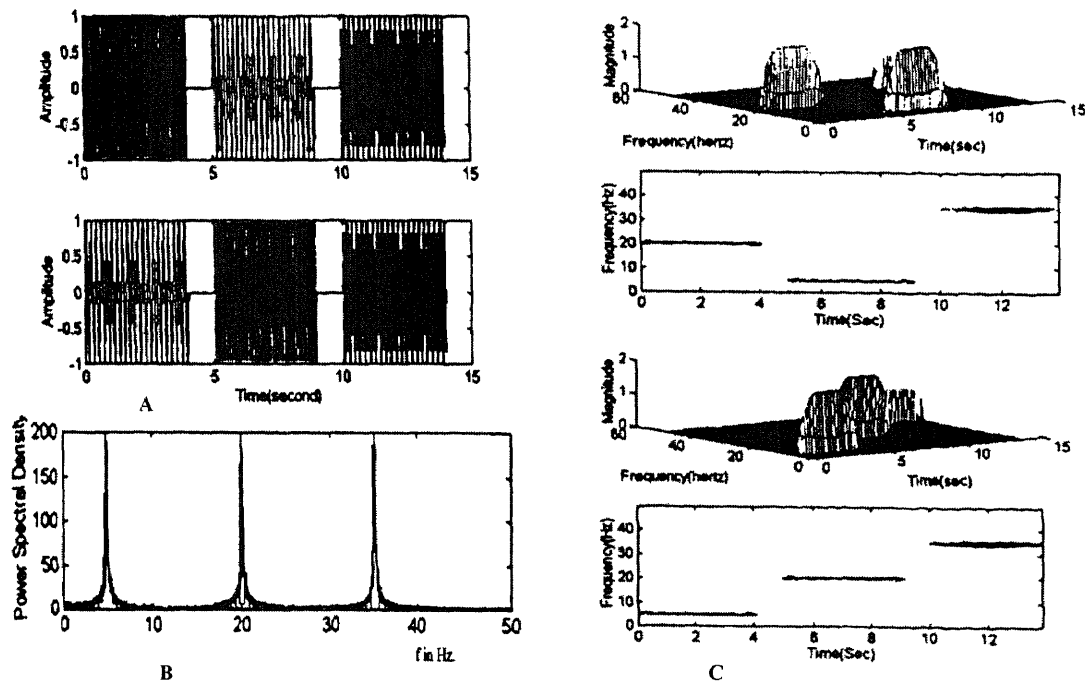


Figure 2.2 Illustration of how time-frequency analysis allows for a dynamic display of the spectral characteristics as opposed to a static display provided by power spectrum analysis. **A**, Two plots illustrating sine waves of three different frequencies present for different time intervals. **B**, Power spectrum for both plots in **A**. **C**, Time-frequency plots for the sine waves in **A**. (From S. Reisman, EE 667 Lecture Handout, ts. *New Jersey Institute of Technology*, Fall 1998.)

If the sine wave is windowed, or cut to a finite time, the spectrum widens in the frequency domain [8]. Therefore, there exists an inverse relationship between the length of a signal in the time domain and the width of the spectrum in the frequency domain. The greater the time localization of the signal, the less the frequency localization, and vice versa. The use of Fourier transform techniques is not feasible to localize a signal in both time and frequency. Though this limitation does not allow a localization in both time and frequency through the use of Fourier transform techniques, it can be overcome through the use of time-frequency analysis (Figure 2.3).

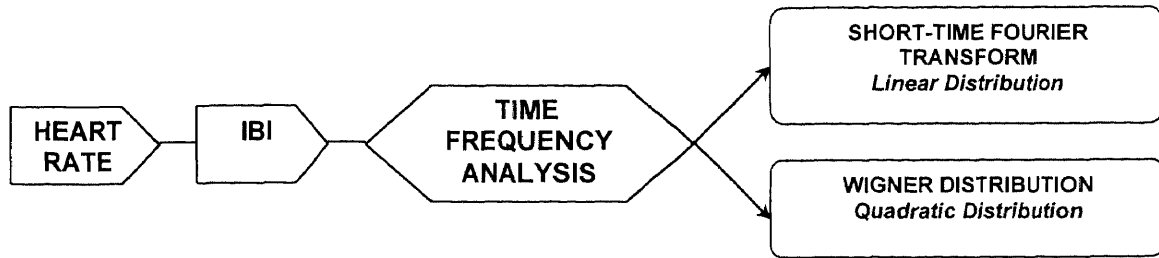


Figure 2.3 Flow-chart of time-frequency analysis methods.

When using the Fourier transform to separate the contents of the short window period into its frequency components, the short-time Fourier transform is used. The equation for the short-time Fourier transform is as follows [15]:

$$X_{st}(\omega) = \frac{1}{\sqrt{2\pi}} \int_{-\infty}^{\infty} e^{-j\omega\tau} x_{\tau}(\tau) d\tau \quad (2.2)$$

$X_{st}(\omega)$ represents the short-time Fourier transform as a function of frequency and $e^{-j\omega\tau}$ represents a set of complex exponential or sinusoidal functions. The function $x_{\tau}(\tau)$ represents $x(\tau)$ multiplied by the window function, $h(\tau)$ to give a weighted signal of width τ centered about time t . The equation for $x_{\tau}(\tau)$ is as follows:

$$x_{\tau}(\tau) = x(\tau)h(\tau) \quad (2.3)$$

However, when the short-time Fourier transform is used, frequency resolution is sacrificed for the sake of time resolution. This is attributable to the uncertainty principle because the window periods used are narrow about the point of interest, giving a wide spectrum.

The short-time Fourier transform can be considered as a linear distribution and possesses many shortcomings in the joint time-frequency analysis of a signal. In order to resolve this, a class of quadratic distributions was developed producing results with a comparably superior time-frequency resolution. The Wigner distribution, employed in

this study, was introduced by Wigner in 1932 for the purpose of quantum mechanics and later used for signal analysis by Ville in 1948 [8, 15, 20]. The distribution is expressed according to the following equation:

$$D_w(t, f) = \int_{-\infty}^{\infty} e^{-j2\pi f\tau} x^*\left(t - \frac{\tau}{2}\right) x\left(t + \frac{\tau}{2}\right) d\tau \quad (2.4)$$

where $D_w(t, f)$ represents the Wigner distribution, and $e^{j2\pi f\tau}$ represents a set of sinusoidal or complex exponential functions. In the above equation, the signal is shifted to the right by $\frac{\tau}{2}$ and then multiplied by the signal when shifted to the left by $\frac{\tau}{2}$. This is done for each time t to yield $x^*\left(t - \frac{\tau}{2}\right) x\left(t + \frac{\tau}{2}\right)$ as seen above. The Fourier transform is then taken of the signal $x^*\left(t - \frac{\tau}{2}\right) x\left(t + \frac{\tau}{2}\right)$ (note that $\int_{-\infty}^{\infty} e^{-j2\pi f\tau} d\tau$ represents the Fourier transform) to give us a result for the Wigner distribution. After the Wigner distribution is performed for each period along the IBI signal, the result is partitioned into its high and low frequency components to give us a high and low frequency point at each time t . This generates two time series of points representing the sum of all signals over time within the designated high and low frequency ranges.

In equation 2.3 on the previous page, the variables x and x^* represent an analytical signal and the complex conjugate of the analytic signal, respectively [21]. Under normal circumstances, the signals are real-valued. The spectrum of a real signal is always symmetric, i.e.

$$x(\omega) = x^*(\omega), \text{ or } |x(\omega)|^2 = |x(-\omega)|^2. \quad (2.5)$$

In this case, the negative frequency components of the spectrum, not only introduce redundancy, but also create cross-terms with the positive frequency components of the spectrum [21]. In order to reduce both the cross-term interference and the redundancy, the real signal needs to be converted to an analytic signal before using the Wigner distribution algorithm. An analytic signal of an original real signal is obtained by:

$$x(t) = x_{original}(t) + jx_{lm}(t) \quad (2.6)$$

where $x_{lm}(t)$ is the Hilbert transform of the original signal $x_{original}(t)$.

In addition to the generation of cross-terms, another disadvantage of the Wigner distribution is its behavior in noise. Noise that occurs at one time will appear in the Wigner distribution at other times (i.e. it is non-local) [8]. The noise will spread over larger time duration than in the original signal. Also, the distribution can become negative, and negative regions cannot be interpreted. Nevertheless, despite these disadvantages, the Wigner distribution possesses strengths that are very pertinent to time-frequency analysis. For example, the Wigner distribution not only provides a good picture of the time-frequency structure of a signal but can also calculate the instantaneous frequency precisely. In addition, the Wigner distribution reveals components in a multi-component signal.

CHAPTER 3

EXPERIMENTAL METHODS AND PROCEDURES

3.1 Introduction

The experimental protocol yielding the data utilized for this study was performed by Peckerman, et al., at the East Orange DVA Medical Center. The data signals acquired include ECG, blood pressure and respiration; however respiratory data was not used in this particular study [22].

This chapter presents the experimental protocol, including subject selection criteria, laboratory setup, and signal acquisition, as described by Peckerman, et al. [22].

3.2 Subject Selection

Fifty-one Gulf veterans with chronic fatigue (CF), labeled GCF, and 42 Gulf veterans without health complaints, labeled GHC, participated in the study. Diagnosis of CF was given if the veteran met CDC-established criteria for CFS or its slightly less severe form, idiopathic chronic fatigue (ICF) [11]. The initial recruitment phase consisted of a health survey conducted among enrollees of the Gulf War Registry established by the Department of Veterans' Affairs (DVA) Office. The survey was designed to identify ill Gulf veterans with health complaints consistent with CFS. Veterans fitting this profile on the paper-and-pencil instrument were invited to come to the East Orange DVA Medical Center for a 2-day study. Control subjects were recruited among survey respondents who gave no indications of war-related illnesses and were generally in good health. On site, evaluation included a comprehensive health and physical exam. On the basis of this

evaluation, the physician determined if the patient had CFS or ICF as defined by the 1994 case definition [11].

Briefly, the diagnosis of CFS requires a clinically corroborated substantial decrease in activity from pre-illness levels and four or more "minor" symptoms from a specified list for at least 6 months in duration. The 1994 CDC list of minor symptoms includes: problems with memory and concentration, muscle or joint pain, headache, unrefreshing sleep, sore throat, tender lymph nodes, and post-exertional malaise. In addition, for each minor symptom, a rating of severity was obtained by the medical examiner on a 0-5 scale, where 0 was none, 3 substantial and 5 very severe. The diagnosis of ICF was given if a patient fulfilled criteria for CFS, except had less than four symptoms from the 1994 case definition symptom list.

Veterans with medical and psychiatric illnesses listed in the 1994 CDC case definition [11] were not included in the study. As an additional safeguard against the possibility of occult medical disease, veterans older than 57 years of age were not invited to participate in the study. Psychiatric evaluation for post traumatic stress disorder (PTSD) was conducted using the Q-DIS, a computerized diagnostic interview for DSM-III-R Axis-I psychiatric disorders, which was conducted by a trained psychometrician under supervision of a Ph.D. level clinical psychologist. In addition, each veteran completed a version of the Mississippi Scale for combat related post-traumatic stress disorder (PTSD) adapted for use in GVs.

Veterans recruited as healthy control subjects underwent identical medical and psychiatric evaluations. None of the subjects included in the study disclosed a history of cardiovascular, respiratory, and neurological disorders, or used medications with central

or peripheral adrenergic activity. Clinically, the most prevalent (reported by more than 50% of ill veterans) symptoms from 1994 CDC minor list, that had severity ratings 3 or higher, were: neurocognitive (short-term memory and concentration) decline (74%), unrefreshing sleep (69%), and myalgia/arthralgia (57%). The mean (SE) self-reported reduction in activity was 47(3)%. The attributes of our sample, including clinical characteristics, and illness-related differences in rank and smoking rates were similar to what has been described in an epidemiological survey [11].

As a part of the health survey, each veteran entering the study filled out the Fort Devens Operation Desert Storm Reunion Survey form that included questions on exposures to environmental pollutants and peridostigmine bromide (anti-nerve gas prophylactic) during deployment.

The resulting sample populations for this study consist of twenty-five GCF subjects (Gulf veterans with chronic fatigue) and thirty-two GHC subjects (Gulf veterans without health complaints). A statistical analysis was performed with SAS System for Windows, Release 6.12, to assess whether the two sample means differ for the given level of statistical significance for the variables evaluated applicable to this study. The variables include gender, age, height, weight, and the level of light-headedness before standing and after standing. According to the results, there is no significant difference between the two groups for the variables evaluated, with the exception of the level of light-headedness after standing.

3.3 Protocol

Each veteran participated in an identical 2-day study protocol, with a minor exception described below. Clinical and diagnostic evaluation was performed on the first day, and laboratory testing was conducted on the second day. All laboratory testing was completed within a single uninterrupted 4-4.5-hour session in all but 8 subjects (7 controls, 1 CF) who participated in a similar but somewhat expanded protocol interrupted by a rest period. In this subgroup, autonomic assessment was conducted in the morning and behavioral stress testing was performed in the afternoon. In all other subjects, the study began with autonomic testing in the morning, and behavioral stress testing was completed in the early afternoon. All subjects were required to abstain from nicotine for 2 hours and from caffeine and related substances for a minimum of 4 hours prior to laboratory testing. The experimenter in contact with the subject was blind to the veteran's clinical status.

The testing session consisted of a series of autonomic and behavioral stress tests that took approximately 4 hours to complete. The autonomic testing protocol was performed first. It included a 2-minute period of paced breathing at 15 breaths per minute, a 2-minute deep breathing test at their vital capacity, at 6 breaths per minute, 5 minutes of active standing, and a Valsalva maneuver. The results of autonomic testing will be reported elsewhere. Reported in this study are data on equilibrated homeostatic adaptation to orthostatic stress. Measurements were taken in the supine, standing, and sitting postures, respectively. Supine data was collected during the last 2 minutes of a 10-minute period of quiet rest. Following that, the subject was asked to stand up quickly and remain standing still for 5 minutes. Recordings were made over the entire 5 minute

period. Measurements in the sitting posture were made during the last 5 minutes of a 20-minute rest period.

The behavioral stressors were administered in the sitting posture. They included an aversive sensory stressor, i.e. the forehead cold pressor test, and two cognitive stressors, i.e. simulated public speaking and mental arithmetic tasks. The aversive sensory stressor increases peripheral resistance and blood pressure and acts as a pain stimulus. This stressor yields information on the reflex of the thermoregulatory response and on vasomotor reactivity. The two cognitive stressors are mental stressors meant to yield a mixed cardiovascular response, including information on heart rate and blood pressure.

The cold pressor test was given first, and speech and arithmetic tasks were given next in a counterbalanced order. A 20-minute rest period preceded the cold pressor test and the speech-arithmetic series of stressors.

3.3.1 The Forehead Cold Pressor Test

A pliable plastic bag containing 4.5 cups of crushed ice and a half-cup of water (1 °C) was applied to the forehead for 2 minutes. During the test period, pain was rated on a 0 (no pain) to 10 (almost intolerable pain) scale at 5-second intervals in response to audio signals.

3.3.2 The Speech Task

The subject was provided with a scenario and was given 3 minutes to prepare and 3 minutes to deliver a speech about the situation into a video camera. The image of the

subject giving a speech was displayed on a monitor in the subject's field of vision. The subject was informed that the recording of the speech would be evaluated by a panel of judges on various aspects of content and delivery.

3.3.3 The Arithmetic Stressor

This task consisted of a series of 18 subtractions on pairs of 2-3 digit numbers delivered at 10-second intervals via an audiotape over a 3-minute period. Subtractions were performed against a background of audiovisual interference created by a daytime television talk show played in the subject's view at a loudness level matching the loudness level of the audiotape (≈ 70 dB). Ratings of perceived stress, challenge, threat, and control were obtained before and after each stressor, so that physiological responses to stressors could be normalized, if necessary, for differences in engagement.

3.4 Data Acquisition of Physiological Measurements

Blood pressure was recorded from the left arm using a Dinamap blood pressure monitor (Model 1846 SX). The Finapres device (Ohmeda, Model 2300) was used to record beat-by-beat blood pressure from a finger on the right hand. The Finapres measurements were used to track acute responses to autonomic probes. Respiration rate and tidal volume (not reported) were recorded using the Resptrace system (Ambulatory Monitoring), and end-tidal CO₂ levels were recorded using an infrared gas analyzer (Criticare POET).

Electrocardiogram was recorded in a modified Lead 1 or Lead 2 position dependent upon which yielded a better signal. ECG signals were obtained via disposable electrodes; no skin preparation was performed prior to electrode placement. The ECG as

well as the blood pressure data were scored, using LabVIEW graphical programming language, as will be described in detail in subsequent sections. Scoring the data involves detecting and marking each successive heart beat in order to obtain the heart rate variability of the respective physiological signal.

Two 30-second samples of the physiological signals mentioned above were collected at 1.5-minute intervals during the last 2 minutes of the supine, standing, and sitting rest periods, and two 30-second samples were obtained during the last 1.5 minutes of the 2- and 3-minute stressor periods. These measurements were averaged to represent the baseline and test response levels.

All data was initially recorded at 1000 Hz and was later resampled and reduced for analysis. The raw data was recorded and digitized using Data Translations' Global Lab, version 03.00. Both ECG and blood pressure data were reduced to 200 Hz and respiration data to 20 Hz. The data was exported as ASCII files through Global Lab in which form it could be further analyzed in LabVIEW.

3.5 Data Files

The data measurements pertinent to this study were obtained during the supine and standing positions of the protocol. The total duration of this series of events is approximately 7 minutes. The first 2 minutes of data consist of measurements acquired in the supine position, and the latter 5 minutes, consist of measurements acquired in the standing position, in addition to measurements obtained during the transition period from the supine to the standing position.

Each subject produced four raw data files: one file consisting of the raw ECG signal obtained during the supine position, one file consisting of the raw ECG signal obtained during the standing position, one file consisting of the raw respiratory signal obtained during both the supine position and the standing position, and one file consisting of the raw blood pressure signal also obtained during both the supine position and the standing position. Because this study was concerned with investigating the autonomic response during the transition period of the protocol, the two ECG files were combined into one data set prior to HRV analysis.

CHAPTER 4

ANALYSIS METHODS AND PROCEDURES

4.1 Introduction

All signal processing techniques were performed with LabVIEW graphical programming language. This chapter describes the use of LabVIEW in this study and the algorithms by which the different physiological signals were analyzed. All other calculations were executed with Microsoft Excel, and the results will be discussed.

4.2 LabVIEW

LabVIEW is a graphical programming language from National Instruments, used mostly in data acquisition and instrumentation control. LabVIEW is short for Laboratory Virtual Instrument Engineering Workbench [23]. In comparison to other programming languages, which involve typing the code, it is drawn with blocks; i.e. it relies on graphic symbols rather than textual language to describe programming actions. LabVIEW utilizes a graphical programming language, G, to create programs in a flowchart-like form called a block diagram, eliminating many the syntactical details. It provides the flexibility of a powerful programming language without the associated difficulty and complexity because its graphical programming methodology is inherently intuitive to scientists and engineers. LabVIEW applications vary widely and include data acquisition and control, data analysis, and data presentation. This study utilized LabVIEW version 4.0.1 to execute the Wigner time-frequency analysis and the power spectrum analysis of heart rate; in addition, version 5.1 was utilized to perform the power spectrum analysis of

blood pressure. This application of the different versions of LabVIEW is attributable to the availability of the respective versions at the time that each program was written.

LabVIEW programs are labeled virtual instruments (VIs) because their appearance and operation imitate actual instruments; however, they are analogous to main programs, functions, and subroutines of such programming languages as C or BASIC. VIs have both an interactive user interface and a source code equivalent where data can be passed between them. A VI has three main parts (Appendix B):

The front panel is the interactive user interface of a VI, so named because it may simulate the panel of a physical instrument.

The block diagram is the VI's source code constructed in LabVIEW's graphical programming language, G. The components of a block diagram, icons, represent lower-level VIs, built-in functions, and program control structures. Wires are drawn to connect the icons together, indicating the flow of data in the block diagram.

The icon and connector of a VI allow other VIs to pass data to the VI. The icon represents a VI in the block diagram of another VI. The connector defines the inputs and outputs of the VI. VIs are hierarchical and modular; therefore, they may be used as top-level programs, as subprograms within other programs, or even within other subprograms. A VI used within another VI, analogous to a subroutine, is called a subVI. Modular programming allows the execution of each subVI independently. This is very useful in that many low-level subVIs often perform tasks common to several applications and can be used independently by each individual application, as is the case in this study.

4.3 Wigner Time-Frequency Analysis

The Wigner time-frequency analysis program (Sympar.vi) consists of several subVIs that are connected (refer to Wigner Diagram, Appendix B). The time-frequency analysis was performed using raw ECG data. The ECG signal was read from a spreadsheet file (Read From Spreadsheet File.vi) as a single column of space delimited data. The data was filtered through a high-pass filter (HP_FILT.vi) after which point the R wave locations were detected automatically (Search BP.vi). The array of R wave locations was then used to calculate the heart rate and to generate graphs of both the ECG signal with detected R waves and of the heart rate, respectively, where the raw ECG signal appeared with markers at each corresponding detected R wave. These graphs appear on the control panel of the Correct.vi. It is in the Correct.vi block that a cursor is provided allowing the user to manually detect missing peaks or undetect "bad" peaks by turning the marker on or off, respectively. Missing peaks result due to saturation, motion, or noise during acquisition of the ECG signal; consequently, peaks must be manually interpolated in place of the missing data. "Bad" peaks consist of peaks that are not characteristically R waves, such as those generated by noise artifact. Manual detection of R waves continues until the switch created in the Correct.vi is turned off, indicating in the program that all detection of R waves is complete. The output of the Correct.vi consists of the IBI as calculated from consecutive R waves detected in the ECG which was then saved to a spreadsheet file to be utilized for further analysis, as will be discussed. The IBI was interpolated and decimated (Interpolation & Decimation.vi) to generate a decimated IIBI waveform which was analyzed utilizing the Wigner distribution (Symbar (Wigner).vi). The Wigner distribution is written in a MatLab program and incorporated into the VI.

After execution of the final subVI in this program, two-dimensional time-frequency graphs of both parasympathetic, or HF, activity and of the combined parasympathetic and sympathetic, or LF, activity were generated on the control panel of Symbar (Wigner).vi. The control panel also displayed graphs of the decimated IIBI waveform, as well as the LF/HF ratio with respect to time.

4.4 Power Spectrum Analysis of Heart Rate

The power spectrum analysis program (Energy Spectrum with No R-wave Detection.vi) consists of several subVIs that ultimately generate graphs of the LF area and HF area of the corresponding ECG signal (refer to Power Spectrum Diagram, Appendix B). As with the Wigner program, the signal is read from a spreadsheet file as a single column of space delimited data (Read From Spreadsheet File.vi); however, in this case the data consists of the previously recorded IBI of the heart rate obtained from the Correct.vi block in the Wigner time-frequency analysis program rather than the raw ECG signal. The use of the IBI array is justified because the subVIs utilized by the Wigner program to obtain this array are duplicated in the power spectrum analysis program; moreover, the sequence of data flow through these subVIs is identical in both programs. Therefore, it would follow that the IBI generated by the Wigner time-frequency analysis program is equivalent to that generated by the power spectrum analysis program. Essentially, the use of the previously generated IBI provides several benefits, such as saving time in the analysis process, and more importantly, it provides consistency in the data being analyzed. This factor is significant when considering the possibility of variation resulting during the manual interpolation of missing data in the ECG signal.

The IBI data flows through the Spectrum1.vi block where it is interpolated. Here, the IBI undergoes a series of analyses and mathematical calculations through subVIs that are provided by LabVIEW programming language. First, the IBI is inputted into the Mean.vi block, where the mean average is computed, and then the resulting output is zero padded (Zero Padder.vi). After this point, the power spectrum is computed and divided to display the graph of the heart rate power spectrum as well as the values of the LF area, the HF area, and the length of the data file in minutes. The graph and calculated data are displayed on the control panel of Energy Spectrum with No R-wave Detection.vi. Because of its interactive nature, the program allows for adjustment of sampling frequency as well as the upper and lower bounds for the VLF, LF, and HF ranges.

4.5 Power Spectrum Analysis of Blood Pressure

The power spectrum of the blood pressure (BP) signal is directly obtained from Energy Spectrum Using BP-NO Rwave Detection.vi. Again, the physiological signals are read from a spreadsheet file (Read From Spreadsheet File.vi) as two, consecutive, space delimited data columns, where one column consists of the IBI data obtained from the raw ECG signal and the other column consists of the raw blood pressure signal. Each signal is independently analyzed and displayed on the control panel of Energy Spectrum Using BP-NO Rwave Detection.vi (see Diagram, Appendix B). In this case, the heart rate is graphically displayed as both the raw ECG and the heart rate because the IBI is used in place of the raw ECG signal.

Similar to the raw ECG signal, the raw blood pressure signal passes through a high-pass filter (HP_FILT.vi) and successively into a peak detection block (Search

BP.vi). The filtered BP array is then analyzed for the detection of each systolic peak, or the R peak. Unlike the peak detection block for the ECG signal, the location of each consecutive peak is not directly detected, but rather it is the peak amplitude of the systolic blood pressure waveform, which is directly detected. It is the detection of the amplitude of each peak that indicates the peak location. The ECG waveform allows for easy detection of each R wave over time because it is characteristically the sharpest, most prominent peak. However, such is not the case with the blood pressure signal. Due to the smoother nature of the blood pressure waveform, several points at the maximum amplitude may occur over time, therefore making it very difficult to accurately assess the true location of the R peak in relation to the time at which it occurred. Consequently, because there is only one value for the maximum amplitude for each peak, this value is detected to indicate each R peak. In the event that multiple points occur at this maximum peak amplitude value, the first point in time that occurs is detected to indicate peak location.

The array of peak locations and the array of peak amplitude, both obtained from automatic detection, then flow into the Correct BP.vi block where the BP IBI is generated. Unfortunately, this block does not allow for the manual detection of peaks, and the resulting BP IBI is dependent solely on the accuracy and efficacy of the automatic detection by the program. Therefore missing data due to calibration of the Finapres cannot be manually interpolated and detected. The significance of this has not yet been determined.

However, the merits of manual interpolation may not be an issue when dealing with analysis of the blood pressure signal. Detection of the BP peak location is

dependent upon the maximum amplitude of the peak, i.e. the y-axis. The first maximum value of amplitude that occurs in the peak is detected. This value is then interpolated over the interval till the next successive peak amplitude is detected. Therefore, if there are several missing peaks in succession, such as during calibration, the last amplitude detected is automatically interpolated over this period of missing data till the next consecutive peak is detected. This means that the systolic blood pressure of the subject is kept constant for that period of interpolation over the missing data. Manual interpolation, therefore, would require estimating the systolic blood pressure of the subject at that given time. Because the systolic blood pressure does not fluctuate greatly due to homeostatic responses, it would be very difficult to predict the behavior of the blood pressure and estimate such a value. On the contrary, detection of R wave location in the ECG signal is directly dependant upon the time at which each heart beat occurs, i.e. the x-axis. The LabVIEW subVI that automatically scores the signals places a marker at the location of the peak with respect to the x-axis, or time. Consequently, it allows for manual detection along the x-axis. This function, however, is not feasible for manual detection of systolic blood pressure peaks. Thus, there may be more merit in not manually interpolating the missing peaks in the blood pressure signal, as they are accounted for during automatic interpolation of the IBI.

The BP IBI is then interpolated (Weighted Coherence HR-BP.vi) to generate the IIBI. Each peak amplitude value is interpolated over the period of time between each successive peak amplitude detection. For example, if the first peak in succession has an amplitude of 1.135, the next detected peak has an amplitude of 0.850, and there is a period of 200 points between the two detected peaks, then the value of the first detected

peak, or 1.135, is interpolated over the 200 points so that each point possesses this amplitude until the next detection at 0.850. The resulting array then undergoes a series of analyses and mathematical calculations, similarly to the heart rate IIBI, to graphically display the BP power spectrum. This graph in addition to graphs of the heart rate power spectrum, the raw BP signal, and the BP IBI are displayed on the control panel of the Energy Spectrum Using BP-NO Rwave Detection.vi. In addition to the graphical displays, the calculated values of the LF area, the HF area, and the length of the data file in minutes can be found on the control panel. Because of its interactive nature, the program allows for adjustment of sampling frequency as well as the upper and lower bounds for the VLF, LF, and HF ranges.

4.6 Preliminary Study

A preliminary study was performed on a sample of five subjects to determine whether blood pressure data scored using an automated software system, provided by the East Orange DVA Medical Center, could be utilized as opposed to the scored ECG data using LabVIEW to yield an accurate assessment of heart rate variability.

The data from this study came from the first five files available from the protocol records at the East Orange DVA Medical Center, including: GHC-AR, GHC-DU, GCF-JE, GHC-SD, and GHC-TR.

4.6.1 Introduction

The purpose of this preliminary study was to investigate whether or not there was a difference in the calculated heart rate variability generated from the two analysis

methods. The first method utilized the blood pressure data acquired during the steady-state supine position. The blood pressure signal was previously scored using an automated software system, provided by the East Orange DVA Medical Center, East Orange, NJ [22]. The second method utilized the raw ECG data acquired during the steady-state supine position. The ECG signal was scored using the LabVIEW program developed at the New Jersey Institute of Technology, Newark, NJ. The data acquired during the steady-state supine position was utilized in this preliminary study to reduce the possibility of error in detection of noise artifact or missing data that may occur due to standing. After each consecutive systolic peak and R wave was scored in the BP and ECG signals, respectively, the data was further analyzed with the power spectrum analysis program developed in LabVIEW.

The findings of this preliminary study would determine whether or not the scored blood pressure data could be used interchangeably with the scored ECG data. Several factors associated with the blood pressure signal were considered in this preliminary study, such as the possibility of long periods of undetected blood pressure data during calibration. In addition, the fact that there is a pulse transition time, i.e. the time delay between the detection of a systolic peak and the actual time of the associated heart beat was also considered in the analysis of the final results.

4.6.2 Findings of Preliminary Study

The power spectrum of the previously scored blood pressure signal varied greatly from that of the ECG signal scored in LabVIEW, as can be seen in the Figures 4.1 through 4.4 and also in Appendix C.

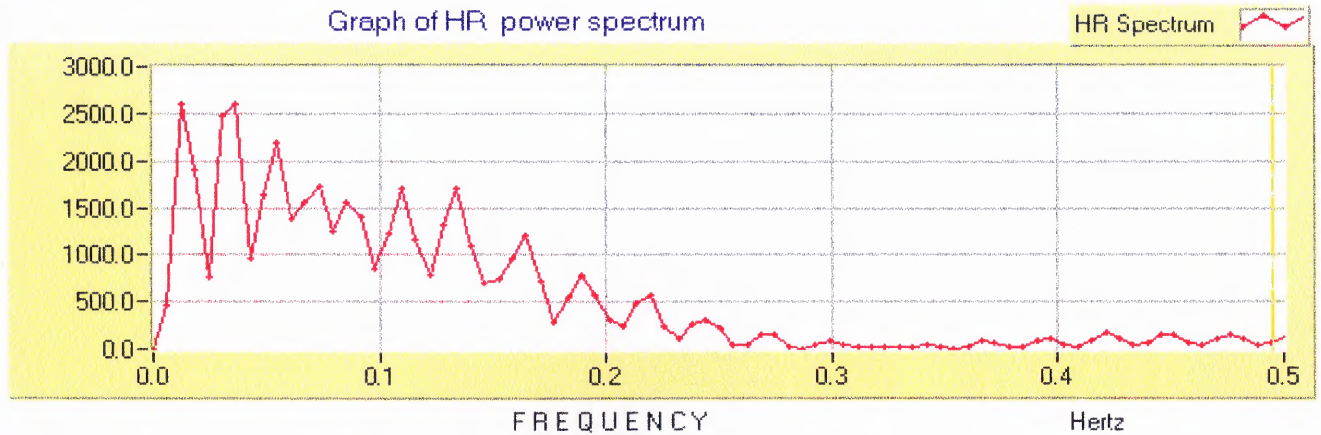


Figure 4.1 HRV Power spectrum using the BP signal, acquired in supine position. (Subject GHC-AR.)

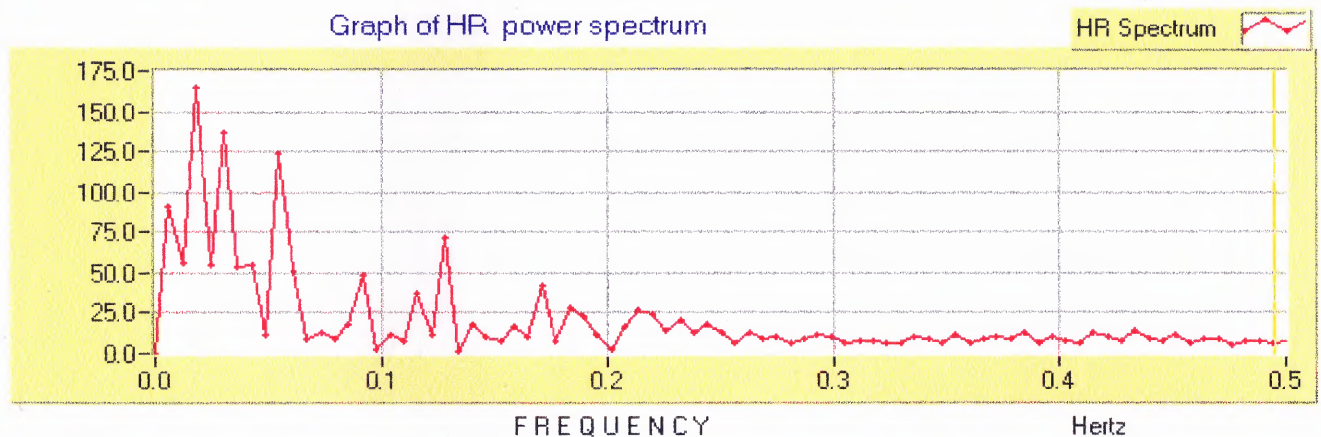


Figure 4.2 HRV Power spectrum using the ECG signal, acquired in supine position. (Subject GHC-AR.)

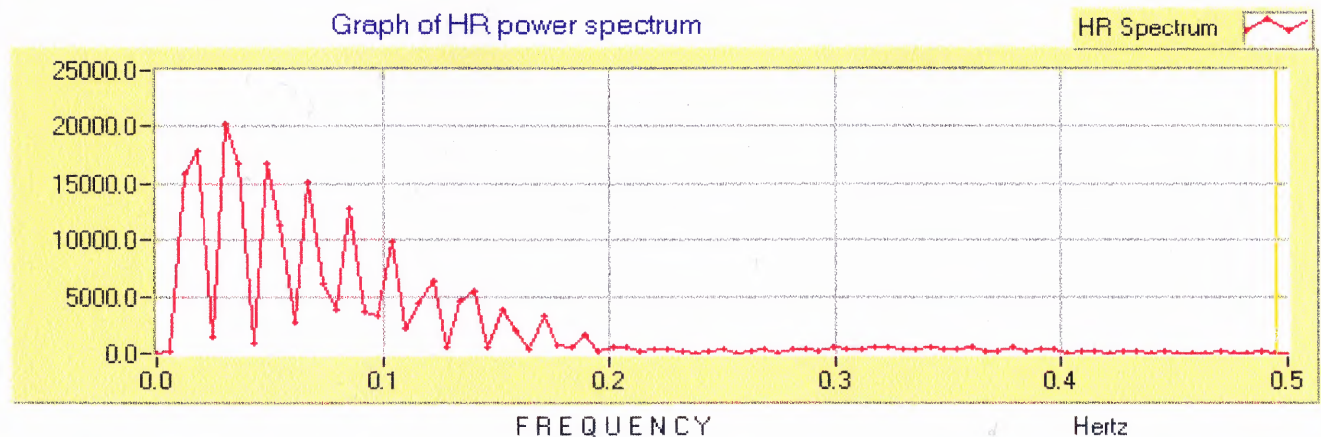


Figure 4.3 HRV Power spectrum using the BP signal, acquired in supine position. (Subject GHC-DU.)

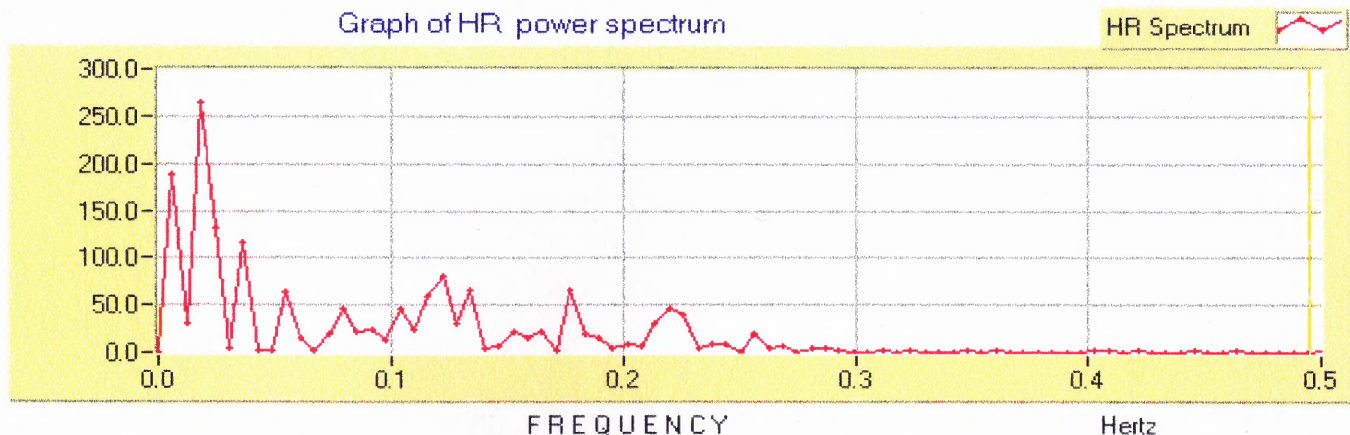


Figure 4.4 HRV Power spectrum using the ECG signal, acquired in supine position. (Subject GHC-DU.)

The power spectra of the ECG signal clearly show peaks which occur distinctly in the very low frequency, low frequency or high frequency regions; therefore the occurrence of various peaks can be attributed to some physiological function, such as respiration. Whereas the power spectra of the BP signal indicates sharp peaks that fluctuate in a periodic manner. The appearance of the power spectra generated by the BP signal is characteristic of that generated by a noise signal. A comparison of the LF/HF ratio calculated by the two methods also confirms that there is a difference in the calculated heart rate variability generated from the ECG analysis method and the BP analysis method (Table 4.1). Consequently, the great difference between the power spectra generated by the two signals led to further examination of both the data and the method of analysis.

Table 4.1 A comparison of the calculated heart rate variability generated from the two analysis methods utilized in the preliminary study.

A COMPARISON OF THE CALCULATED LF/HF RATIO BETWEEN ECG vs. BP ANALYSIS METHODS		
SUBJECT	LF/HF (ECG)	LF/HF (BP)
GHC-AR	0.89	2.40
GHC-DU	1.42	4.21
GCF-JE	1.35	4.89
GHC-SD	0.94	4.60
GHC-TR	3.83	3.51

Upon investigation of the scored blood pressure signal, it was discovered that periods of undetected data (Figure 4.5), caused by calibration of the Finapres, were extracted and considered as missing data. This in effect deletes the periods of time during calibration, which consequently leads to inaccurate results when carrying out an analysis where time is a variable.

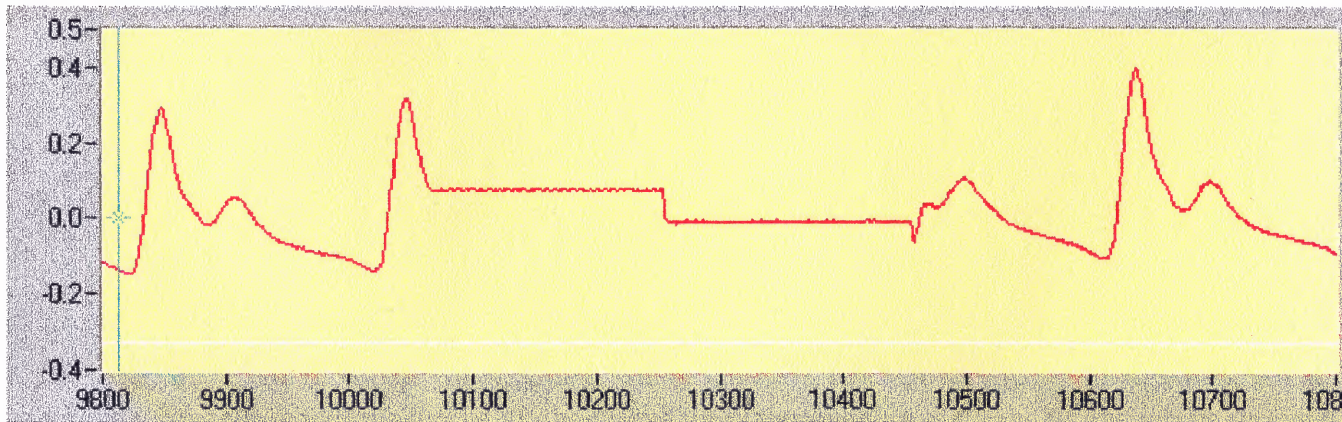


Figure 4.5 Blood pressure waveform as displayed in LabVIEW graphical programming language. The graphical display shows the period of undetected data during calibration of the Finapres. (Subject GHC-TR.)

It was also discovered that there is a major difference in the manner in which heart rate variability can be obtained via ECG versus blood pressure. This is due to the smoother nature of the blood pressure waveform, as opposed to the sharp R peaks of the

ECG waveform, as can be seen in Figures 4.6 and 4.7. The result is a frequent occurrence of repetitive maximum values in an individual systolic waveform.

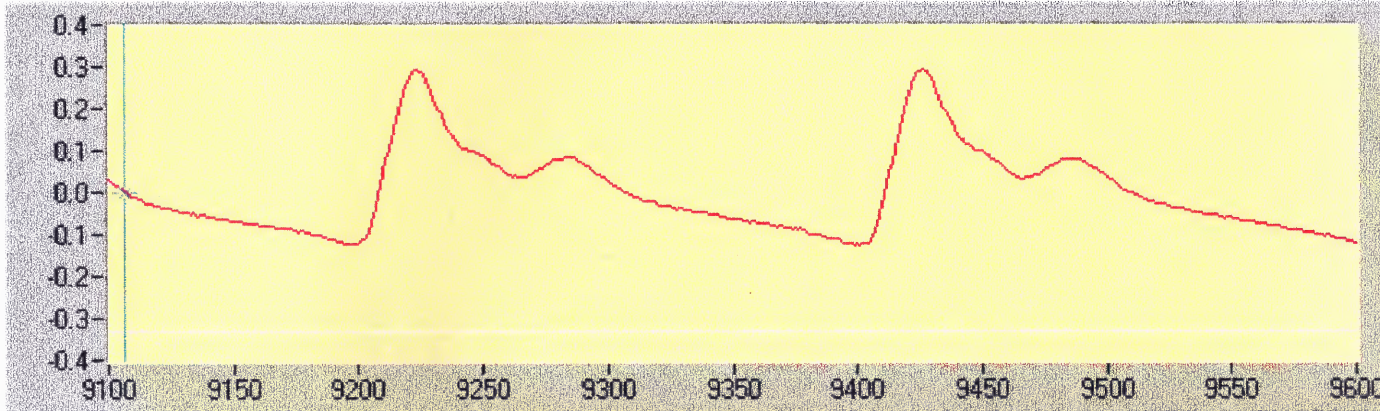


Figure 4.6 Blood pressure waveform as displayed in LabVIEW graphical programming language. The graphical display shows the smoother and more rounded systolic peaks. (Subject GHC-TR.)

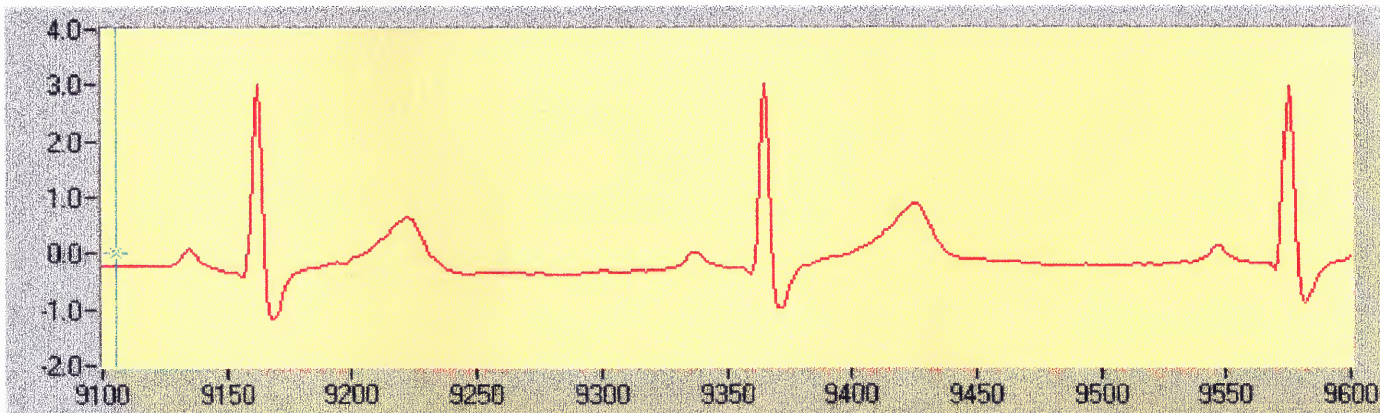


Figure 4.7 ECG waveform as displayed in LabVIEW graphical programming language. The graphical display shows the sharp distinct R peaks. (Subject GHC-TR.)

Although several points may occur at the maximum amplitude of the systolic blood pressure, there is only one value that repeatedly occurs at this maximum. In such an event that repetitive maximum values occur in an individual systolic waveform, the first occurring maximum value was detected. Consequently, the analysis of the BP signal

cannot be carried out in the same manner as the ECG signal. Therefore, the scored BP cannot be used interchangeably with the scored ECG to calculate heart rate variability using the given power spectrum analysis program.

4.6.3 Conclusions of Preliminary Study

This preliminary study provided evidence supporting the conclusions that there is a difference in the calculated heart rate variability generated from the two physiological signals and that the blood pressure data scored using an automated software system, provided by the East Orange DVA Medical Center could not be used interchangeably with the ECG data scored using the LabVIEW program developed at the New Jersey Institute of Technology.

Finally, a recent study by Carrasco, et al., was carried out comparing heart rate variability parameters obtained from the electrocardiogram and the blood pressure wave during several experimental conditions, including a supine position and a standing position [24]. According to their results, values of heart rate provided by the Finapres are not completely interchangeable with those obtained from the ECG during the standing position.

4.7 Limitations of Data Analysis

As with any study, the scope of this study was limited by the capabilities of both the data acquisition and their respective data analysis methods and tools.

The ECG data used in this study included periods of noise, misdetecting beats, movement, as well as missing data due to saturation of the curve. Studies indicate that

ectopic beats, arrhythmic events, missing data, and noise effects may alter the estimation of the power spectral density of HRV (using the ECG signal) [6]. However, proper interpolation (or linear regression or similar algorithms) on preceding and successive beats on the HRV signal may decrease this error. Preferentially, short-term recordings (approximately 5 minutes) that are free of ectopy, missing data, and noise should be used. Subjects that had significant periods of unusable data (i.e. consecutive periods of 30 seconds or more), were excluded from this research because the estimated occurrence of each interpolated beat in time would influence the outcome of the time-frequency analysis, where time is a variable. However, acceptance of short-term recordings where only short periods were interpolated may introduce significant selection bias. In such cases, certain undetected factors may have warranted exclusion of the subject, and the possibility of the final results being influenced by this exclusion should be considered.

Also, in spectral analysis, the number of outlying beats can present problems; if necessary, the outliers are to be removed without influencing the results to a great extent, again, by interpolating between the preceding and following intervals of the outlier [25]. Regardless, ECG recordings should be made with care, so as to minimize noise, artifacts, hum and related measuring problems. In addition, the ECG equipment used should satisfy the current voluntary industrial standards in terms of signal-to-noise ratio, common mode rejection, bandwidth, and so forth [6].

The blood pressure signal also contained frequent short periods of missing data followed by several undetected peaks, both of which are attributable to the calibration function of the Finapres. Due to the nature of peak detection and interpolation in the program for power spectrum analysis of blood pressure, missing data and undetected

peaks could not be manually detected nor manually interpolated. However, because time-frequency analysis was not performed on the blood pressure signal, time was, therefore, not a variable in this case. Consequently, subjects were not excluded based on the amount of missing data in the blood pressure signal, but those with significantly large periods of missing data were noted. Since missing data and noise effects may alter the estimation of the power spectral density of HRV when using the ECG signal, it may similarly follow that such events also alter the estimation of the power spectral density of HRV when using the blood pressure signal. Therefore, the Finapres should remain active after the first 10 minutes allowing it to stabilize after which point the servo-reset (calibration) mechanism should be disabled to permit continuous collection of cardiac beats [26]. By doing so, periods of missing data followed by undetected beats can be eliminated.

4.8 Statistical Analysis of Data

The statistical analysis was performed to describe the relationships between the GHC group and the GCF group using the acquired blood pressure and ECG signals to generate the heart rate variability. It was also performed to describe the relationships between the different methods used in this study to assess heart rate variability, namely the LF/HF ratios calculated from the blood pressure variability and heart rate variability, respectively, in addition to the $LF_{(BP)}/HF_{(ECG)}$ ratio. The statistical analysis deals with inferences about the true nature of the relationships between variables, even though the data include errors, and also offers an efficient means to describe and summarize data. Consequently, it provides measures of the relationships and observations made.

The statistical hypothesis, called a null hypothesis, specifies that the sample means are the same and that any observed difference between sample means is merely the product of sampling error. In this case, the t test was performed to test for equivalence between means of the various sample groups.

The t distribution is based upon the assumption that samples have been drawn from normally distributed populations, and that these populations have the same variance [29]. In fact, the t test is fairly robust. This means that even if the proper assumptions cannot be met exactly, the probability of obtaining significant t 's under the null hypothesis will still be quite close to the confidence levels (p) given in a table of critical values for t for the specified degree of freedom (df).

In order to use the t distribution, the assumption is made that the populations from which the samples come have equal variances. This assumption is used when combining the sum of squares and degrees of freedom from each sample into one common estimate of the population variance. This estimate is then used to determine the estimated standard error of the difference between means ($S_{\bar{X}_1 - \bar{X}_2}$):

$$S_{\bar{X}_1 - \bar{X}_2} = \sqrt{\frac{\sum X_1^2 - \frac{(\sum X_1)^2}{n_1} + \sum X_2^2 - \frac{(\sum X_2)^2}{n_2}}{n_1 + n_2 - 2} \left(\frac{n_1 + n_2}{n_1 n_2} \right)} \quad (4.1)$$

where X is the value of each observation, \bar{X} is the sample mean, and n is the number of observations constituting a sample.

The interest lies in testing whether or not the difference between two sample means is significantly different from zero, or that the two means are the same. Therefore, t is given as the ratio of the difference between sample differences and hypothesized

population mean differences, divided by the estimated standard error of the sample mean differences, having $(n_1 + n_2 - 2)$ *df*:

$$t = \left(\frac{\bar{X}_1 - \bar{X}_2}{S_{\bar{X}_1 - \bar{X}_2}} \right). \quad (4.2)$$

However, if the populations seem to have unequal variances, which can be determined by performing tests for the significance of the difference between sample variances, then there are some special modifications of the *t* test which should be used.

First, if the population variances are unequal, the sums of squares and degrees of freedom from both samples should not be combined to arrive at a common estimate of the population variance. Under these circumstances, $(S_{\bar{X}_1 - \bar{X}_2})$ should be calculated as follows:

$$S_{\bar{X}_1 - \bar{X}_2} = \sqrt{\frac{S_1}{n_1} + \frac{S_2}{n_2}} \quad (4.3)$$

where *S* is an estimate of the standard deviation derived from a sample of *n* observations.

Second, there is a change in the procedure for determining the *t* required for any given level of significance. The required *t* cannot be obtained directly from a *t* table; it must be calculated from the following formula which is an approximation. When the population variances are assumed to be unequal, the *t* needed for significance is given by the formula below:

$$t = \frac{t_1 \frac{S_1^2}{n_1} + t_2 \frac{S_2^2}{n_2}}{\frac{S_1^2}{n_1} + \frac{S_2^2}{n_2}} \quad (4.4)$$

where $t_{1,2}$ are taken directly from the t table and are the values of t required for significance at the level set by the experimenter; t_1 is the t required for $(n_1 - 1)$ df , and t_2 is the t required for $(n_2 - 1)$ df .

Another t test should be utilized when some reasonable basis exists for matching subjects [30]. In this case, it is usually advantageous to make use of the matched pairs t test because matching subjects, or using the same subject as his/her own control, usually results in a fairly high correlation between the two sets of scores on the dependent variable which reduces the variability of the difference (D) scores; this consequently reduces the estimated standard error of the mean of paired difference scores ($S_{\bar{D}}$). The reduction in $S_{\bar{D}}$ means that the distribution of the sample mean differences will cluster more tightly about the sample mean difference and this increases the power of the t test. This matched t test for correlated measures calculates t for the specified $(n - 1)$ df in a different manner.

Assume that a sample of paired scores has been extracted from this population and that by subtracting the second score from the first, a difference score, D , is obtained. The sample of difference scores obtained will have a sample mean, \bar{D} , and can consequently be used to provide an estimate of the standard deviation, S_D , in the sample population of difference scores. Therefore the estimated standard error of this sampling distribution which takes this correlation into account is given by:

$$S_{\bar{D}} = \sqrt{S_{D_1}^2 + S_{D_2}^2 - 2rS_{D_1}S_{D_2}} \quad (4.5)$$

where r is the correlation coefficient calculated with the following formula:

$$r = \frac{\sum X_1 X_2 - \bar{X}_1 \bar{X}_2}{n S_1 S_2} \quad (4.6)$$

The t ratio for correlated measures is given by:

$$t = \frac{\bar{D}}{S_{\bar{D}}} \quad (4.7)$$

CHAPTER 5

RESULTS AND DISCUSSION OF ANALYSES

5.1 Introduction

This chapter will present and discuss the findings of this research in comparison to findings from previous studies.

5.2 Observations and Results of Time-Frequency Analysis

The Wigner time-frequency graphs clearly indicate several consistent features that occur both in the Gulf veterans with chronic fatigue, labeled GCF, and the Gulf veterans without health complaints, labeled GHC, as can be seen in Figures D-GHC-BS, D-GHC-JR, and D-GHC-LL vs. D-GCF-AY, D-GCF-JB, and D-GCF-JA of Appendix D. A prominent peak occurs in both the graph of parasympathetic activity (HF), as well as the graph of the combined parasympathetic and sympathetic activity (LF), at the transition period from the supine to standing position for all the subjects tested. The maximum amplitude of this prominent peak is consistently greater in the LF region than in the HF region. The period following the transition peak, i.e. the standing period, also yields a greater amplitude in the LF region in comparison to the HF region. The period before the transition peak, i.e. the supine period, indicates amplitudes and peaks that, on average, are visually similar and consistent between both graphs. A significant difference between the GCF group versus the GHC group is not clearly apparent and requires a more mathematical analysis that should be approached in future work on this study.

5.3 Observations and Results of Power Spectrum Analysis

The power spectrum analyses performed on the ECG and blood pressure signals, respectively, yielded the low frequency and high frequency areas of each. These components were then used to calculate the different low frequency to high frequency ratios, as discussed sections 2.3.1 and 2.4. Several typical HRV power spectrum curves obtained utilizing the ECG signal and the blood pressure signal can be seen in Appendix D and Appendix E, respectively. The individual subject data, including averages, standard deviations, and variances of each component, is summarized in Table 5.1 below.

Table 5.1 Summary of data obtained from power spectrum analyses.

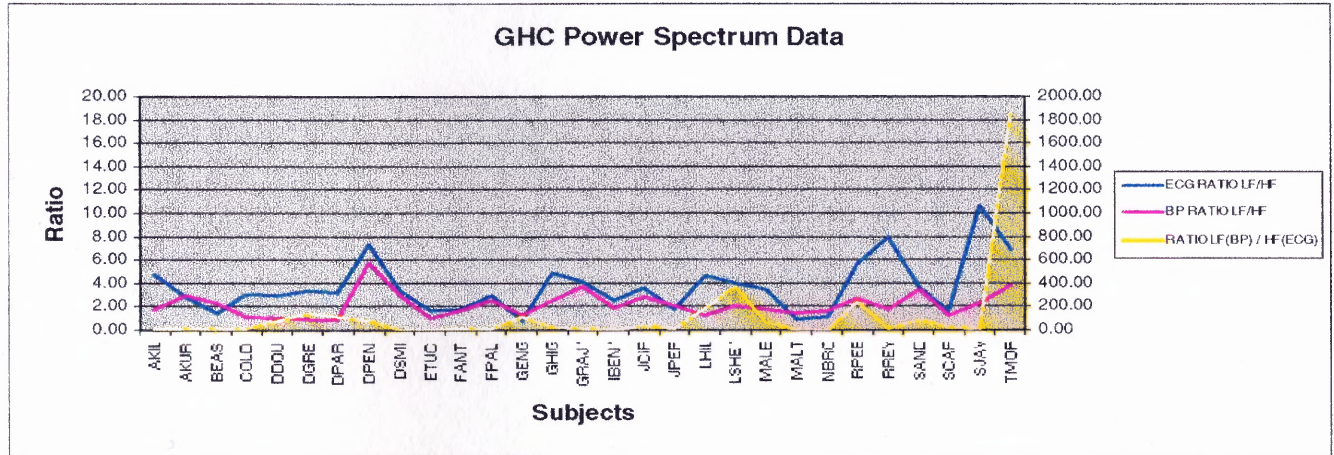
POWER SPECTRUM ANALYSIS								
Combined Files								
SUBJECT		ECG SIGNAL		BP SIGNAL		ECG RATIO	BP RATIO	RATIO
GHC		HF area	LF area	HF area	LF area	LF/HF	LF/HF	LF(BP) / HF(ECG)
GHC-AL	AB	67.26	323.30	683.71	1204.68	4.81	1.76	17.91
GHC-AR	AB	174.21	481.90	757.92	2196.01	2.77	2.90	12.61
GHC-BS	AB	482.12	702.15	2337.00	5322.21	1.46	2.28	11.04
GHC-CD	BS	46.98	145.10	530.45	644.46	3.09	1.21	13.72
GHC-DU	AB	236.51	705.34	19066.45	19620.81	2.98	1.03	82.96
GHC-DE	AB	28.68	93.93	4521.92	4150.71	3.28	0.92	144.72
GHC-DR	AB	21.94	71.03	2720.86	2605.00	3.24	0.96	118.73
GHC-DN	AB	179.11	1298.44	2482.70	14479.50	7.25	5.83	80.84
GHC-DI	AB	202.22	662.32	315.98	934.00	3.28	2.96	4.62
GHC-EC	AB	180.74	305.83	301.66	314.57	1.69	1.04	1.74
GHC-FT	AB	137.51	243.70	1408.41	2292.64	1.77	1.63	16.67
GHC-FL	AB	239.53	710.73	683.12	1712.34	2.97	2.51	7.15
GHC-GE	AB	107.12	87.66	8957.77	11942.26	0.82	1.33	111.48
GHC-GI	AB	148.35	719.99	1717.53	4357.40	4.85	2.54	29.37
GHC-GJ *	AB	114.70	472.70	490.80	1854.30	4.12	3.78	16.17
GHC-IN *	AB	58.47	152.17	38.37	73.17	2.60	1.91	1.25
GHC-JP	BS	482.21	1716.29	6577.29	18344.80	3.56	2.79	38.04
GHC-JR	AB	246.91	435.86	1122.97	2244.96	1.77	2.00	9.09
GHC-LL	AB	65.50	302.63	9477.63	12441.33	4.62	1.31	189.94
GHC-LE *	AB	159.11	629.51	29326.84	59668.22	3.96	2.03	375.01
GHC-MB	BS	302.17	1034.52	12064.11	21152.76	3.42	1.75	70.00
GHC-MT	AB	990.98	852.58	1687.21	2295.71	0.86	1.36	2.32
GHC-NO	AB	184.51	217.36	130.95	218.11	1.18	1.67	1.18

Table 5.1 (Continued) Summary of data obtained from power spectrum analyses.

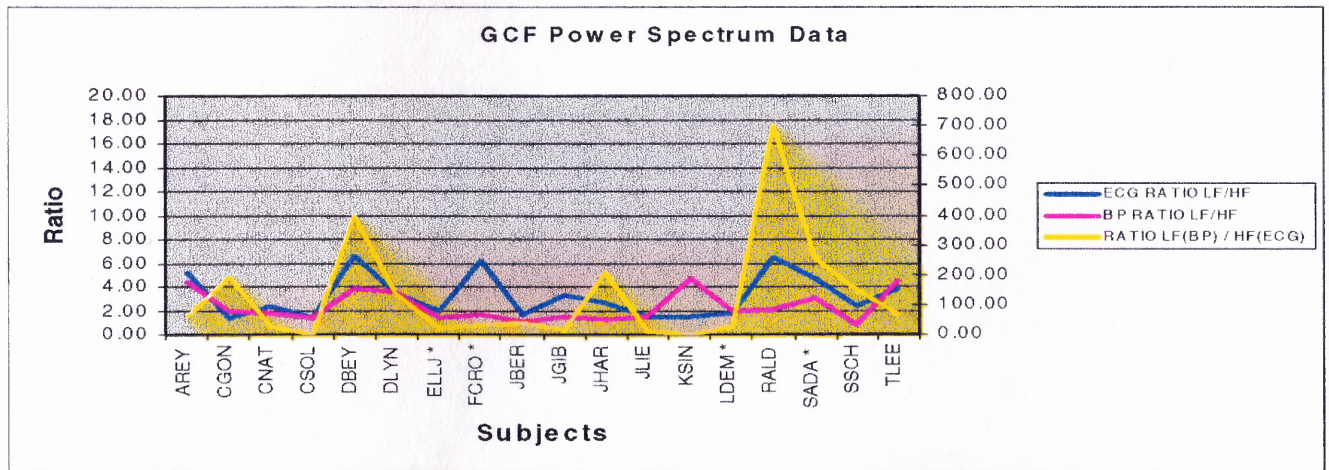
GHC-RE	BS	275.29	1566.07	23919.81	65534.37	5.69	2.74	238.06
GHC-RY	BS	96.27	762.39	699.67	1264.02	7.92	1.81	13.13
GHC-SD	AB	146.17	531.51	4049.93	13918.01	3.64	3.44	95.22
GHC-SR	BS	174.69	295.49	3653.52	4615.21	1.69	1.26	26.42
GHC-SV	BS	78.71	839.80	380.71	858.82	10.67	2.26	10.91
GHC-TR	AB	52.07	357.89	25043.31	96823.24	6.87	3.87	1859.48
AVERAGE		195.86	576.49	5694.78	12864.95	3.68	2.17	124.13
STD. DEV.		191.10	421.92	8286.06	22697.09	2.27	1.09	344.54
VARIANCE		36520.01	178018.60	6.866E+07	5.152E+08	5.15	1.18	118709.38
POWER SPECTRUM ANALYSIS								
Combined Files								
SUBJECT		ECG SIGNAL		BP SIGNAL		ECG RATIO	BP RATIO	RATIO
GCF		HF area	LF area	HF area	LF area	LF/HF	LF/HF	LF(BP) / HF(ECG)
GCF-AY	AB	75.14	394.22	1030.81	4551.12	5.25	4.42	60.57
GCF-CN	AB	98.03	135.71	9527.70	19026.32	1.38	2.00	194.09
GCF-CT	AB	199.44	479.17	3258.14	5745.16	2.40	1.76	28.81
GCF-CL	AB	1028.98	1447.92	473.14	683.24	1.41	1.44	0.66
GCF-DY	AB	129.68	859.22	13315.52	51380.86	6.63	3.86	396.21
GCF-DN	AB	379.13	1297.69	14773.73	52938.12	3.42	3.58	139.63
GCF-EJ *	AB	168.84	327.83	2604.20	3634.19	1.94	1.40	21.52
GCF-FO *	AB	128.69	793.37	2626.42	4170.58	6.16	1.59	32.41
GCF-JE	AB	335.22	567.49	10899.85	12027.14	1.69	1.10	35.88
GCF-JB	AB	62.73	204.56	752.58	1151.58	3.26	1.53	18.36
GCF-JA	AB	55.59	142.45	9421.46	11546.58	2.56	1.23	207.71
GCF-JI	AB	527.92	777.76	3225.45	4840.16	1.47	1.50	9.17
GCF-KN	AB	280.82	428.18	111.40	528.42	1.52	4.74	1.88
GCF-LM *	AB	158.89	283.46	2146.02	4158.99	1.78	1.94	26.18
GCF-RD	AB	66.18	430.59	21614.95	46198.75	6.51	2.14	698.08
GCF-SA *	AB	309.79	1458.70	26293.95	78367.03	4.71	2.98	252.97
GCF-SH	BS	73.50	171.44	13412.47	11071.14	2.33	0.83	150.63
GCF-TE	AB	151.42	584.04	2270.05	10194.13	3.86	4.49	67.32
AVERAGE		235.00	599.10	7653.21	17900.75	3.24	2.36	130.11
STD. DEV.		237.18	429.43	7762.73	22937.09	1.85	1.29	178.14
VARIANCE		56252.61	184410.76	6.026E+07	5.261E+08	3.43	1.66	31734.78
<i>* Notes patients possessing significantly large periods of missing data in their particular blood pressure signals.</i>								

Before the statistical analysis was performed on this data, the three ratios for each subject group were compared graphically to display patterns or trends between each. The graphs in Figure 5.1 A and B visually indicate that there is a greater similarity in the shape and fluctuations of the peaks between the ratios (i.e. the ECG ratio (LF/HF), the BP ratio

(LF/HF), and the new ratio ($LF_{(BP)}/HF_{(ECG)}$) obtained from the GHC group than between the respective ratios obtained from the GCF group. The rise and fall of the peaks of each ratio correspond more often in the GHC group than in the GCF group.



A

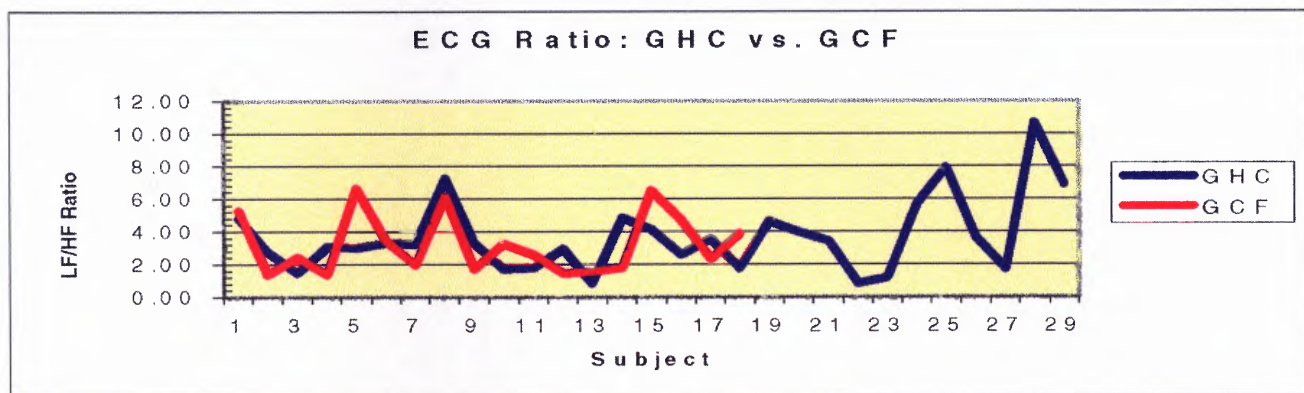


B

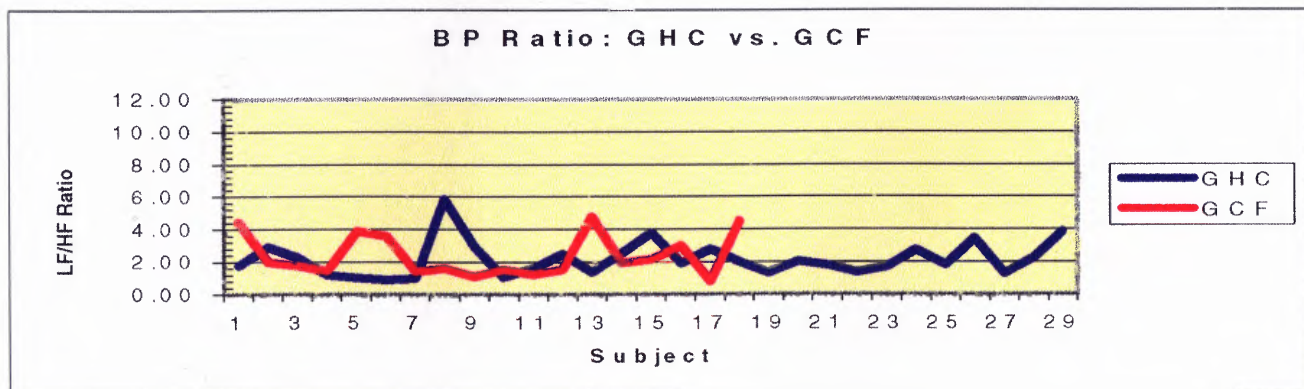
Figure 5.1 A, Graphical comparison between the ECG ratio (LF/HF), the BP ratio (LF/HF), and the new ratio ($LF_{(BP)}/HF_{(ECG)}$) as calculated from the GHC group. **B**, Graphical comparison between the ECG ratio (LF/HF), the BP ratio (LF/HF), and the new ratio ($LF_{(BP)}/HF_{(ECG)}$) as calculated from the GCF group.

Notice the greater similarity between the curves of the GHC power spectrum data than the GCF power spectrum data.

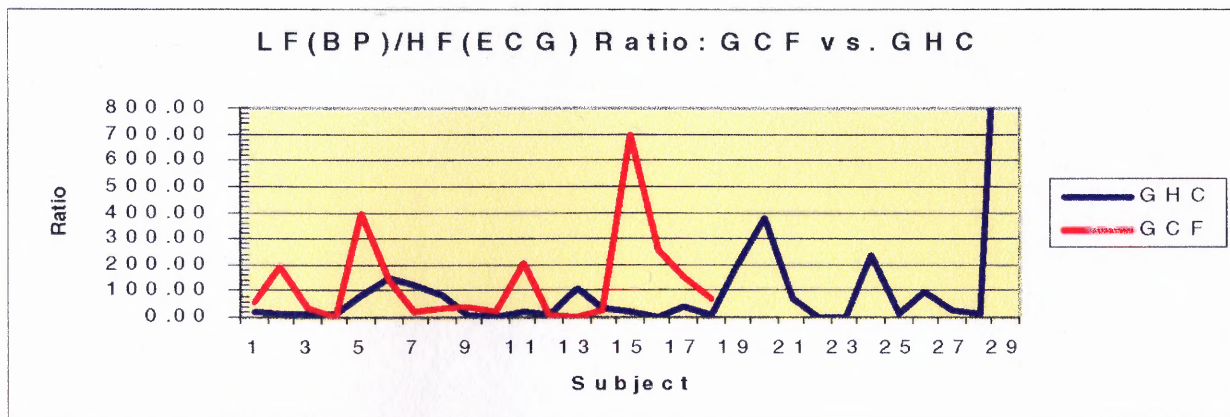
In addition, the appearance of the graphs comparing the GHC group versus the GCF group indicate that there may be a possible direct relationship between the ECG ratio of the two groups (Figure 5.2A); whereas there may be a possible inverse relationship between the $LF_{(BP)}/HF_{(ECG)}$ ratio of the two groups (Figure 5.2B). Finally, the appearance of the graphs indicate that there may possibly be no relationship between the BP ratio of the two groups (Figure 5.2C). These assumptions, however, have not been confirmed mathematically and are based upon the indicated peaks in the graphs.



A



B



C

Figure 5.2 Graphical displays of the three different calculated ratios showing comparison between the GHC group vs. the GCF group. **A**, Graphical comparison of the calculated ECG LF/HF ratio. **B**, Graphical comparison of the calculated BP LF/HF ratio. **C**, Graphical comparison of the calculated $LF_{(BP)}/HF_{(ECG)}$ ratio.

In addition to a graphical comparison, the percent difference between each measure was calculated and can be found in Table 5.2 below.

Table 5.2 Comparison of average percent difference between GHC subjects vs. GCF subjects based on data obtained from power spectrum analyses.

AVERAGE PERCENT DIFFERENCE BETWEEN GHC SUBJECTS vs. GCF SUBJECTS							
	ECG SIGNAL		BP SIGNAL		ECG RATIO	BP RATIO	RATIO
	HF area	LF area	HF area	LF area	LF/HF	LF/HF	$LF(BP) / HF(ECG)$
AVERAGE	-19.98	-3.92	-34.39	-39.14	12.06	-8.98	-4.82
STD. DEV.	-24.11	-1.78	6.32	-1.06	18.35	-18.54	48.30
VARIANCE	-54.03	-3.59	12.23	-2.13	33.32	-40.51	73.27

NOTE: A negative percent difference indicates that the GCF values are on average greater than the GHC values.

Although the difference between the averages of the $LF_{(BP)}/HF_{(ECG)}$ ratio of the GHC and the GCF group, respectively, is much greater than the differences between the averages of the other calculated ratios, the percentages indicate otherwise. Conversely, the percent difference between the HF area of the BP signal and the LF area of the BP signal appear

to be significantly large. In order to confirm these conjectures, t tests were performed on the data. The various LF/HF ratios calculated were tested for equivalence of the means between various sample groups utilizing the appropriate t test; the corresponding t test was based upon the assumptions required of the two sample groups being tested.

Several two-tailed t tests were performed at a 5% significance level using the data outlined in the table above. The t tests selected for each comparison took into account the assumptions being made. For example, in a comparison between the $LF_{(BP)}/HF_{(ECG)}$ ratio of the GHC subjects versus that of the GCF subjects, there was a significant difference between their respective variances, therefore warranting use of the modified t test. The assumptions and equations for each of the t tests employed are described in section 4.7.

The aim was to test the hypothesis that the sample population means are equivalent for the sample groups being compared. Rejecting this hypothesis would indicate that the difference between these sample means is significant at the 5% level. A summary of the hypothesis tests is outlined in Table 5.3 below.

Table 5.3 Summary of t tests comparing equivalence of means of the ratios between the two sample groups.

SUMMARY OF t TESTS PERFORMED BETWEEN SAMPLE GROUPS				
COMPARISON	SAMPLE GROUP 1	SAMPLE GROUP 2	t STATISTIC FOR GIVEN df	t VALUE TO TEST SIGNIFICANCE ($p < .05$)
<i>ECG RATIO vs. ECG RATIO</i>	GHC SUBJECTS	GCF SUBJECTS	0.7252	1.95996
<i>BP RATIO vs. BP RATIO</i>	GHC SUBJECTS	GCF SUBJECTS	0.5212	1.95996
<i>LF(BP)/HF(ECG) RATIO vs. LF(BP)/HF(ECG) RATIO</i>	GHC SUBJECTS	GCF SUBJECTS	0.0781	2.06396
<i>ECG RATIO vs. BP RATIO</i>	GHC SUBJECTS	GHC SUBJECTS	0.7424	2.048

Table 5.3 (Continued) Summary of t tests comparing equivalence of means of the ratios between the two sample groups.

ECG RATIO vs. LF(BP)/HF(ECG) RATIO	GHC SUBJECTS	GHC SUBJECTS	0.6890	2.048
BP RATIO vs. LF(BP)/HF(ECG) RATIO	GHC SUBJECTS	GHC SUBJECTS	0.2803	2.048
ECG RATIO vs. BP RATIO	GCF SUBJECTS	GCF SUBJECTS	0.4754	2.110
ECG RATIO vs. LF(BP)/HF(ECG) RATIO	GCF SUBJECTS	GCF SUBJECTS	1.170	2.110
BP RATIO vs. LF(BP)/HF(ECG) RATIO	GCF SUBJECTS	GCF SUBJECTS	0.5034	2.110
* NOTE: WHEN COMPARED WITH OTHER RATIOS, THE LF(BP)/HF(ECG) RATIO WAS REDUCED BY A FACTOR OF 100 IN ORDER TO COMPENSATE FOR THE DIFFERENCE IN UNITS OBTAINED DUE TO THE DIFFERENT METHODS OF ANALYSES.				

Testing the significance of a difference between means indicates how probable the obtained sample mean difference is on the basis of sampling error alone, when no mean difference exists between the populations being sampled [29]. If the sample mean difference is highly improbable on the basis of sampling error, the null hypothesis that sampling error alone was responsible, can be rejected. This permits acceptance of the alternative hypothesis that the difference between the sample means was the result of sampling from populations with different means.

By applying these principles to this study, if the t value for significance at the 5% level is greater than the t statistic obtained for a given df , the null hypothesis that the two samples have come from populations with the same mean, is accepted. Contrarily, if the t value for significance at the 5% level is less than the t statistic obtained for a given df , the null hypothesis is rejected, and the alternative hypothesis is found true and is thus accepted.

The statistical data indicates that the t statistic required for significance at the 5% level is much greater than the t value obtained for the given df ; therefore, the hypothesis

that the two samples have come from the populations with the same mean cannot be rejected at the .05 level of confidence. Such is the case for all the t tests performed comparing the different ratios between the sample groups.

5.4 Discussion of Results

An upright posture causes translocation of approximately 800mL of blood from the intrathoracic venous compartment to veins of the buttocks, pelvis and legs [31]. The normal compensatory cardiovascular response to this orthostatic stress is a neurogenically mediated increase in heart rate and in systemic vascular resistance.

A previous study conducted by Streeten, et al., drew attention to the possibility that fatigue and exhaustion in some patients with the CFS might be attributable to failure to maintain blood pressure in the erect posture [32]. This factor is evident in the large percent differences between the GCF and GHC groups (Table 5.3) in both low and high frequency areas of the blood pressure signal.

Yataco, et al., compared heart rate variability in patients with chronic fatigue syndrome and controls [33]. The findings of their study demonstrate that autonomic function, assessed using an analysis of heart rate and heart rate variability, does not differ in the baseline state, nor in response to upright tilt testing among patients with chronic fatigue syndrome and normal controls. In each of their patient groups, upright tilt resulted in a similar increase in mean heart rate, decrease in HF power, and increase in LF power consistent with a withdrawal of parasympathetic tone and increased sympathetic tone. Similarly, studies have shown that the standing position, where a high sympathetic tone is present, yields an amplification in the LF power and small but

insignificant fall in the HF power [16, 34]. Although the LF/HF power ratio has been considered an indirect measure of sympathetic activity, it may have been of no significance in this study. Hojgaard, et al., quote a recent study by Hoshikawa and Yamamoto confirming that in settings with high sympathetic tone, but without specific enhancements of LF fluctuations in the sympathetic nerves, the LF/HF ratio is not expected to be useful in assessing autonomic balance [7].

In an effort to find an index that enhanced the diagnosis of postural tachycardia syndromes (POTS), Novak, et al., proposed the use of $LF_{(BP)}/HF_{(ECG)}$ to provide a dynamic estimate of autonomic (sympathovagal) balance [27, 28]. POTS is defined by the combination of orthostatic tachycardia and symptoms of orthostatic intolerance. Novak, et al., reason that while the HF obtained from the ECG RR intervals (RRI), is a valid index of cardiovagal function, the commonly used approach of using RRI variability in the low frequency band as the index of sympathetic function is problematic since it receives both sympathetic and cardiovagal contributions [27, 28]. Therefore, the substitution of the LF obtained from systolic blood pressure for LF obtained from the heart rate results in a more valid sympathetic numerator. It follows that because low frequency powers in blood pressure reflect sympathetic vasomotor drive, and high frequency powers in ECG RRI reflect cardiovagal efferent activity, it is possible to define an index of sympathovagal balance as a ratio of the LF in systolic blood pressure/HF in the heart rate, i.e. $LF_{(BP)}/HF_{(ECG)}$ [27, 28].

According to Novak, et al., the new index is more sensitive than the conventional ratio. The main finding of their study is that it is possible to detect, using the novel approach of Wigner distribution time-frequency analysis of resting and tilt-induced

alterations in BP and heart rate, the presence of autonomic dysfunction and failure, in a subset of patients with orthostatic intolerance [27, 28]. In a comparison of this new index with the commonly used ratio of LF/HF of heart rate (obtained from ECG), the commonly used ratio did not distinguish a group with mild orthostatic intolerance (MOI) from the POTS group during rest or during head-up tilt. In addition, it failed to distinguish MOI from control subjects during supine rest or at the head-up tilt [28]. However, the new index was markedly increased in patients with POTS; and in patients with MOI, it was not significantly different from that in control subjects. In patients with POTS, the sympathovagal index was increased during supine rest and markedly increased during head-up tilt [28].

Their results show that this ratio ($LF_{(BP)}/HF_{(ECG)}$) is a much more reliable index of autonomic (sympathovagal) balance than the commonly used LF/HF ratio obtained from the ECG signal [27, 28]. The commonly used ratio has limitations that contribute to its low sensitivity and specificity, namely (1) spectral powers at low and high frequencies are determined within fixed frequency ranges regardless of the actual respiratory rate, and (2) spectral power at low frequency is not a pure index of the sympathetic cardiac activity. In contrast to the low sensitivity and specificity of the LF/HF ratio, the use of the $LF_{(BP)}/HF_{(ECG)}$ consistently demonstrated sympathovagal imbalance in patients with POTS [28]. This finding is significant to this study because a possible association between CFS and POTS has been suggested due to the presence of common symptoms in both syndromes, including orthostatic intolerance [35, 31]. Therefore, the new index may also provide a better descriptor of dynamic sympathovagal estimate in CFS subjects than the LF/HF ratio.

However, the results of this study were not similar to the findings of studies performed by Novak, et al. There was no significant difference ($p < .05$) between the new index and the conventional ratios, calculated from both the systolic blood pressure and the heart rate, respectively, neither in the GHC group nor in the GCF group. There was also no significant difference ($p < .05$) between the each of the different ratios in a comparison between the GHC and GCF groups. Both the new index and the conventional ratios failed to distinguish the autonomic imbalance in subjects with chronic fatigue syndrome from that in healthy control subjects. However, our study did not have the advantage that Novak, et al., included in their study [28]. The new index, as utilized by Novak, et al., allowed for the oscillations in the heart rate to be explicitly defined and detected according to the actual breathing frequency. This factor should be considered in further work on this study.

Although heart rate variability has been widely used to assess autonomic tone, several recent studies have demonstrated that factors other than the level of parasympathetic and sympathetic tone may affect heart rate variability parameters. The findings of the Yataco study suggest that if an abnormality of autonomic tone is present in patients with chronic fatigue syndrome, it cannot be detected reliably using an analysis of heart rate variability. It also appeared unlikely that heart rate variability will emerge as a useful non-invasive diagnostic tool in subjects with chronic fatigue syndrome [33]. Yataco also concluded that autonomic function, as assessed using an analysis of heart rate variability does not differ (in the baseline supine state, nor in response to upright tilt) among patients with chronic fatigue syndrome and healthy controls. The research presented in this study also concludes that there was no significant difference in the

analysis of heart rate variability between Gulf War veterans with chronic fatigue syndrome and healthy controls.

CHAPTER 6

CONCLUSIONS

6.1 Introduction

A summary of the results from the analyses performed in this study will be presented in this chapter. In addition, suggestions for future work on this study, as well as the clinical relevance of future studies in heart rate variability, will be proposed in this chapter.

6.2 Summary of Results

Different methods of heart rate variability analysis, including time-frequency analysis and power spectral analysis, were used to assess the autonomic system activity of Gulf War veterans with chronic fatigue syndrome versus Gulf War veterans with a healthy diagnosis. The data utilized includes the ECG signal and blood pressure signal acquired during a period in the supine position into the standing position. A statistical analysis using the *t* test was performed comparing the different ratios between the two sample groups. The null hypothesis was rejected at the .05 level of confidence for all the comparisons performed (Table 5.3). The statistical analysis conclusively shows that there is no significant difference in the heart rate variability as well as in the sympathetic activity between Gulf War veterans diagnosed with chronic fatigue syndrome and those diagnosed as healthy. In addition, there is apparently no significant difference between the ratios that serve as a measure of sympathetic activity.

6.3 Future Research

Heart rate variability is a possible quantitative marker of autonomic activity and has been provided as a tool for both research and clinical studies. The areas for future work on the study presented in this thesis, as well as the possible clinical relevance of heart rate variability as a diagnostic and prognostic tool will be addressed in the following section.

6.3.1 Suggestions for Future Work on this Study

A rigorous statistical analysis should be performed on the results of the time-frequency analysis of the experimental data presented. This may be executed by evaluating second order polynomial regression lines in comparison to linear regression lines drawn through areas of interest. Correlation coefficients may also be used to compare the variables of interest.

There are many other sources of technical error with the potential for distorting the power spectrum that need to be minimized or eliminated as much as possible by careful selection of artifact-free data, proper replacement of missing data, and optimal methods of analysis. Therefore, data acquisition should be performed with great caution so as to avoid noise artifact and missing data both in the ECG signal and the blood pressure signal.

Further investigation of interpolation techniques are needed to determine the most accurate method of interpolating missing heart rate and systolic blood pressure data. Although interpolation of missing data was carried out in this study, the degree of error incurred by such a technique and the final effect on the resulting power spectrum are not known.

The limitations of the power spectrum analysis of blood pressure program may have also incurred an error in the final result. This program detects systolic peaks based on the maximum value for the amplitude of each peak; on the contrary, the power spectrum analysis program of heart rate detects the occurrence of each R wave with respect to time. Therefore, the locations of missing R waves can be interpolated because it is the average time of each peak that is being estimated; however, the average amplitude of each missing systolic peak cannot be interpolated because it is the actual systolic blood pressure measurement that would be estimated. This limitation can be eliminated by acquiring a continuous blood pressure signal.

Further studies should be performed taking into consideration respiration in conjunction with heart rate and blood pressure. This study was also limited due to the lack of a data analysis tool to accurately generate the respiratory frequencies in the respiratory signal. All three data signals should be analyzed by using time-frequency mapping based on the Wigner distribution, which provides a good estimate for short nonstationary time series, as well as by frequency domain methods. Cross-Wigner distributions should be computed between respiratory and RR interval and blood pressure signals to determine spectral powers at actual respiratory frequencies at any moment in time. As previously described, respiratory frequency oscillations during slow breathing may encroach into the spectral estimates at nonrespiratory frequencies, in which case the HF component may extend into the LF band of the power spectrum. Therefore, it is important to carefully separate the respiratory frequency powers from the nonrespiratory frequency powers over time. Studies have demonstrated that both respiratory frequency and posture have an important effect on measurements derived from power spectral

analysis of heart rate and systolic blood pressure variability in normal subjects [17, 36]; thus, further supporting the need for extended research in this study.

In addition to the spectrum of the ECG and blood pressure, the coherence is another measure that provides information about the state of the cardiovascular system. The coherence is a measure of the linear association of each frequency of one signal on the same frequency of another signal and is defined as the ratio of the cross-spectral density of the two signals to the product of the individual spectral densities [11]. In this case, it is a frequency domain measure of the similarity between the ECG and blood pressure signals.

6.3.2 Clinical Relevance of HRV

Frequency domain, in addition to joint time-frequency domain, studies would appear to have the added potential for further improving our understanding of the nature of the specific autonomic dysfunction associated with different physiologic and pathophysiologic states, as well as for such purposes as early detection of autonomic neuropathies, monitoring of the progression of disease in terms of changes in autonomic function, risk stratification with respect to mortality, and development of more rational therapeutic approaches by facilitating drug selection in terms of ability to correct autonomic imbalances associated with disease [5].

For instance, spectral analysis of blood pressure and heart rate fluctuations has been proposed as a unique approach to obtain a deeper insight into cardiovascular regulatory mechanisms in health and disease. Availability of techniques for combined beat-to-beat recording of blood pressure and heart rate signals may allow for the extended

evaluation of autonomic dysfunction to daily life conditions [38]. There are conditions characterized by early autonomic dysfunction (e.g. subclinical diabetic patients, asymptomatic alcohol patients, etc.) where the responses to autonomic tests are still within the normal range, but blood pressure and heart rate variability already show specific alterations. In these conditions, time or frequency domain analysis of blood pressure and heart rate fluctuations may represent a complementary approach to early detection of subjects at increased risk of clinically relevant autonomic failure. However, there are a number of problems related to the diagnostic use of spectral analysis of blood pressure and heart rate that need to be addressed. First, no data are yet available on normal reference values for heart rate and blood pressure spectral powers [38]. Second, the ability of heart rate and blood pressure spectra to specifically reflect autonomic cardiovascular modulation is challenged by a number of observations [38]. For example, there are conditions and diseases (e.g. dynamic exercise, congestive heart failure, etc.) in which an enhanced sympathetic activity is accompanied by no change or even a reduction in blood pressure and heart rate LF powers [38]. Thus, great caution is needed in the methods of extrapolation responsible for the generation of these spectral components. Consequently, further studies are needed to better clarify not only the physiologic and pathophysiologic relevance of blood pressure and heart rate variability analysis, but also its possible diagnostic and prognostic value in different pathological conditions.

APPENDIX A

EXPLANATION OF SIGNIFICANCE OF THE USE OF NORMALIZED UNITS

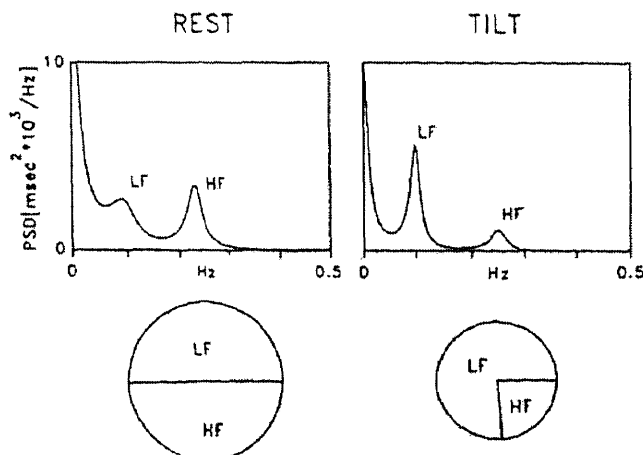


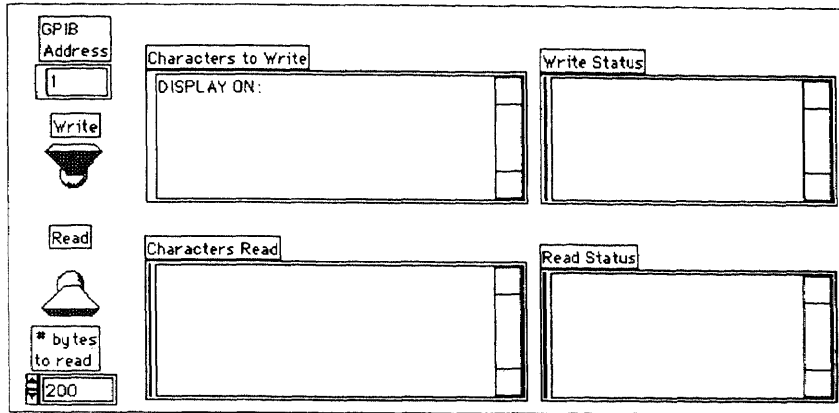
Figure A1 Spectral analysis (AR model) of RR interval variability in a healthy subject at rest and during 90° head-up tilt. At rest, two major components of similar power are detectable at low and high frequencies. During tilt, the LF component becomes dominant, but as total variance is reduced, the absolute power of LF appears unchanged compared with rest. Normalization procedure leads to predominant LF and smaller HF components, which express the alteration of spectral components due to tilt. Pie charts show the relative distribution together with the absolute power of the two components represented by the area.

During rest, the total variance of the spectrum was 1201 ms², and its VLF, LF and HF components were 586 ms², 310 ms² and 302 ms², respectively. Expressed in normalized units (nu), the LF and HF were 48.95 and 47.78 nu, respectively. The LF/HF ratio was 3.34. Thus, note that for instance, the absolute power of the LF component was slightly decreased during tilt while the normalized units of LF were substantially increased. (From Task Force of the European Society of Cardiology and the North American Society of Pacing and Electrophysiology, "Heart rate variability: standards of measurement, physiological interpretation, and clinical use," *Circulation*, vol. 93, pp. 1043-1065, 1996.)

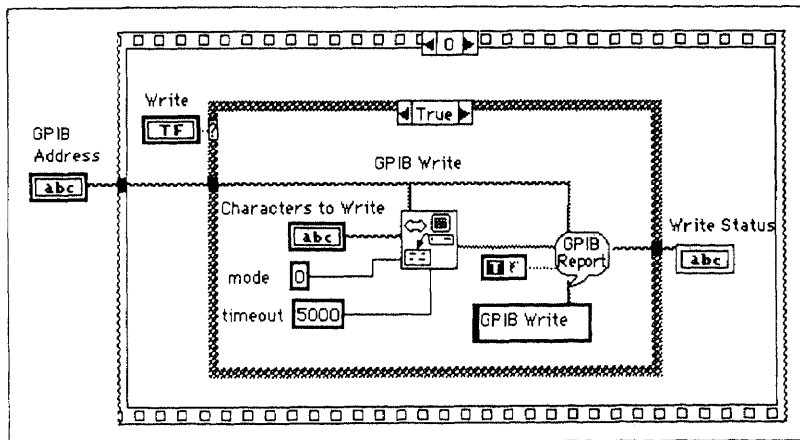
APPENDIX B

LABVIEW DIAGRAMS

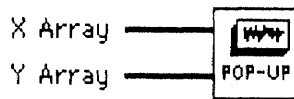
Three Main Parts of a LabVIEW VI



Front Panel



Block Diagram



icon





connector

Wigner Time-Frequency Program

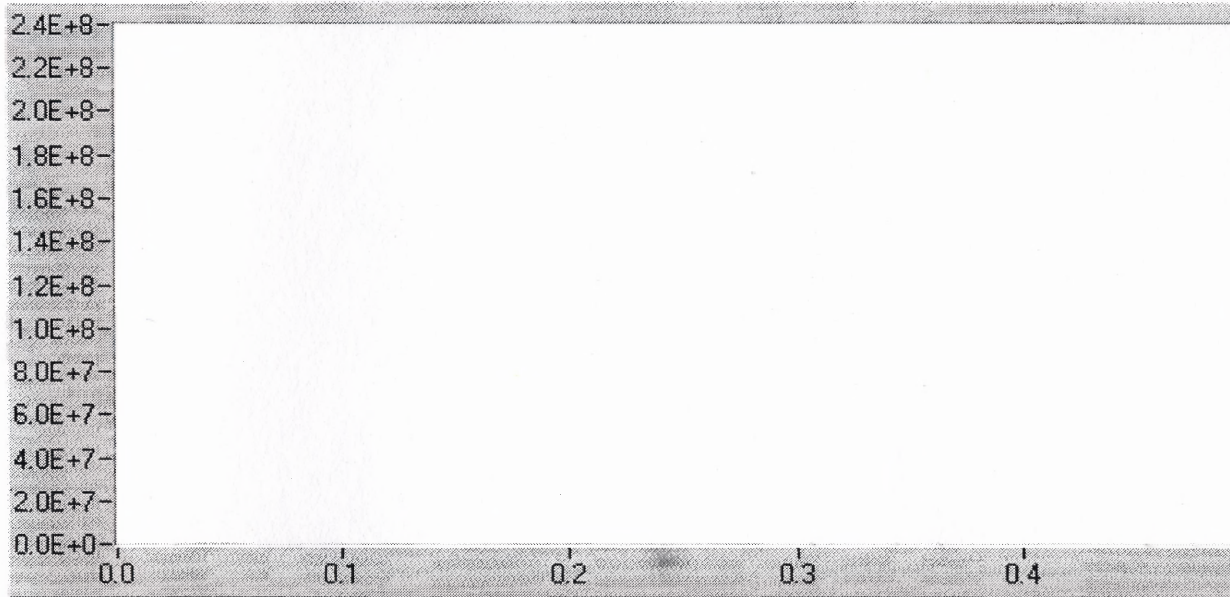
Sympar.vi (Control Panel)

Path to ECG data file

HR Spectrum 
Resp Spectrum 

SF

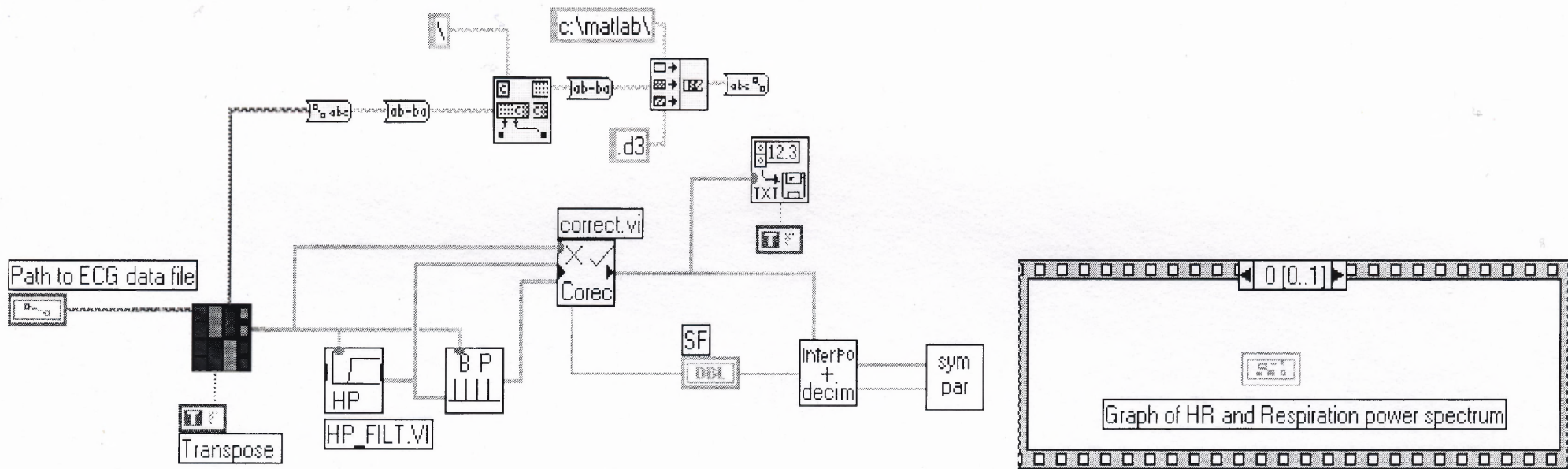
Graph of HR and Respiration power spectrum



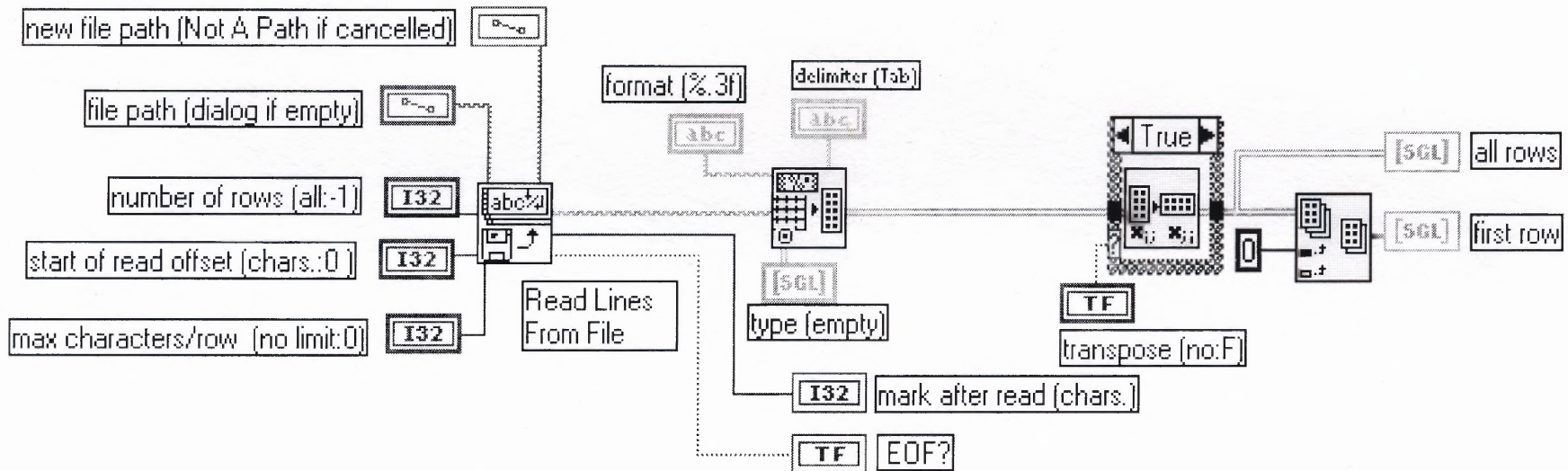
FREQUENCY

Hertz

Sympar.vi (Diagram)



Read From Spreadsheet File.vi (SubVI Diagram)



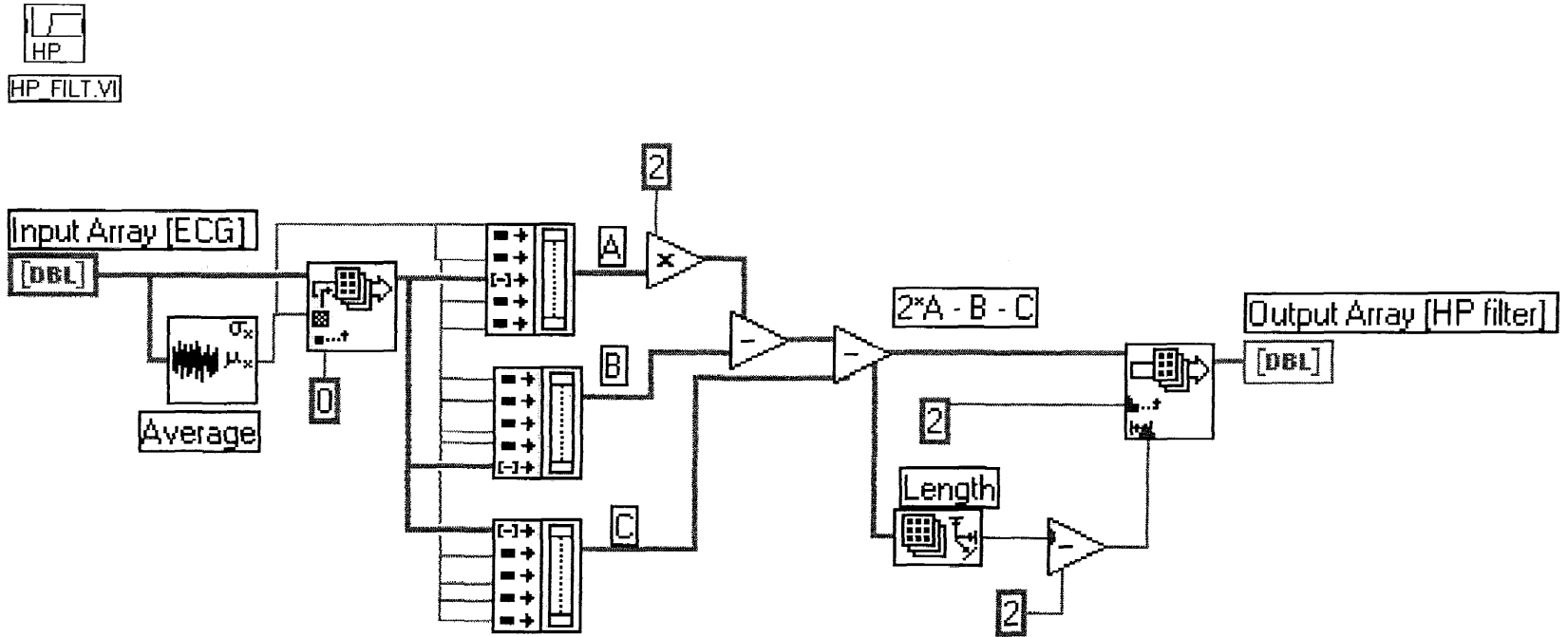
instructions

Spreadsheet String to Array requires that columns are separated with the input delimiter string (Tab default), and rows are terminated with EOL characters. If your spreadsheet string uses a different terminator, use the Search String and Replace VI from the examples/general/strings.llb library (or something equivalent) at the output of Read Lines From File to modify the string.

Spreadsheet String to Array produces a rectangular numeric array, whose number of columns equals the maximum number of columns in all rows that are read. Short rows are padded with zeroes.

You can modify a copy of this VI to return the file contents into arrays of strings by changing **all rows**, **first row**, and **type (empty)** arrays to string arrays and by setting the **format** to %s.

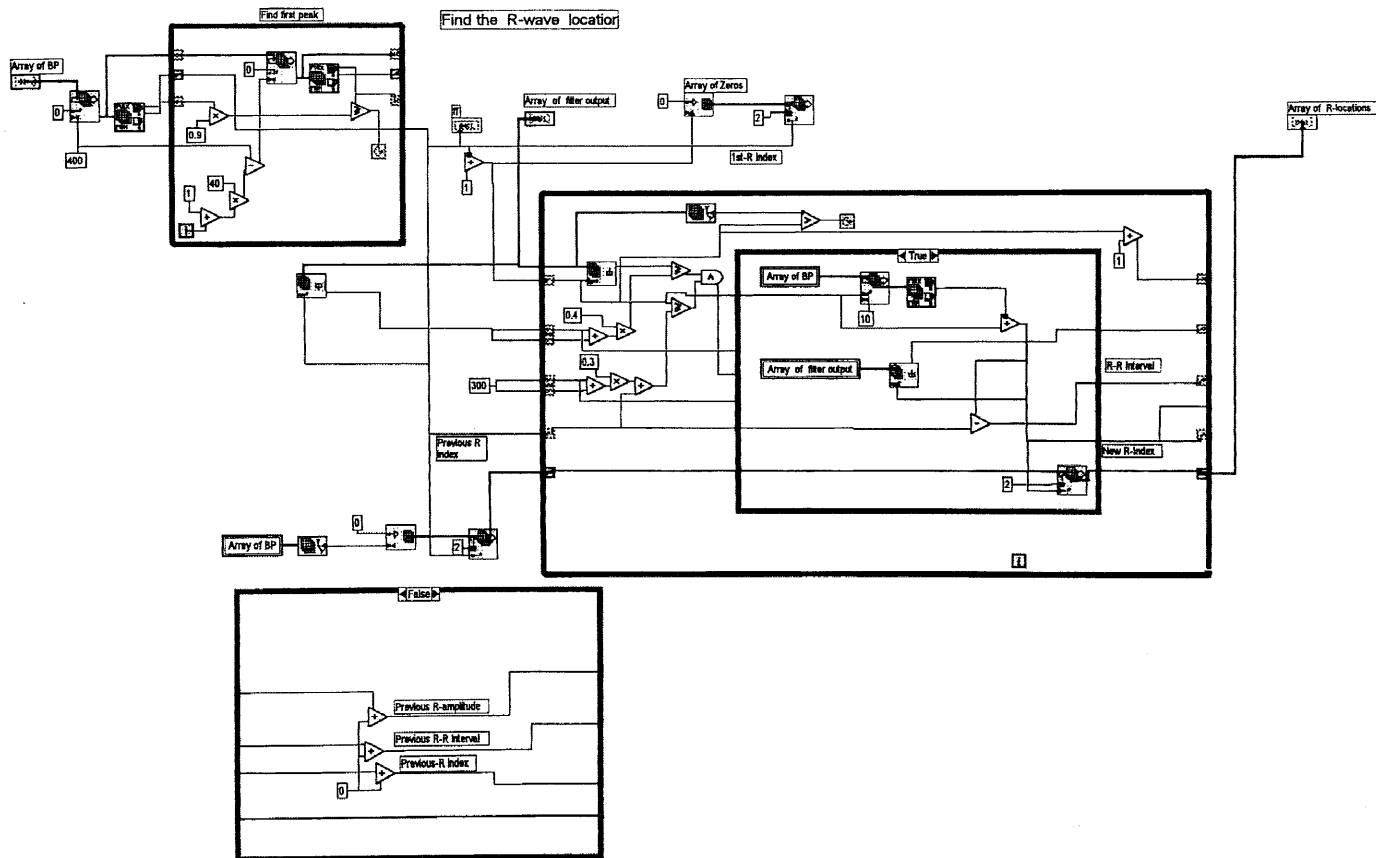
HP_FILT.vi (SubVI Diagram)



High-pass Filter using template.

Filter the input signal according to the template [-1 0 2 0 -1].

Search BP.vi (SubVI Diagram)



Correct.vi (SubVI Control Panel)

correct.vi



HEART RATE

ECG

0 10.00

Filtered

0 10.00

R locations

0 0.00

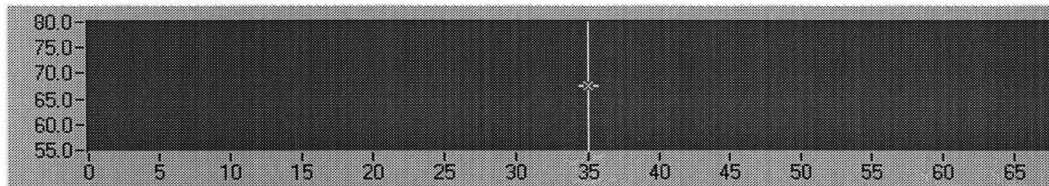
BOTH

Sampling frequency

0.00

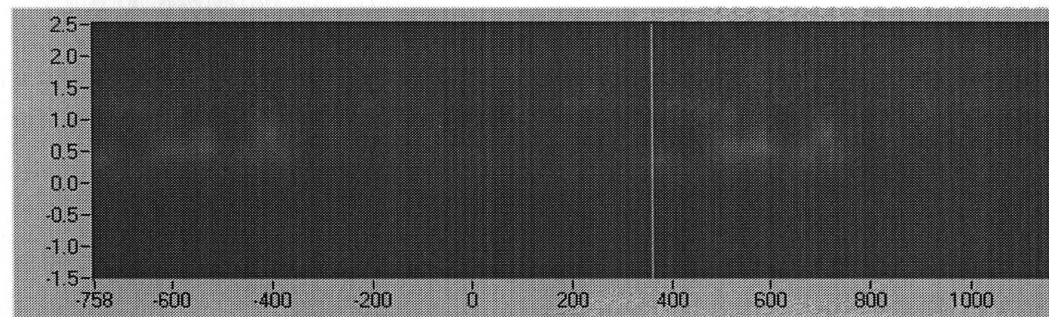
IBI

0 0.00



Cursor 1 35.00 67.50

Move to Heart R

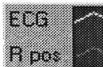


Cursor 2 360.93 122.71

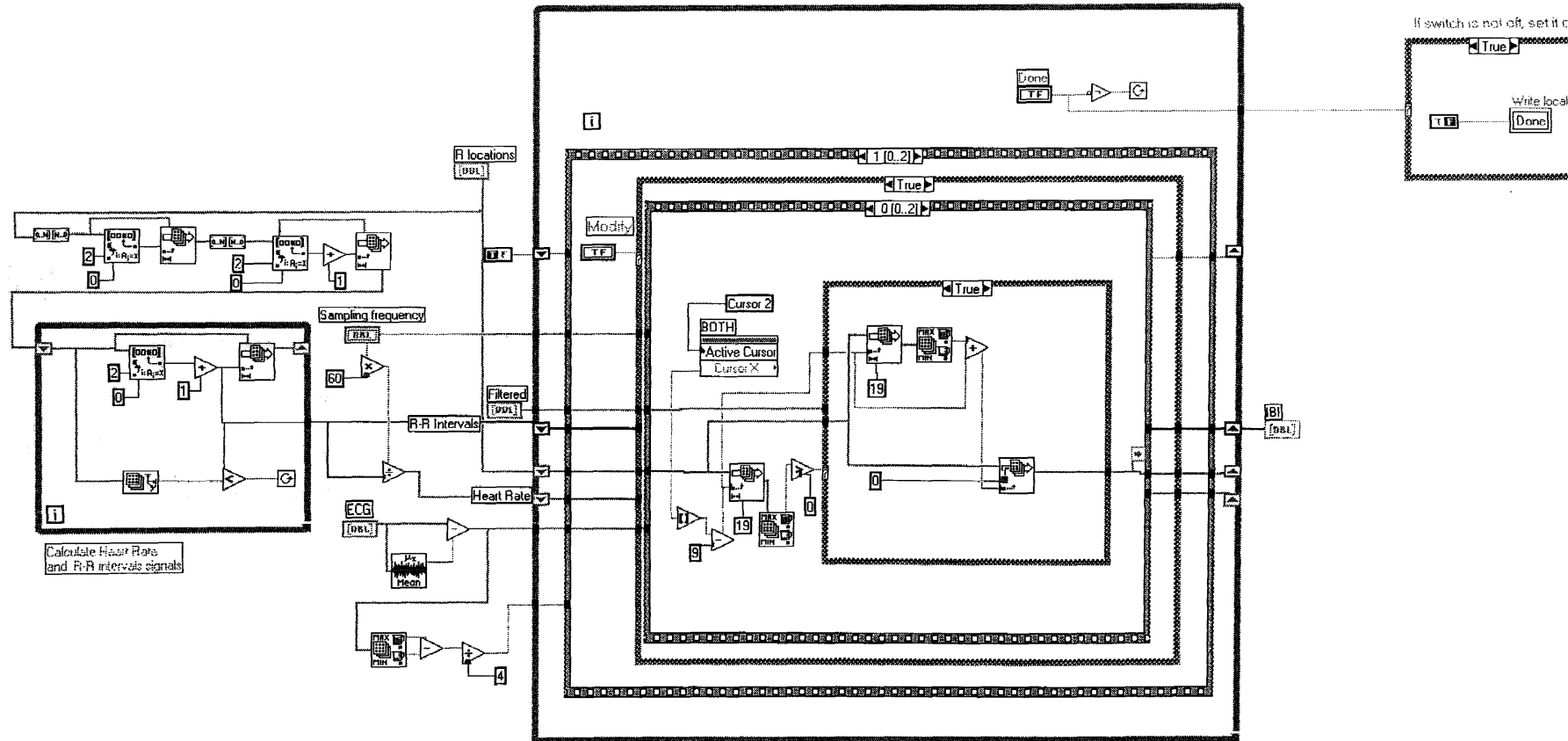
Modify



Done

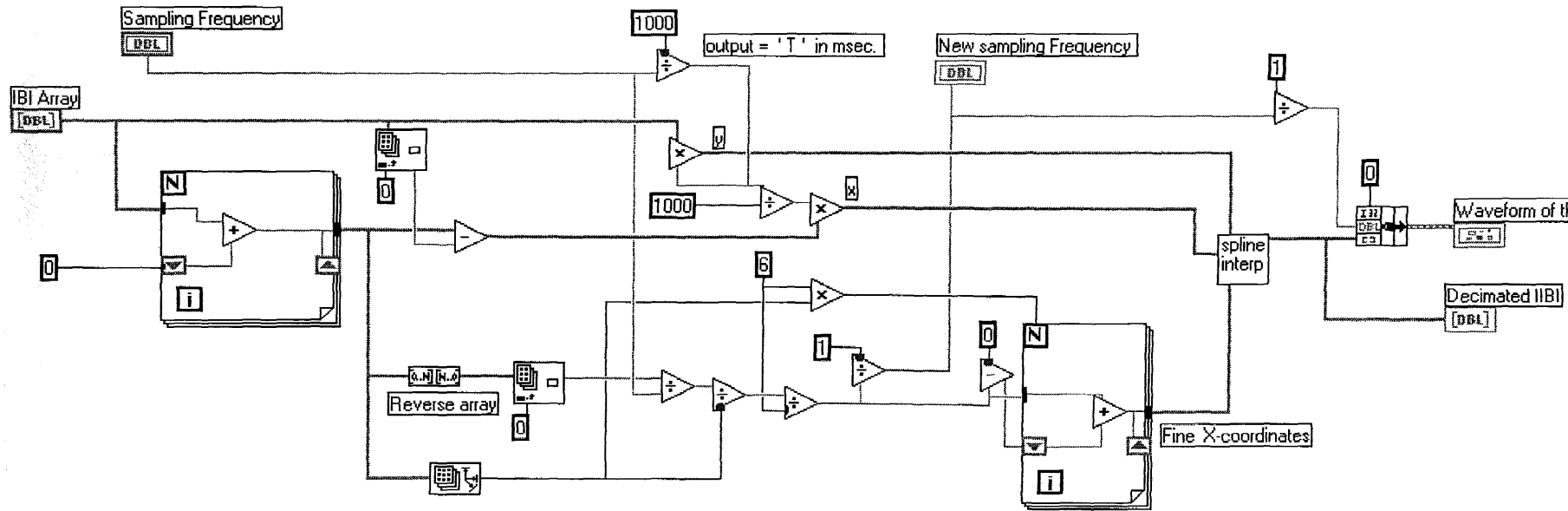


Correct.vi (SubVI Diagram)

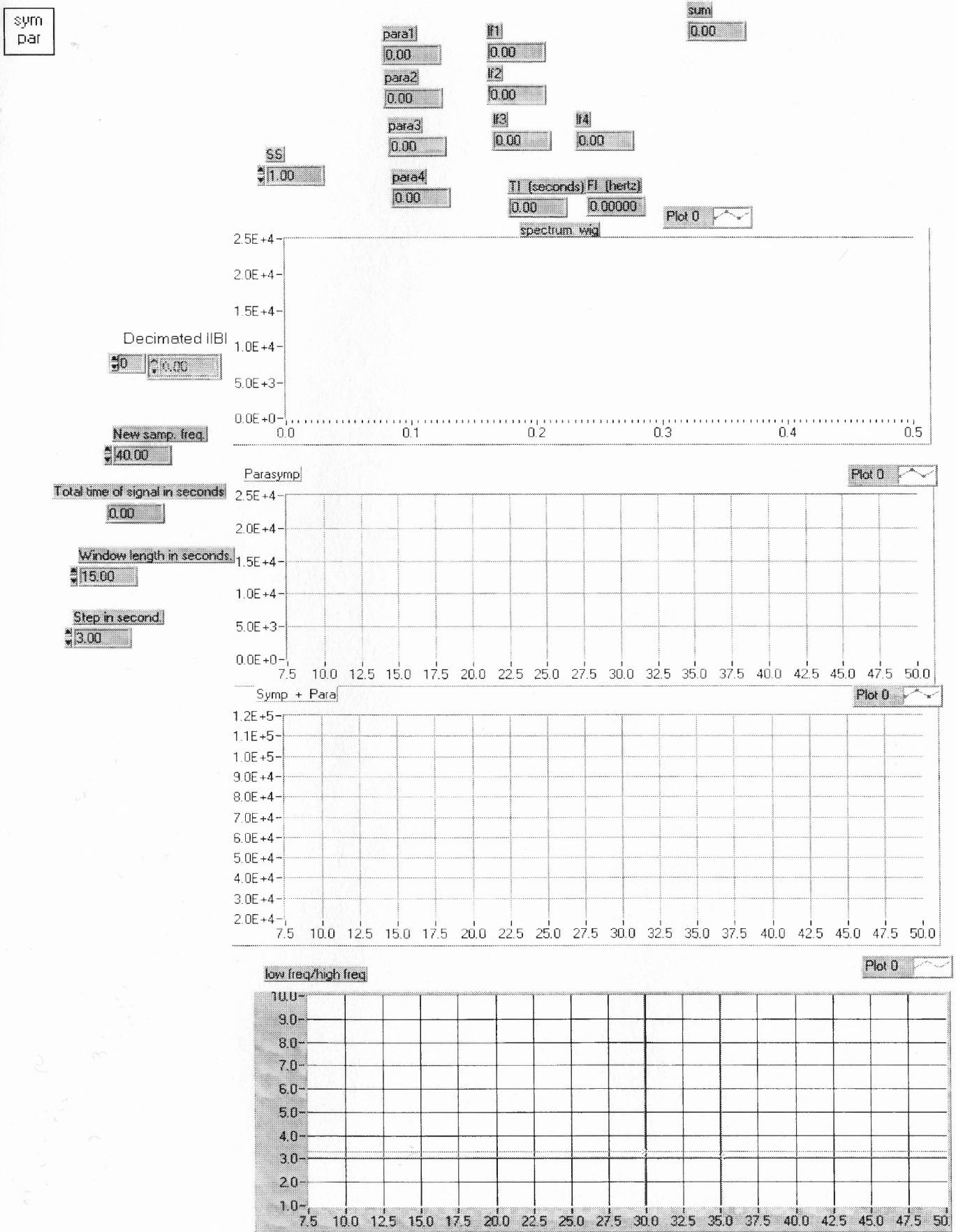


Interpolation & Decimation.vi (SubVI Diagram)

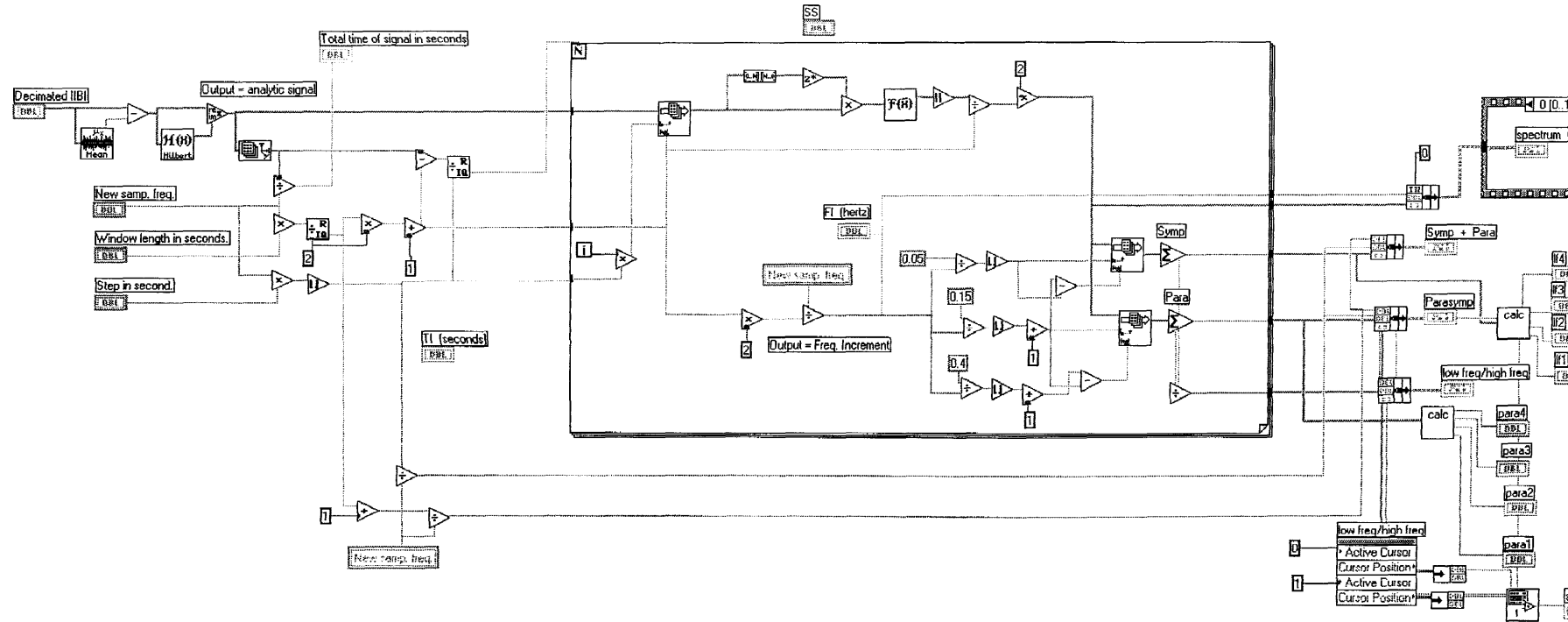
InterPo
+
decim



Symbar (Wigner).vi (SubVI Control Panel)



Symbar (Wigner).vi (SubVI Diagram)



Power Spectrum Analysis Program for Heart Rate

Energy spectrum with no R-wave detection.vi (Control Panel)

Path to ECG data file

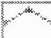
SF

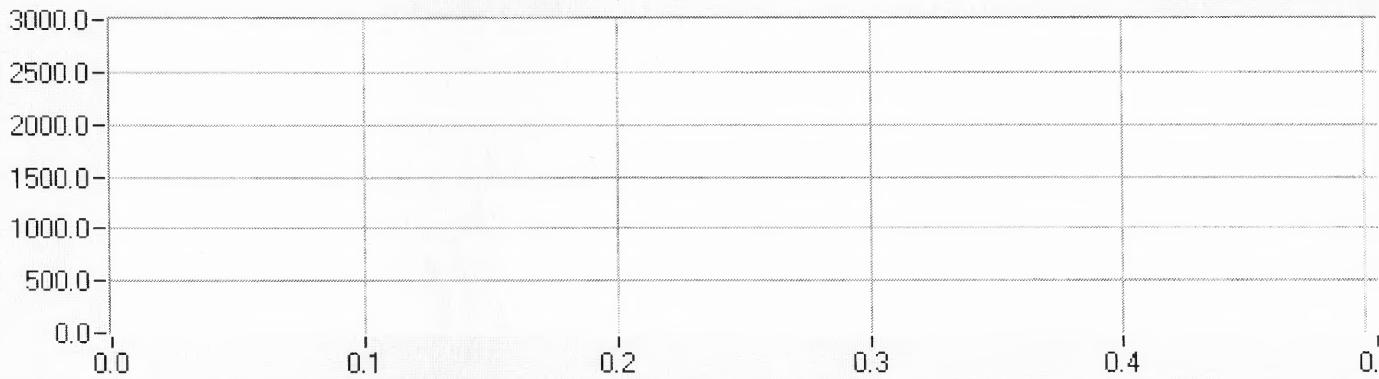
Time of record in minutes

HF Area

LF Area

Graph of HR power spectrum


HR Spectrum 

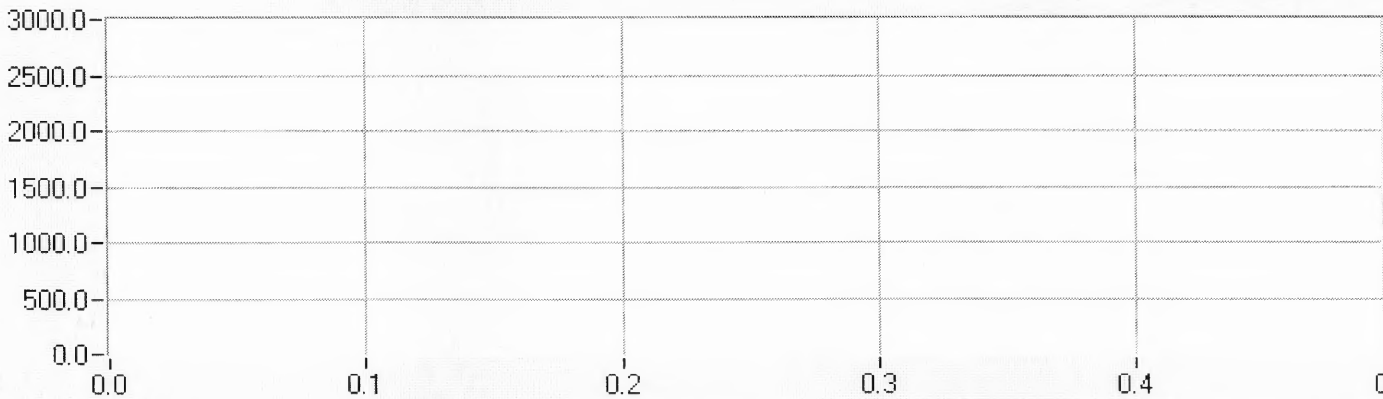


FREQUENCY

Hertz

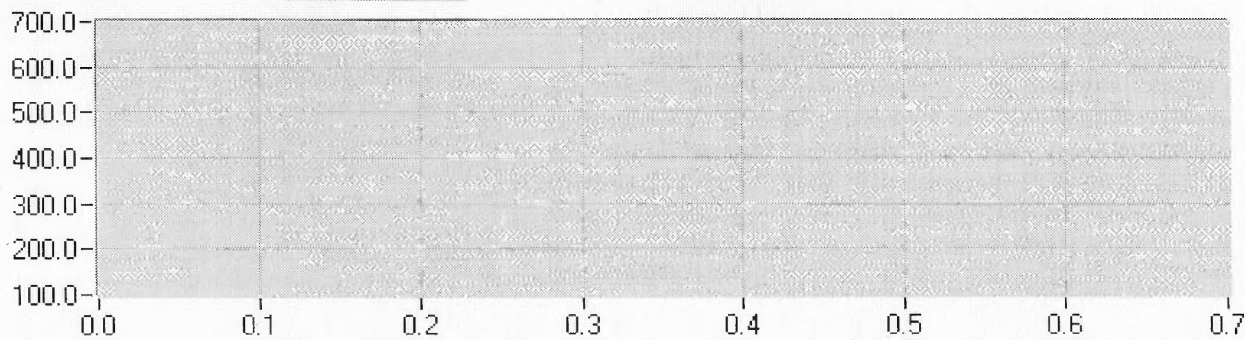
Graph Respiration power spectrum

HR Spectrum 

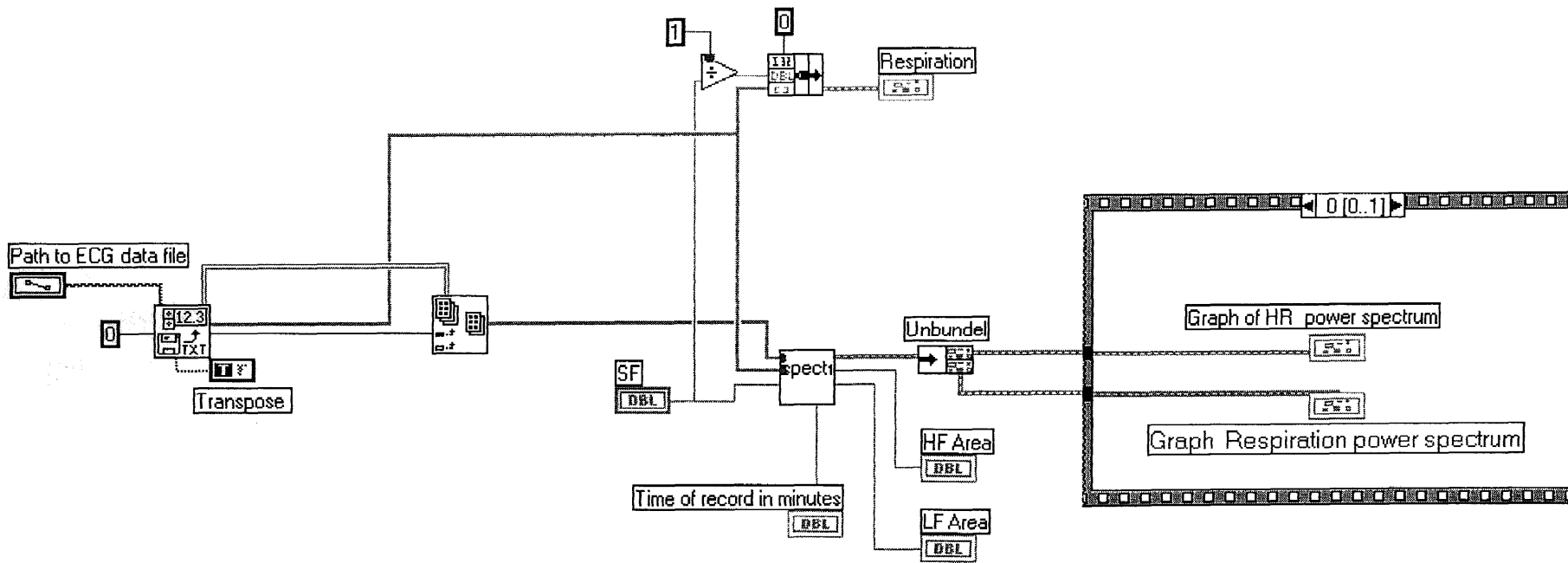


Respiration

Plot 0

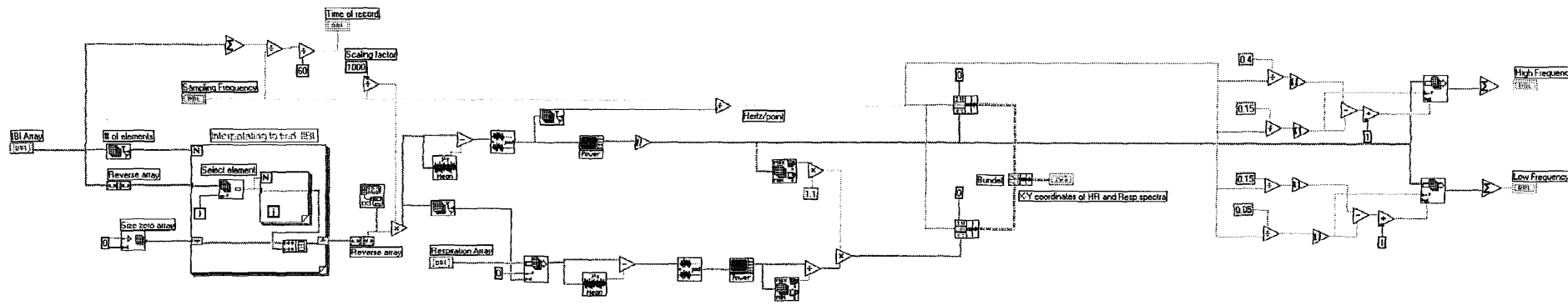


Energy spectrum with no R-wave detection.vi (Diagram)



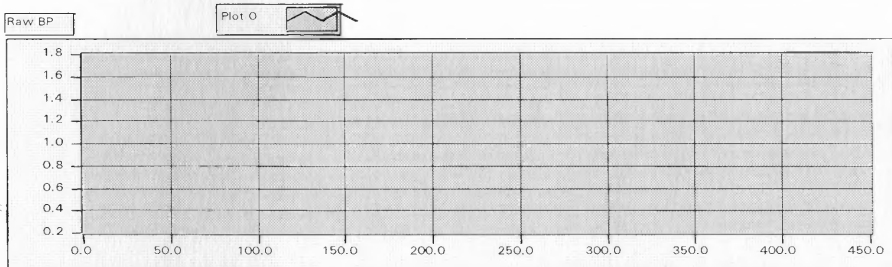
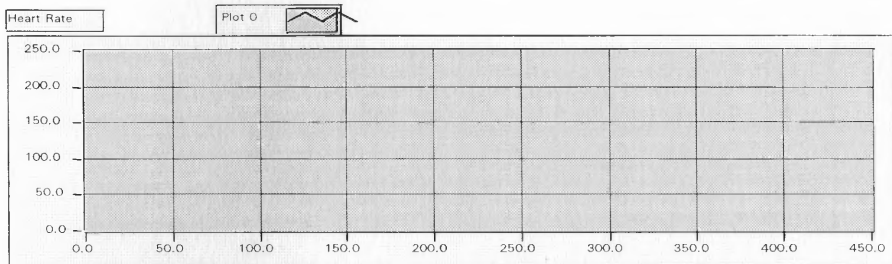
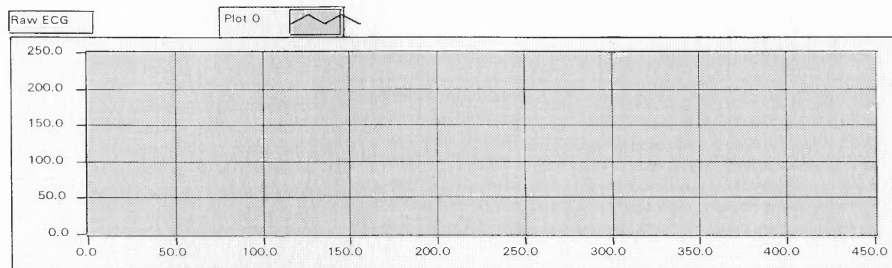
Spectrum1.vi (SubVI Diagram)

spectr



Power Spectrum Analysis Program for Blood Pressure

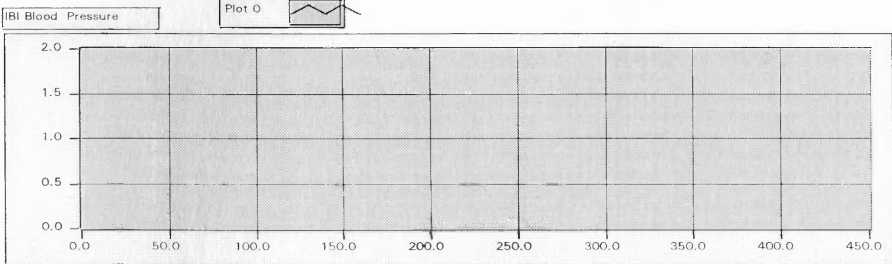
Energy spectrum using BP-NO Rwave detection.vi (Control Panel)



IBI BP file

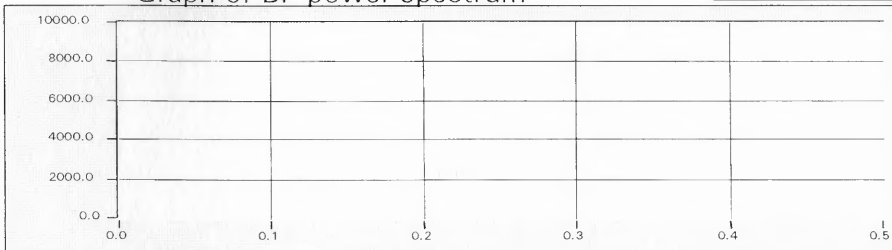
Path to ECG data file

SF



Graph of BP power spectrum

Resp Spectrum



HF Area copy

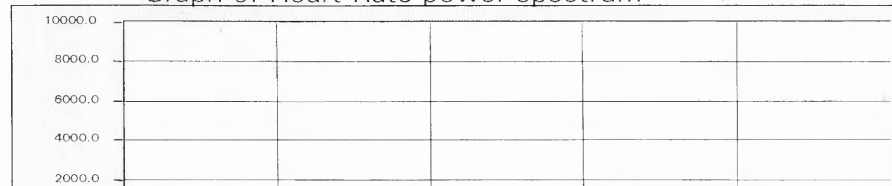
LF Area copy

Time of record in minutes copy

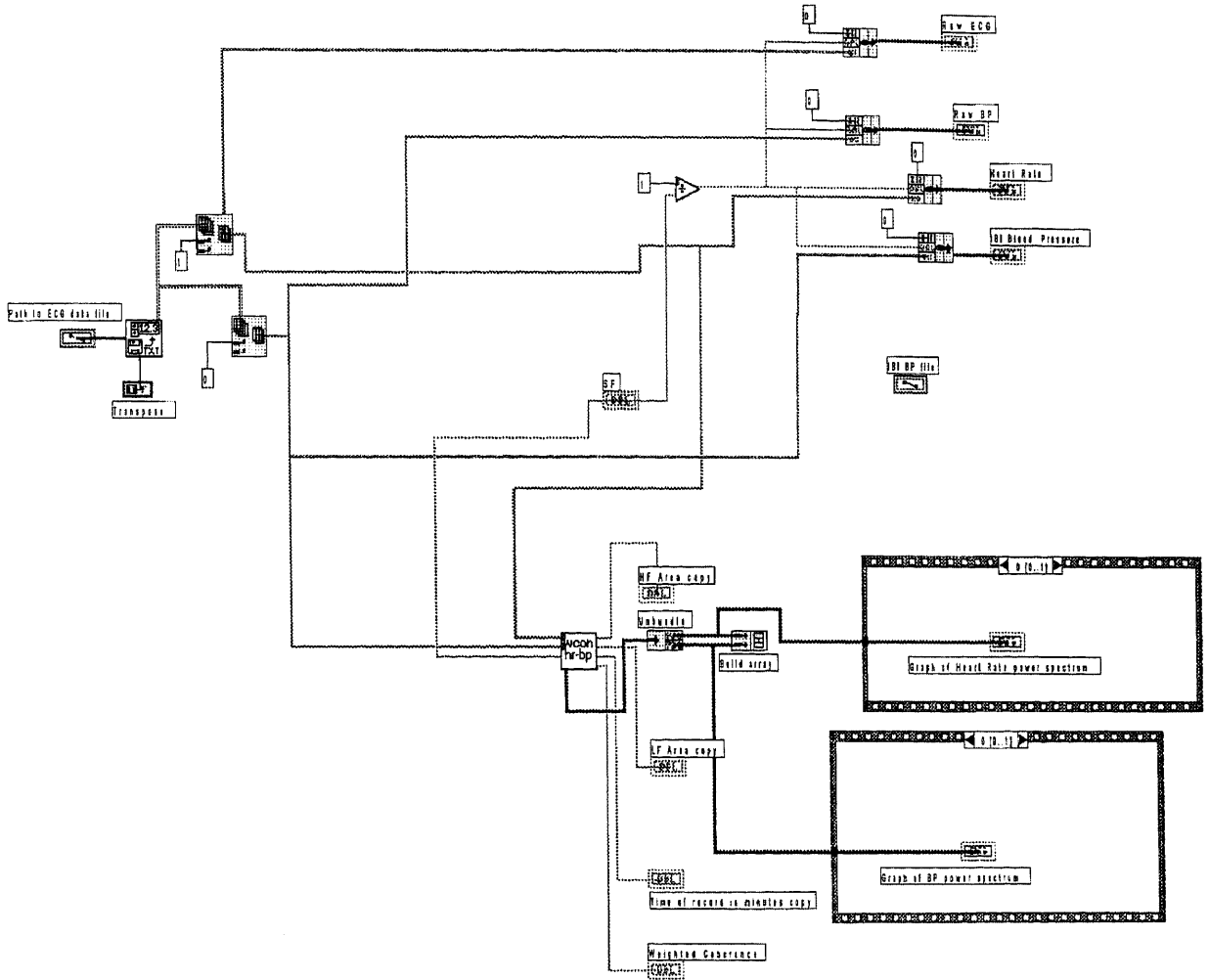
Weighted Coherence

Graph of Heart Rate power spectrum

HR Spectrum



Energy spectrum using BP-NO Rwave detection.vi (Diagram)



APPENDIX C

RESULTS OF HEART RATE VARIABILITY ANALYSIS OF PRELIMINARY STUDY

Power Spectrum Analysis of ECG Signal for the 5 Subjects

(Subject: GHC-AR)

Path to ECG data f

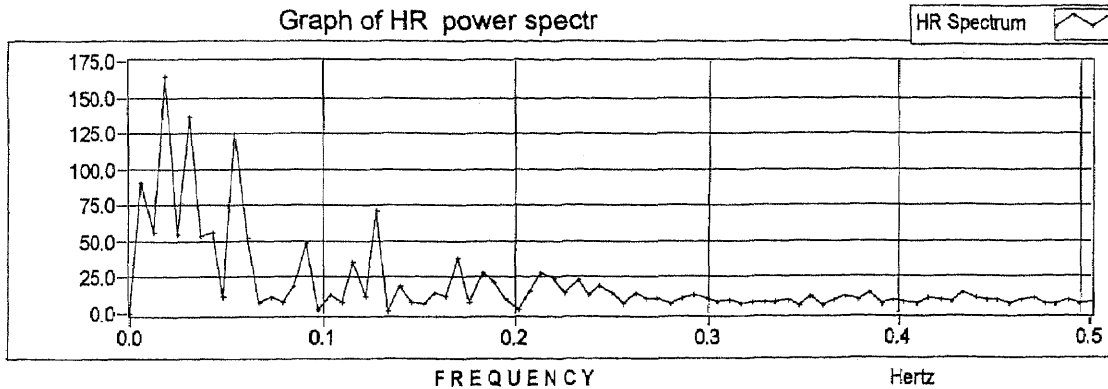
SF

Time of record in minutes

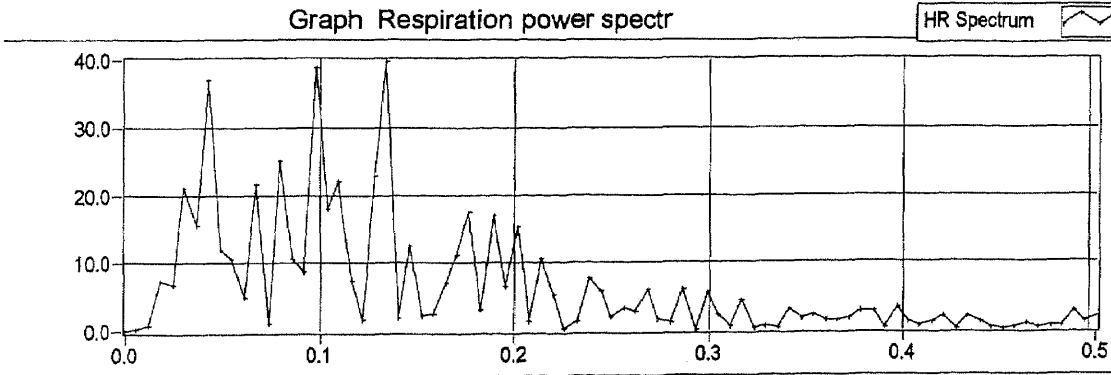
HF Area

LF Area

Graph of HR power spectr

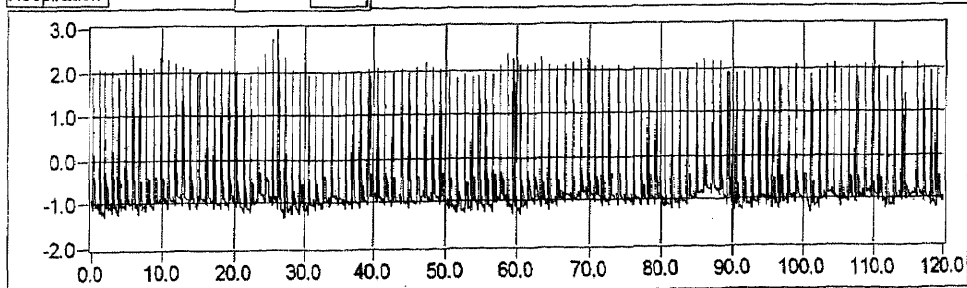


Graph Respiration power spectr



Respiration

Plot 0



(Subject: GHC-DU)

Path to ECG data f

SF

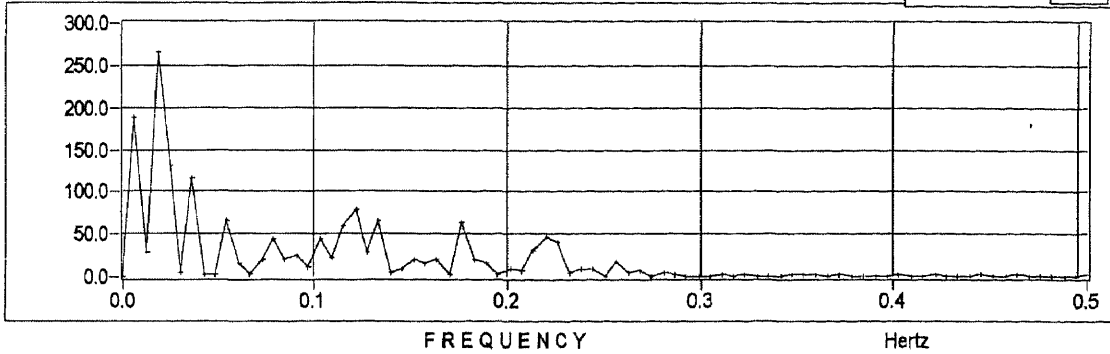
Time of record in minutes

HF Area

LF Area

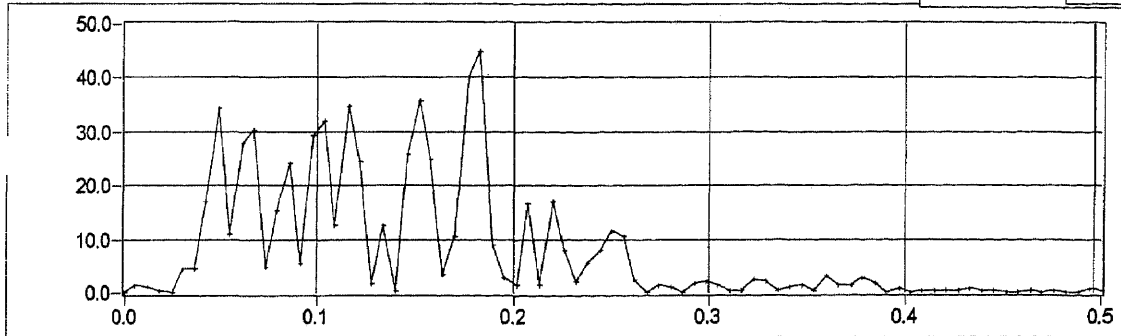
Graph of HR power spectr

HR Spectrum



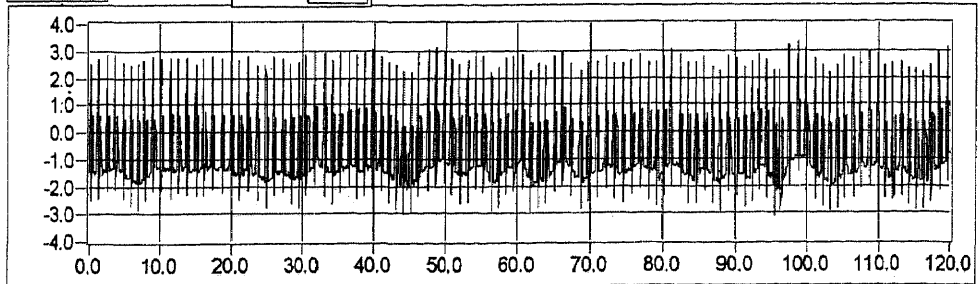
Graph Respiration power spectr

HR Spectrum



Respiration

Plot 0



(Subject: GCF-JE)

Path to ECG data f

SF

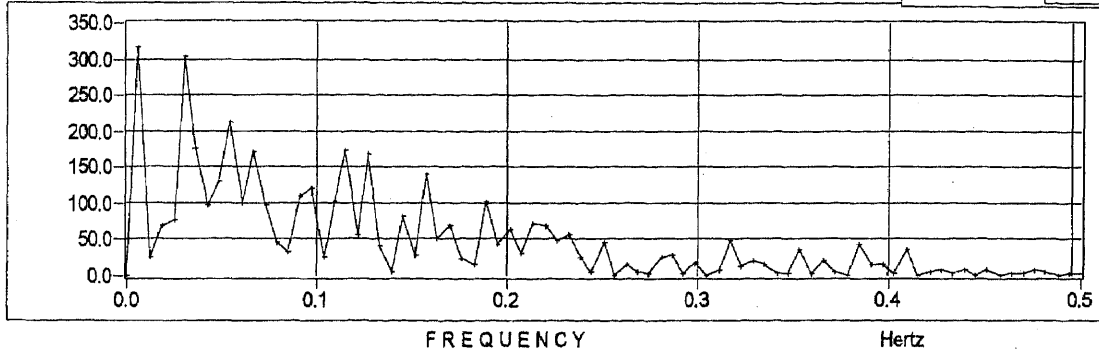
Time of record in minutes

HF Area

LF Area

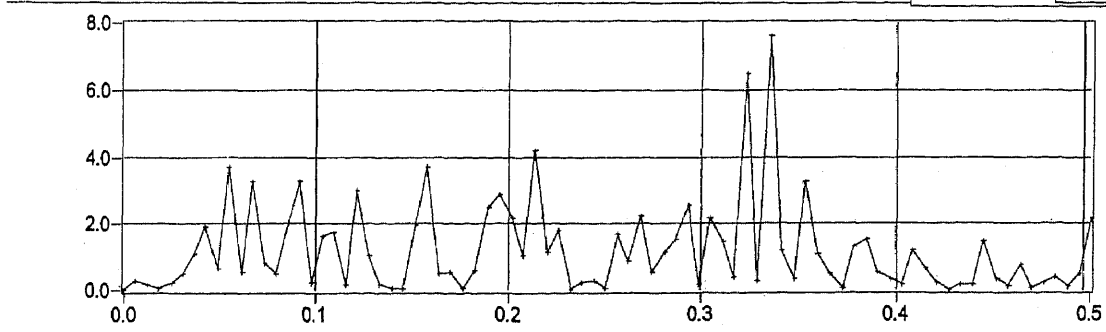
Graph of HR power spectr

HR Spectrum



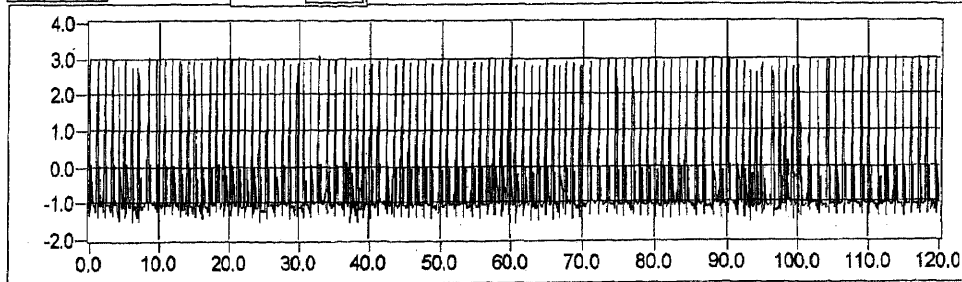
Graph Respiration power spectr

HR Spectrum



Respiration

Plot 0



(Subject: GHC-SD)

Path to ECG data f

SF

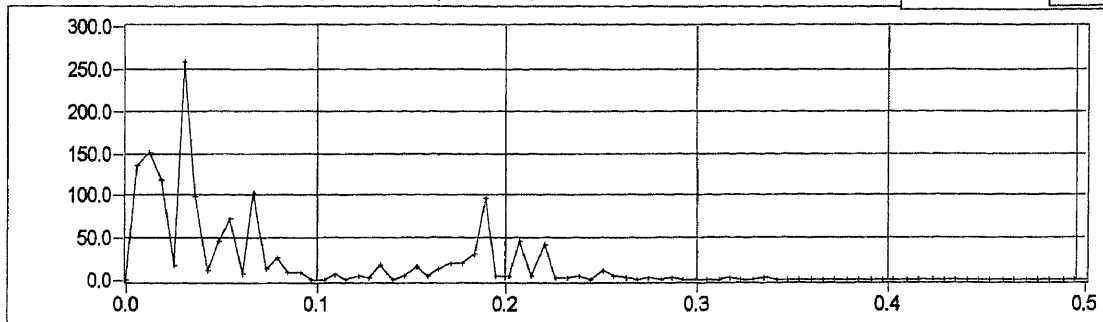
Time of record in minutes

HF Area

LF Area

Graph of HR power spectr

HR Spectrum

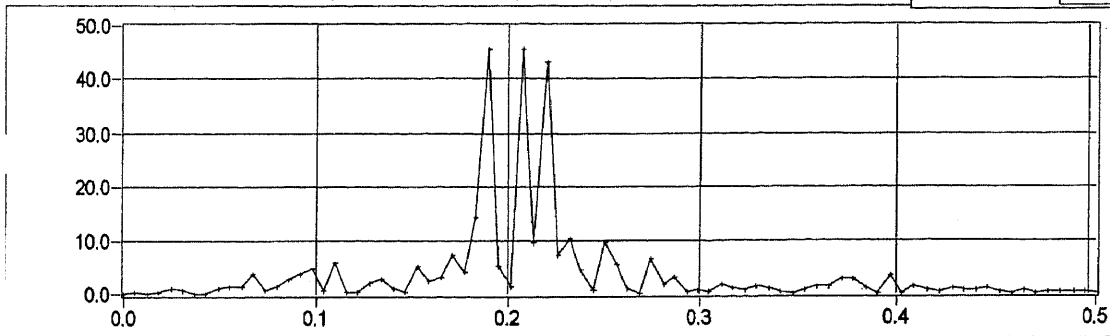


FREQUENCY

Hertz

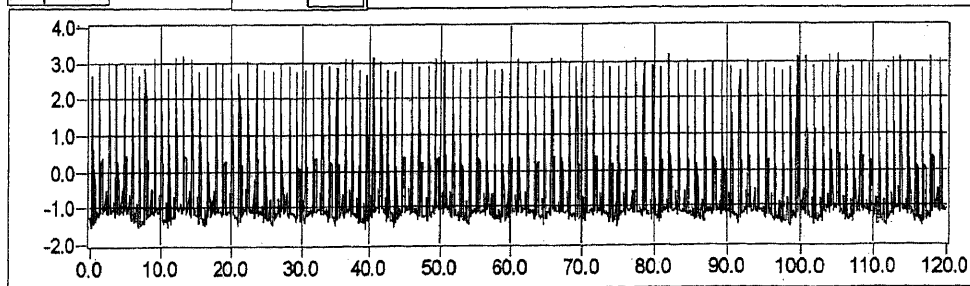
Graph Respiration power spectr

HR Spectrum



Respiration

Plot 0



(Subject: GHC-TR)

Path to ECG data f

SF

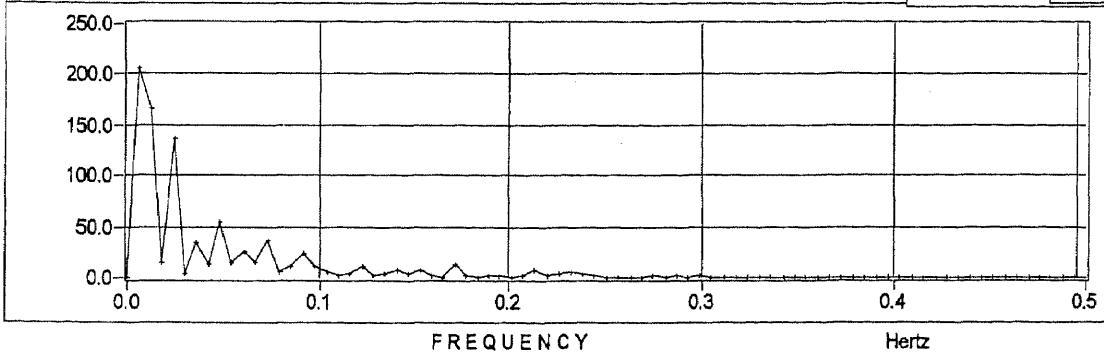
Time of record in minutes

HF Area

LF Area

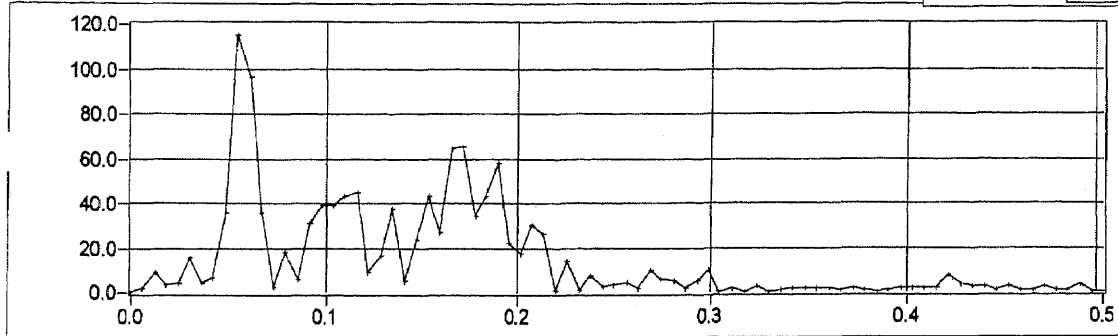
Graph of HR power spectr

HR Spectrum



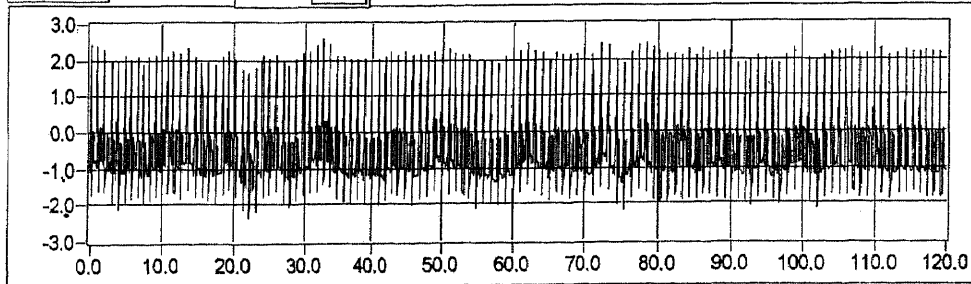
Graph Respiration power spectr

HR Spectrum



Respiration

Plot 0



Power Spectrum Analysis of BP Signal for the 5 Subjects

(Subject: GHC-AR)

Path to ECG data f

SF

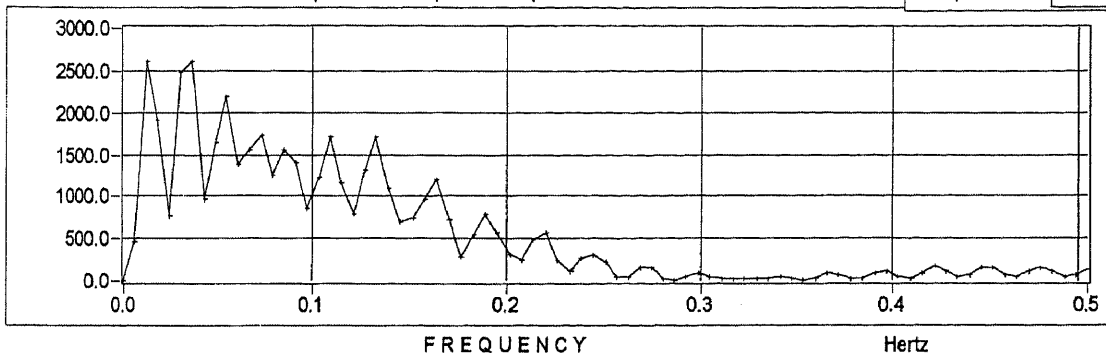
Time of record in minutes

HF Area

LF Area

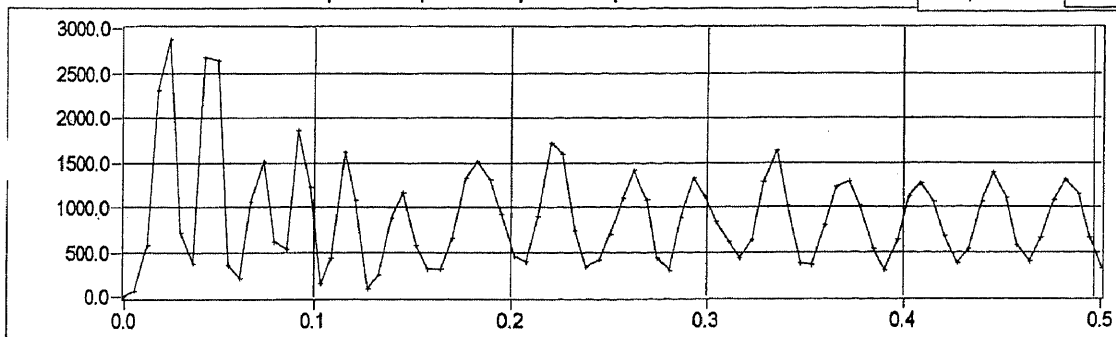
Graph of HR power spectr

HR Spectrum



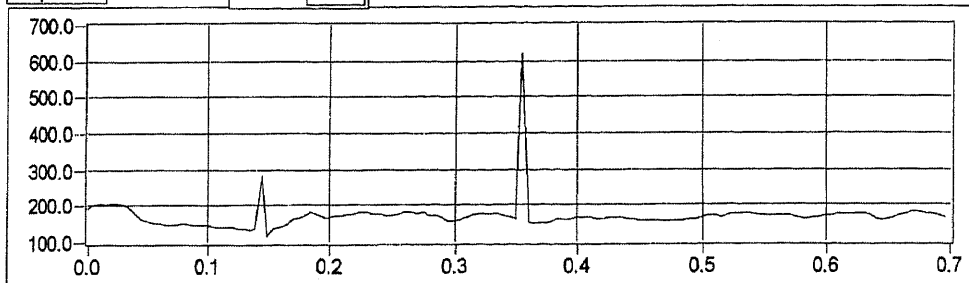
Graph Respiration power spectr

HR Spectrum



Respiration

Plot 0



(Subject: GHC-DU)

Path to ECG data f

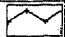
SF

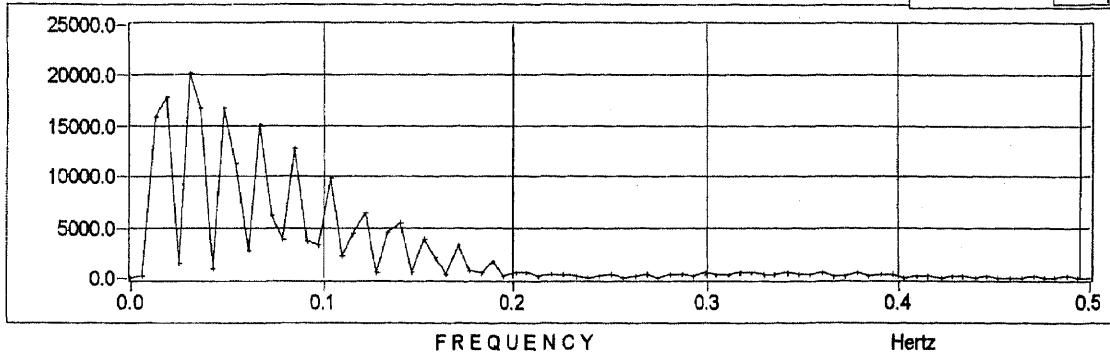
Time of record in minutes

HF Area


LF Area

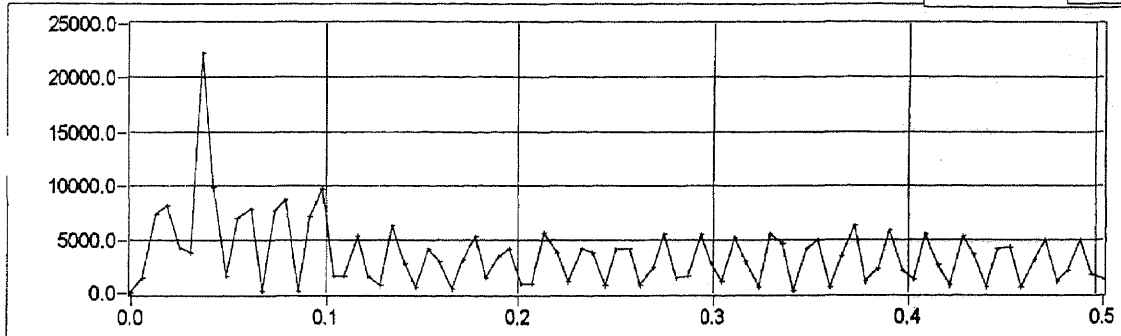
Graph of HR power spectr

HR Spectrum 




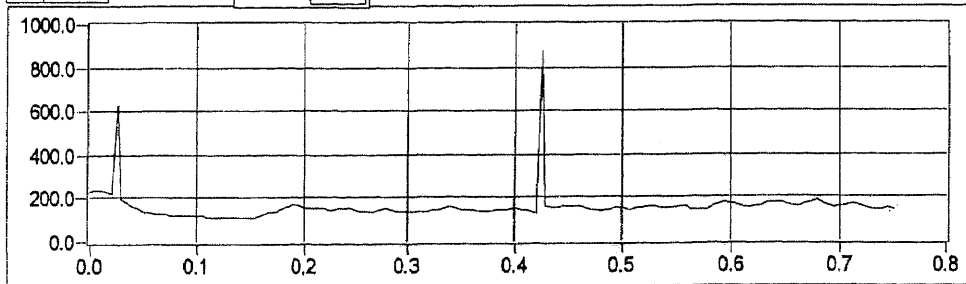
Graph Respiration power spectr

HR Spectrum 



Respiration

Plot 0 



(Subject: GCF-JE)

Path to ECG data f

SF

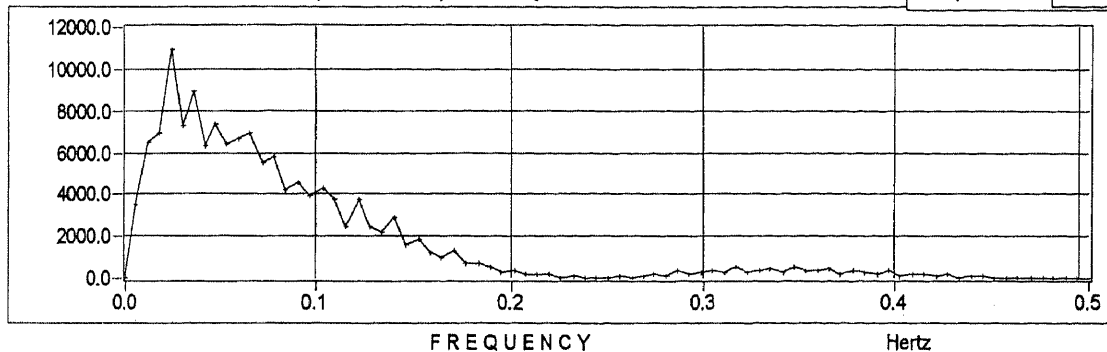
Time of record in minutes

HF Area

LF Area

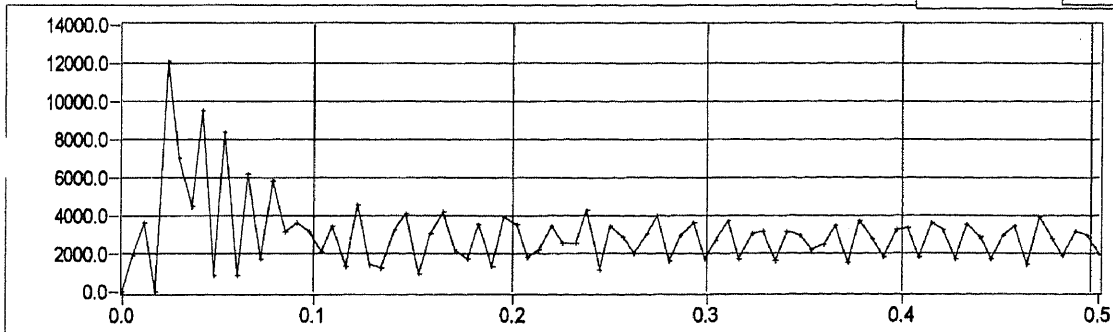
Graph of HR power spectr

HR Spectrum



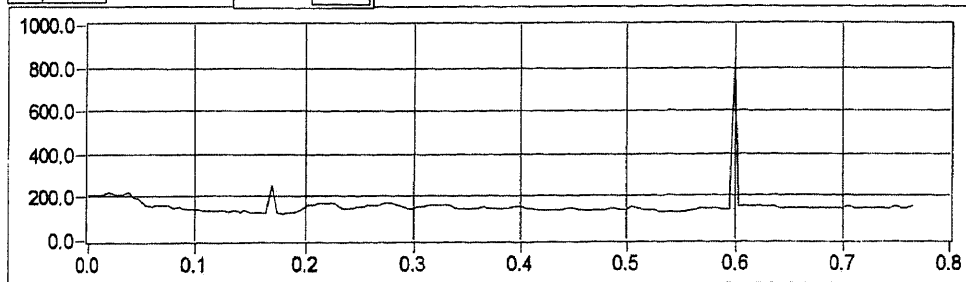
Graph Respiration power spectr

HR Spectrum



Respiration

Plot 0



(Subject: GHC-SD)

Path to ECG data f

SF

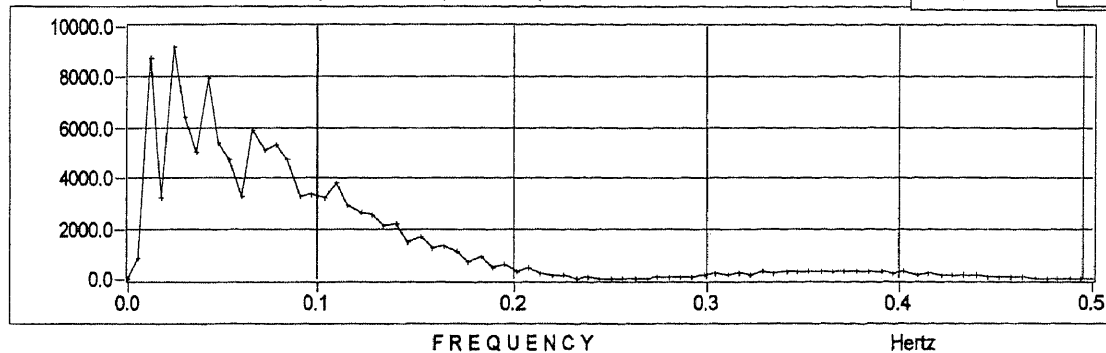
Time of record in minutes

HF Area

LF Area

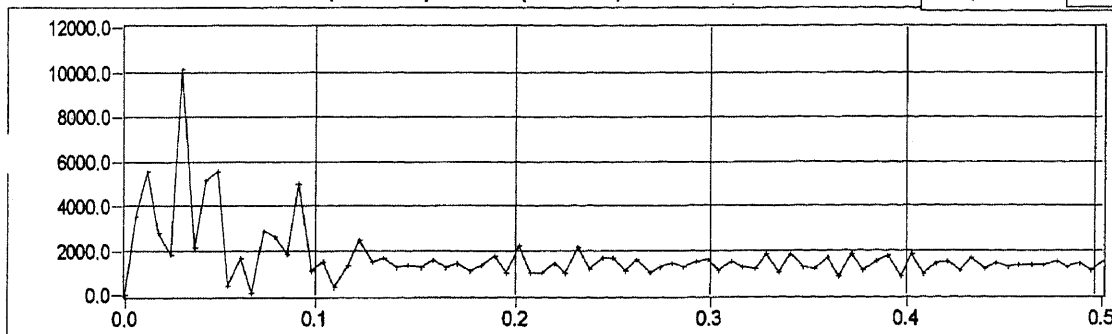
Graph of HR power spectr

HR Spectrum



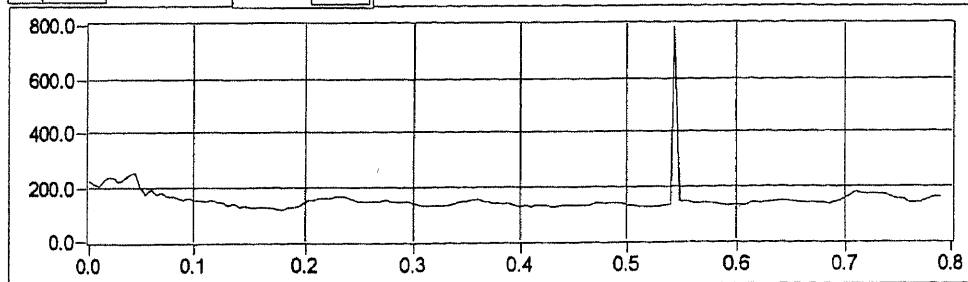
Graph Respiration power spectr

HR Spectrum



Respiration

Plot 0



(Subject: GHC-TR)

Path to ECG data f

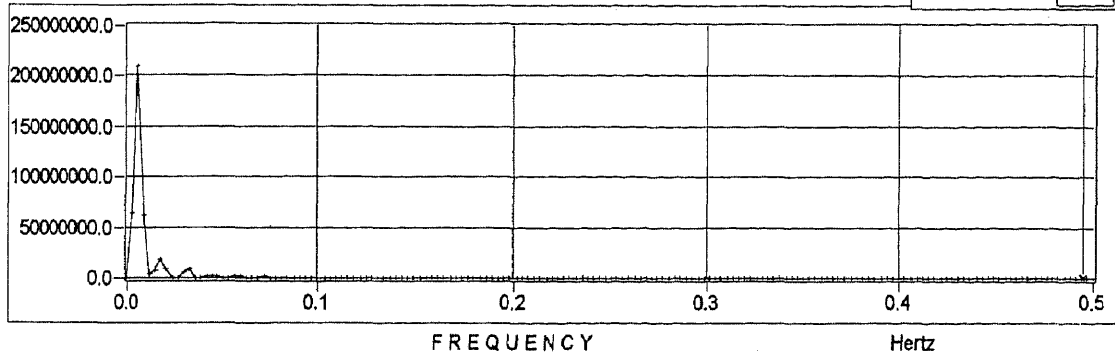
SF

Time of record in minutes

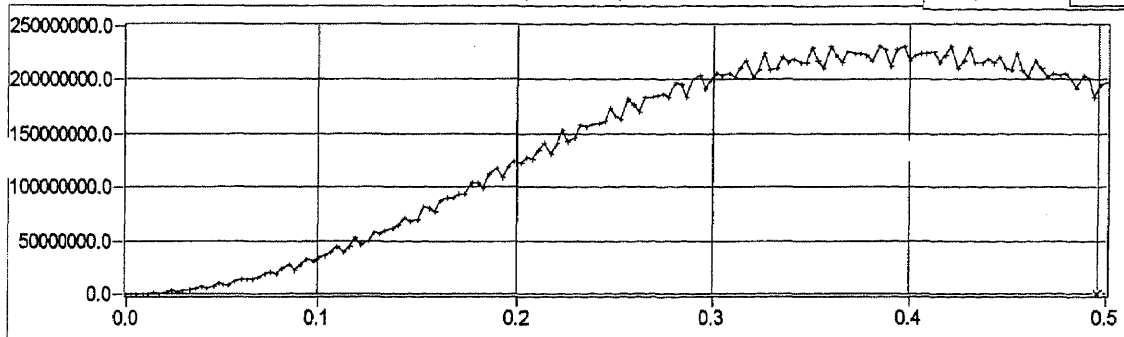
HF Area

LF Area

Graph of HR power spectr

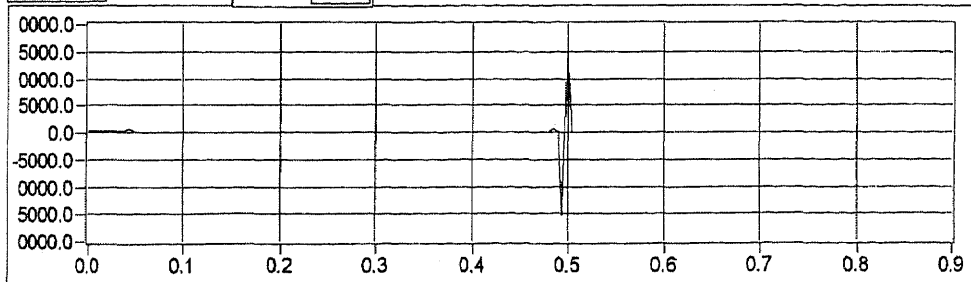


Graph Respiration power spectr



Respiration

Plot 0

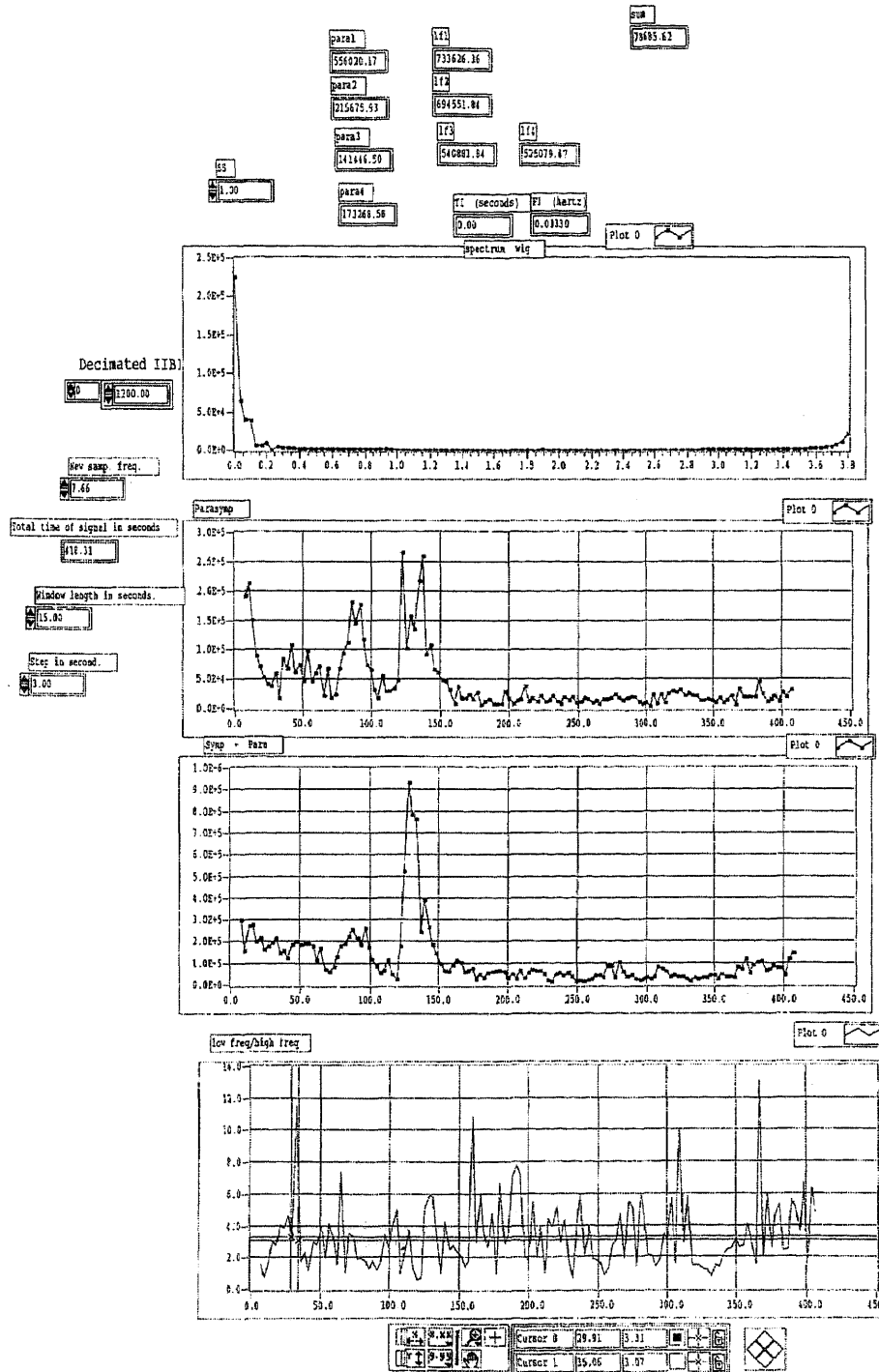


APPENDIX D

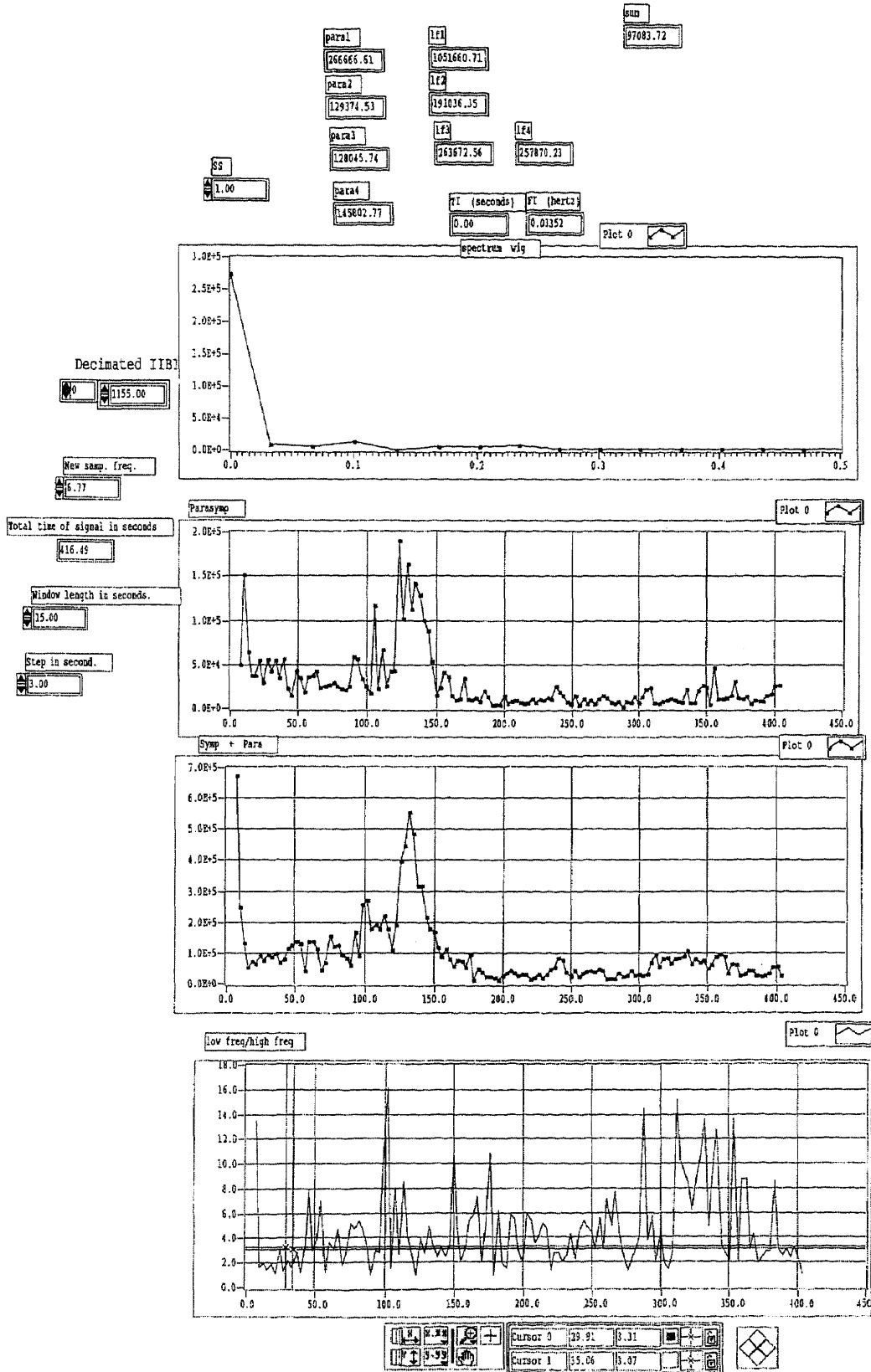
RESULTS OF HEART RATE VARIABILITY ANALYSIS

Time-Frequency Curves Utilizing ECG Signal

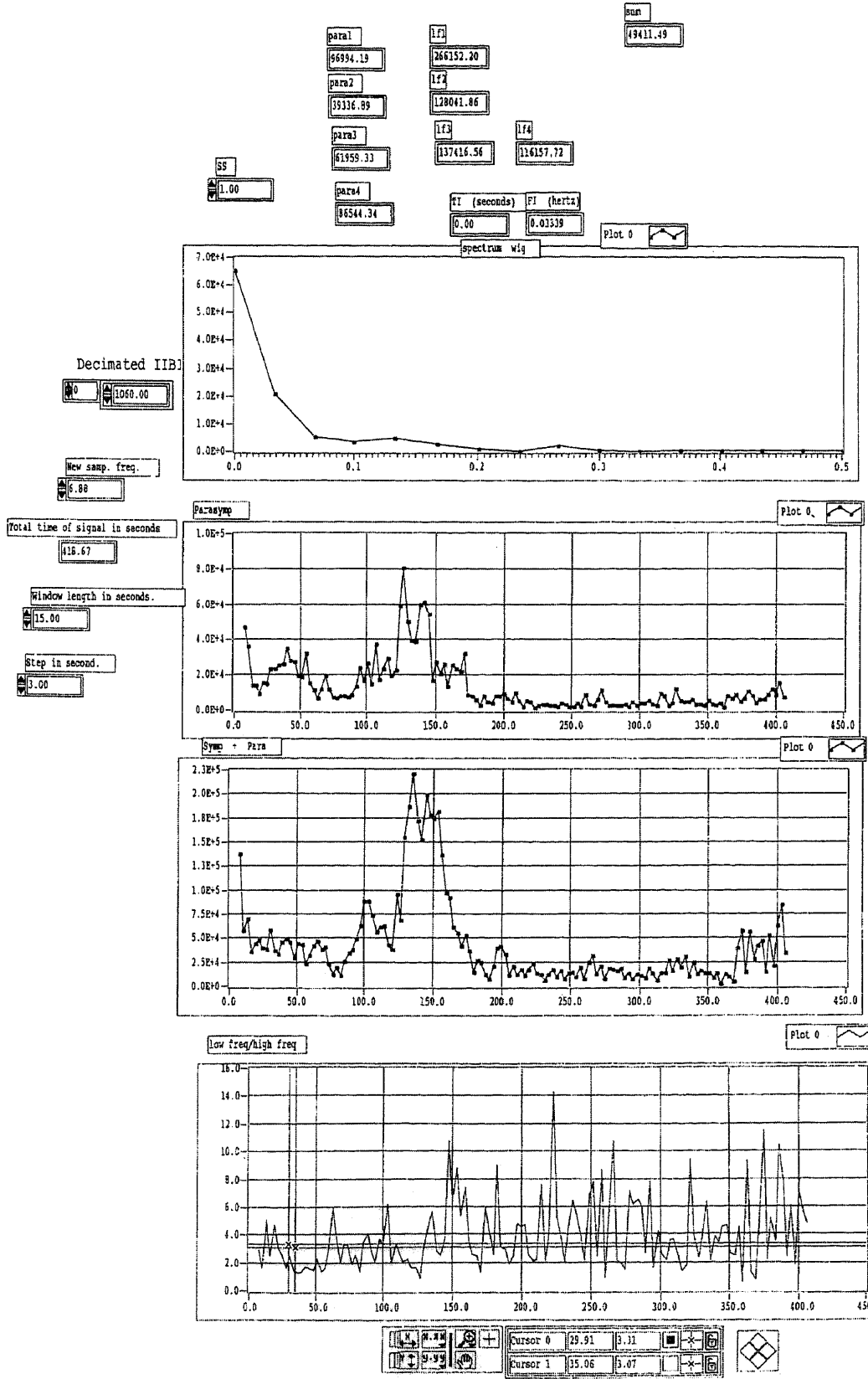
(Subject: GHC-BS)



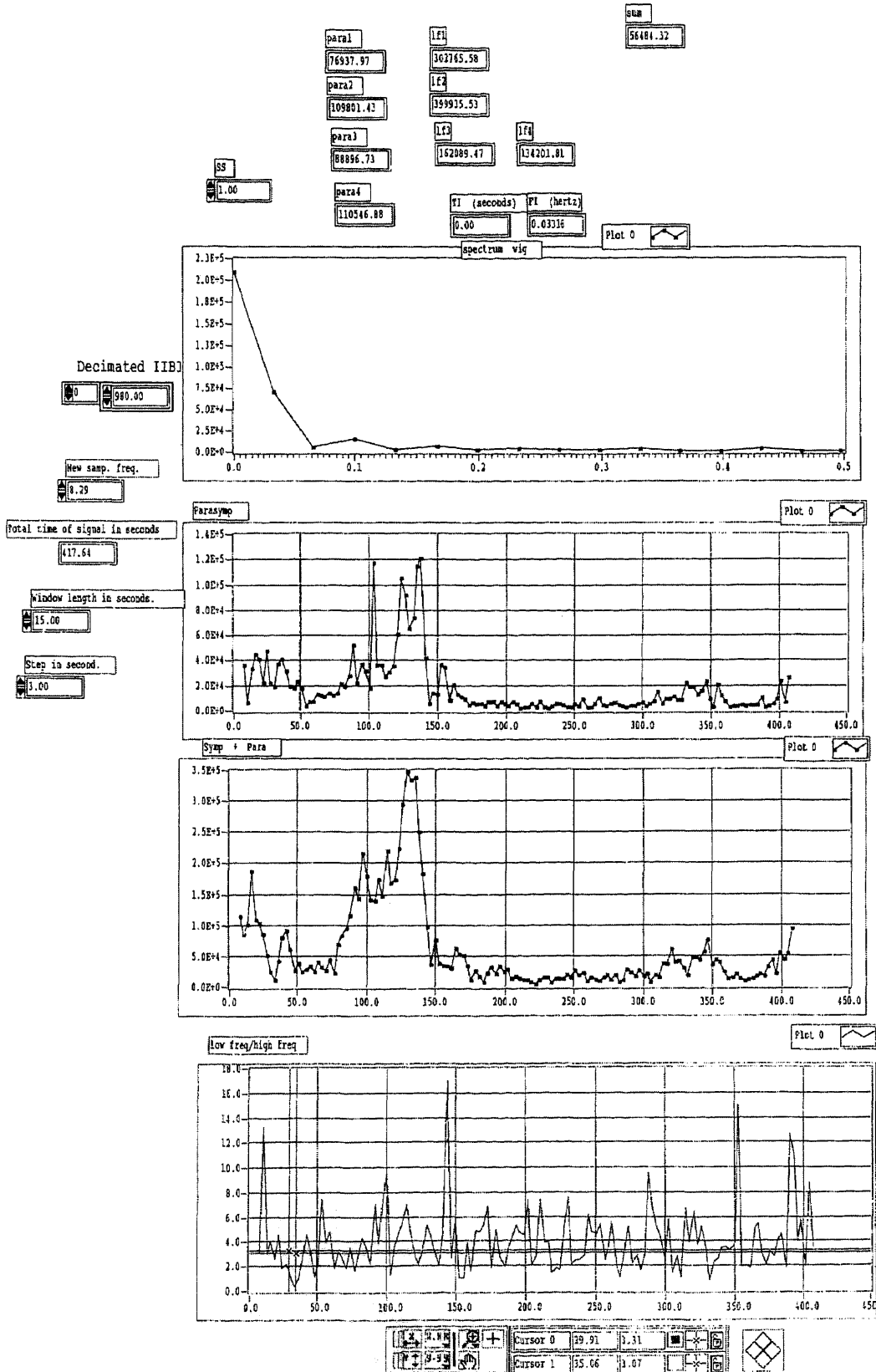
(Subject: GHC-JR)



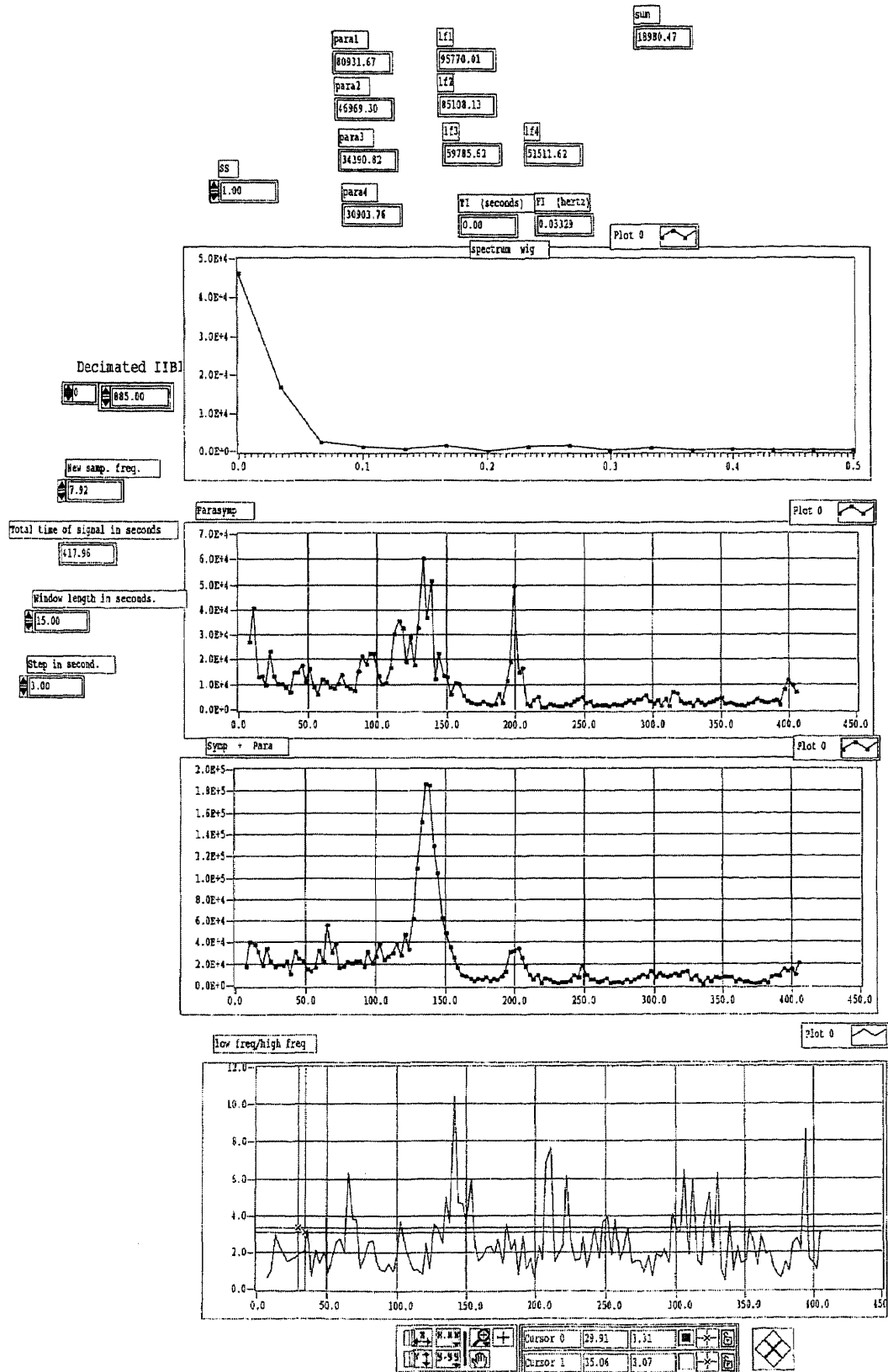
(Subject: GHC-LL)



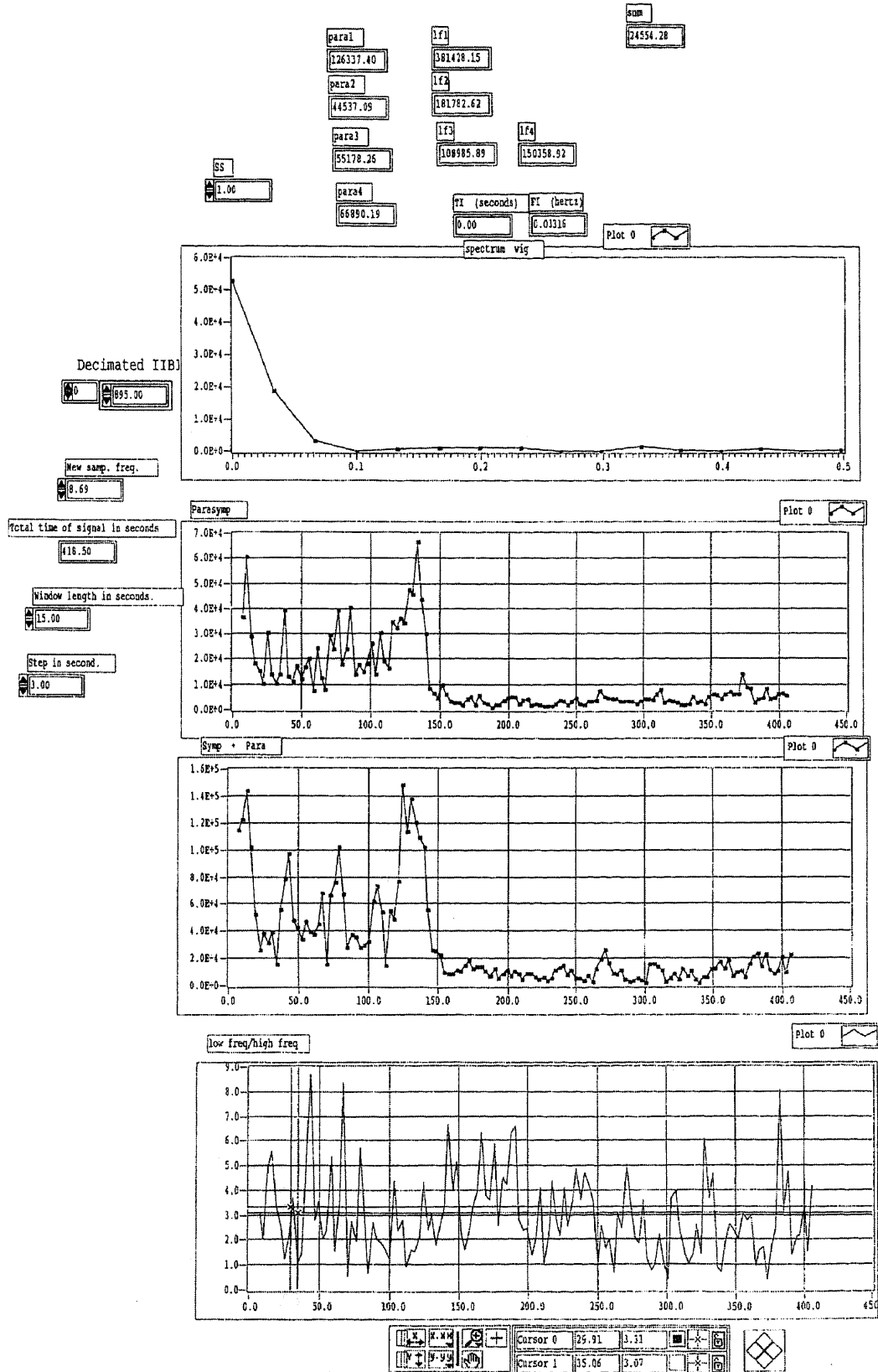
(Subject: GCF-AY)



(Subject: GCF-JB)



(Subject: GCF-JA)



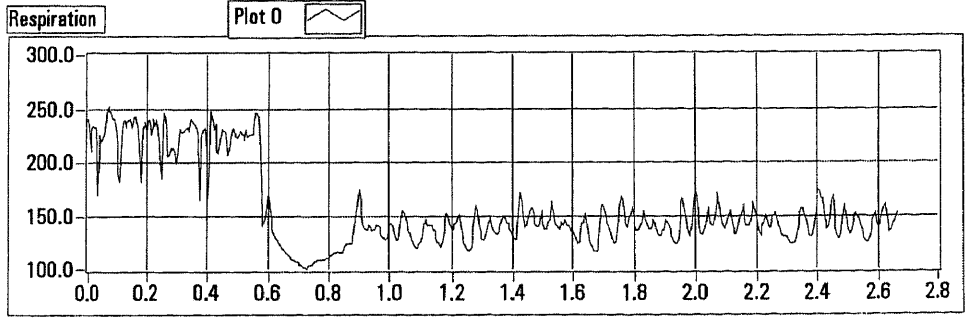
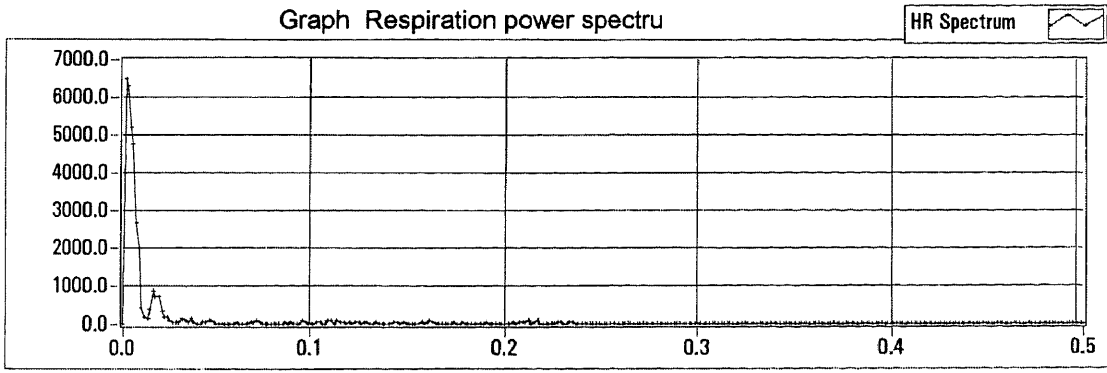
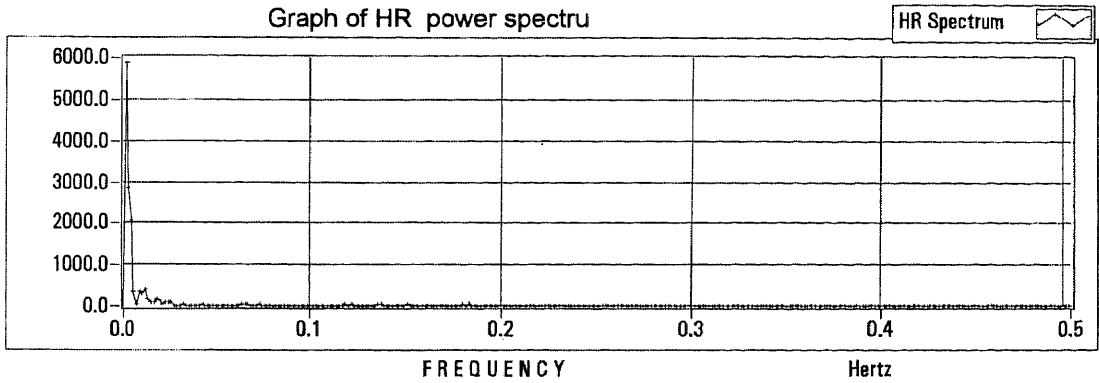
APPENDIX E

RESULTS OF HEART RATE VARIABILITY ANALYSIS

Power Spectrum Curves Utilizing ECG Signal

(Subject: GHC-BS)

Path to ECG data fi SF Time of record in minutes HF Area LF Area



(Subject: GHC-JR)

Path to ECG data fi

JPERAB8&9 - GHC FILE

SF

200.00

Time of record in minutes

6.94

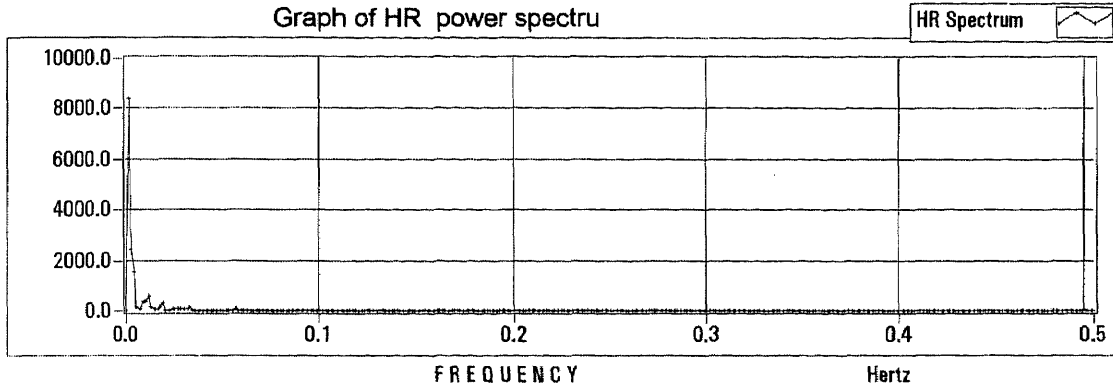
HF Area

246.91

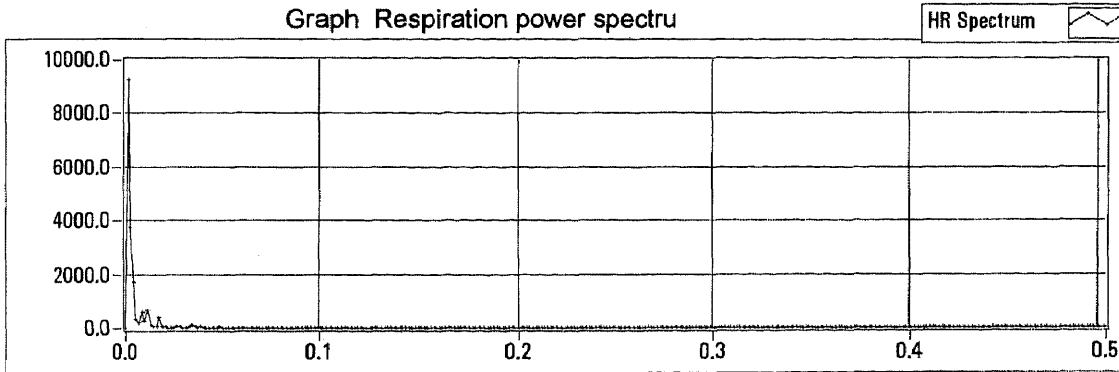
LF Area

435.86

Graph of HR power spectru

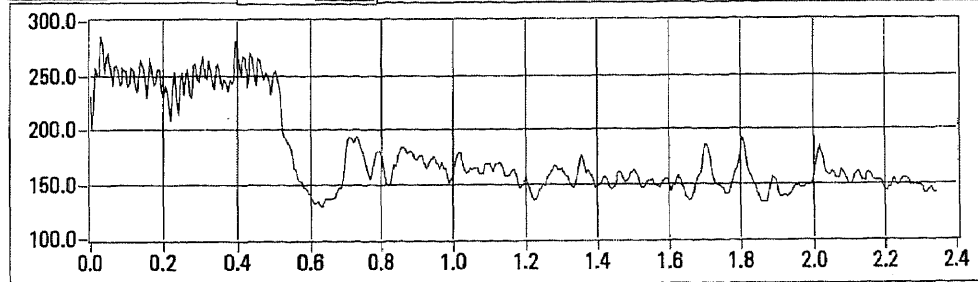


Graph Respiration power spectru



Respiration

Plot 0



(Subject: GHC-LL)

Path to ECG data fi

LHILAB889 - GHC FILE

SF

200.00

Time of record in minutes

6.98

HF Area

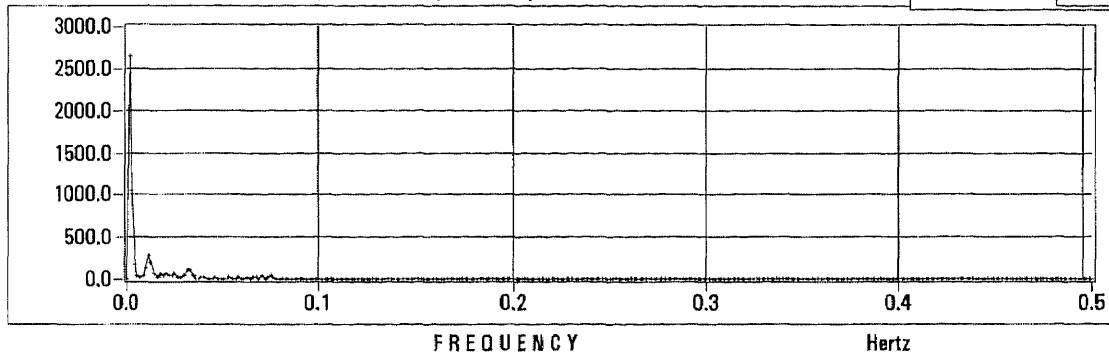
65.50

LF Area

302.63

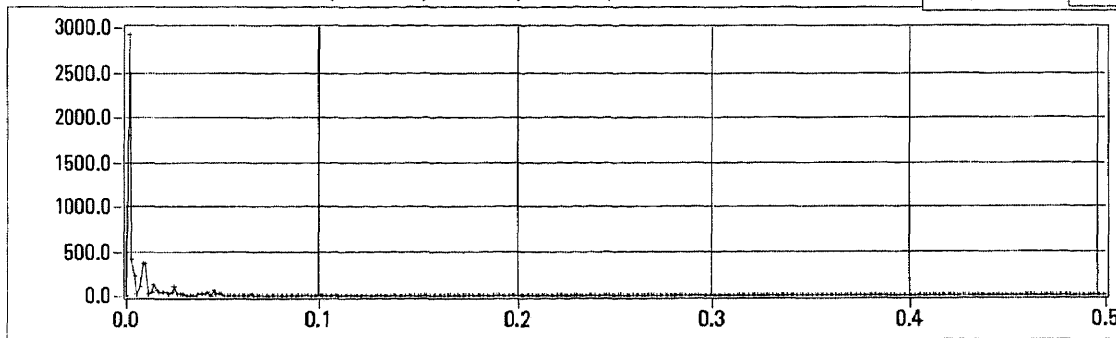
Graph of HR power spectru

HR Spectrum



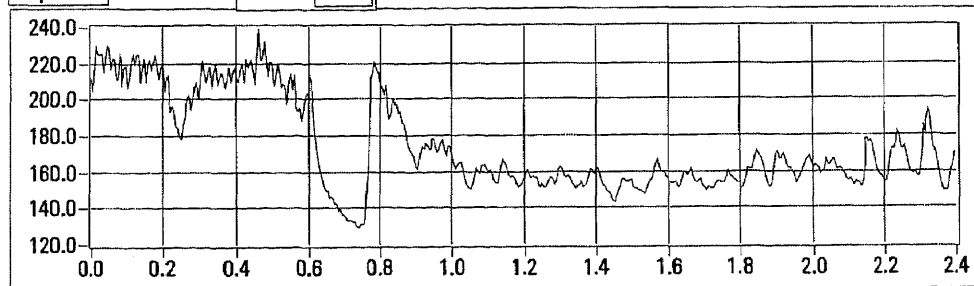
Graph Respiration power spectru

HR Spectrum



Respiration

Plot 0



(Subject: GCF-AY)

Path to ECG data fi

AREYAB8&9 - GCF FILE

SF

200.00

Time of record in minutes

6.96

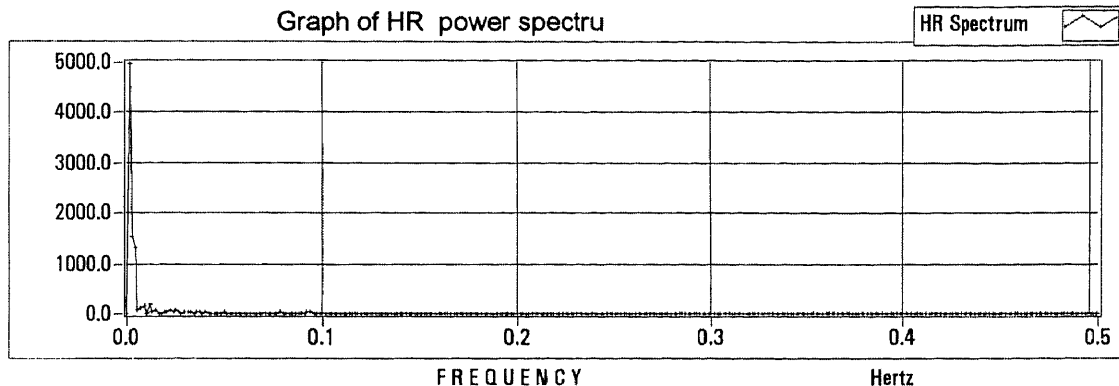
HF Area

75.14

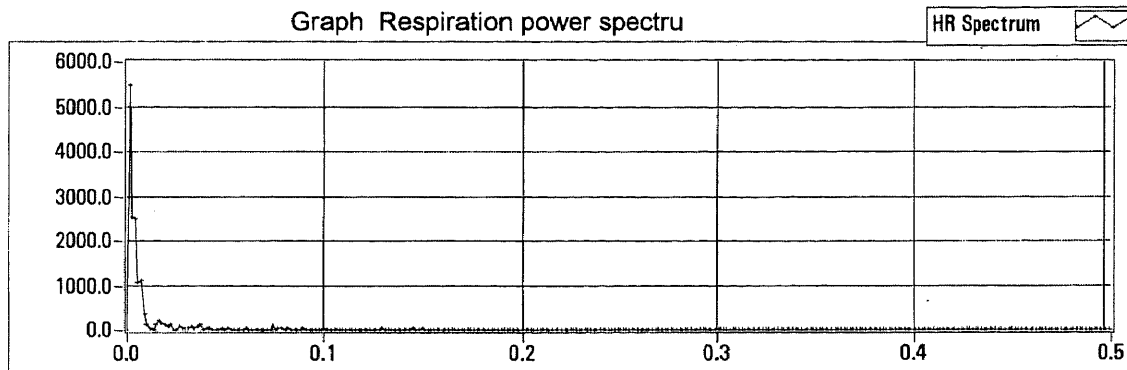
LF Area

394.22

Graph of HR power spectrum

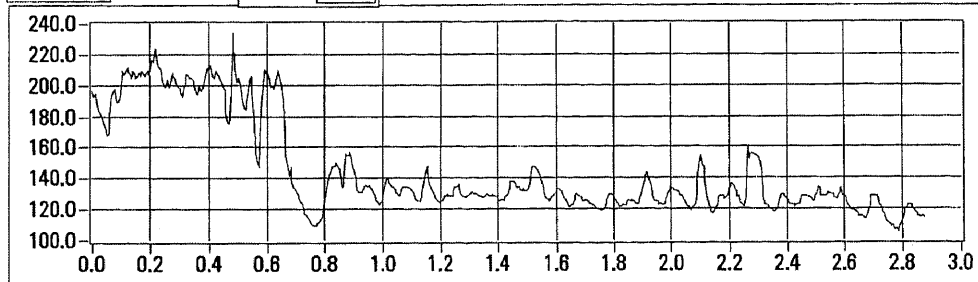


Graph Respiration power spectrum



Respiration

Plot 0



(Subject: GCF-JB)

Path to ECG data fi

JGIBAB8&9 - GCF FILE

SF

200.00

Time of record in minutes

6.97

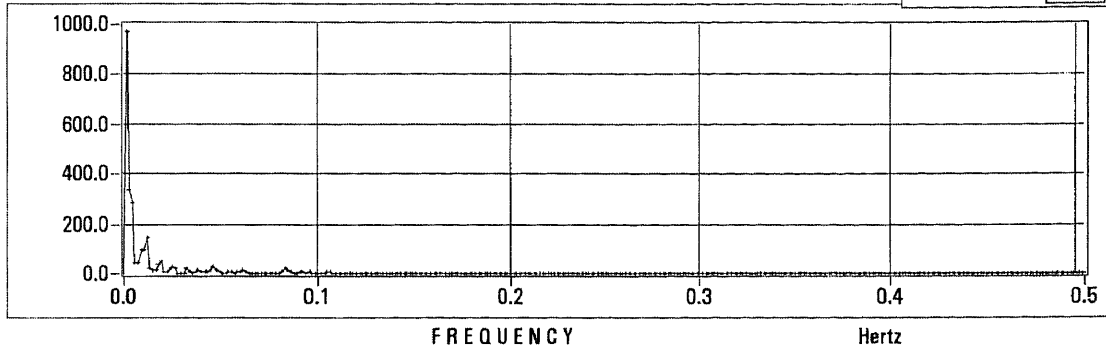
HF Area

62.73

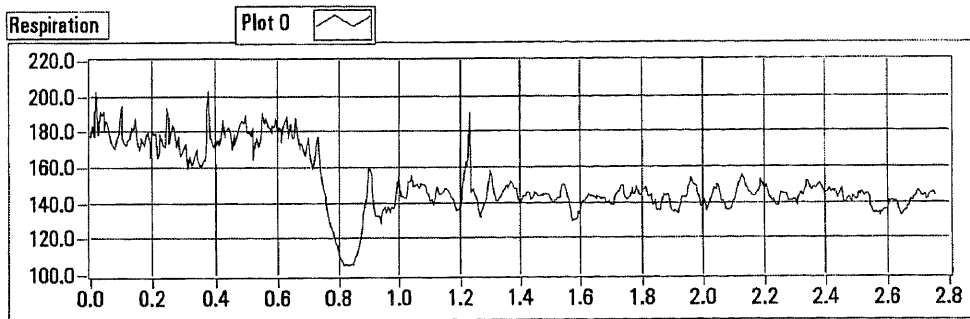
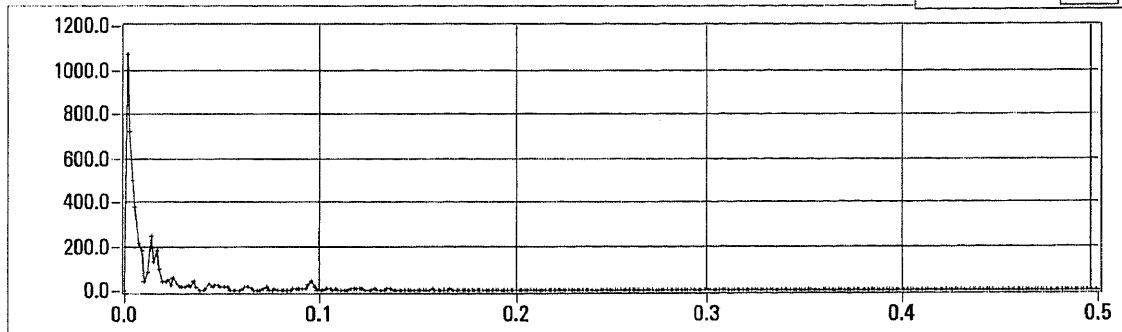
LF Area

204.56

Graph of HR power spectrum



Graph Respiration power spectrum



(Subject: GCF-JA)

Path to ECG data fi

JHARAB8&9 - GCF FILE

SF

200.00

Time of record in minutes

6.97

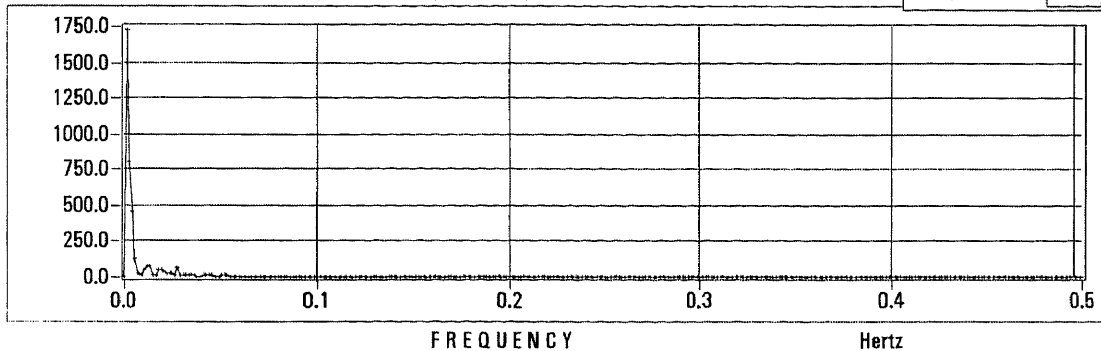
HF Area

55.59

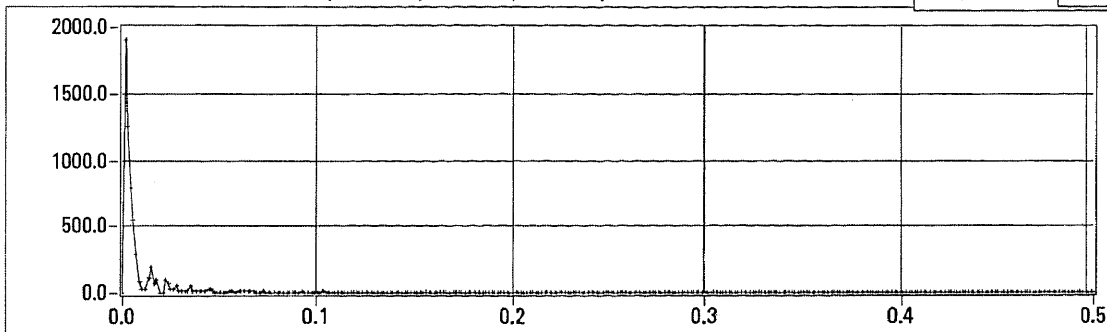
LF Area

142.45

Graph of HR power spectrum

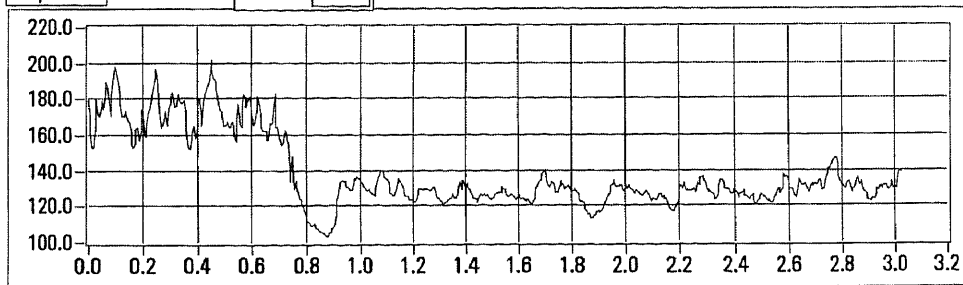


Graph Respiration power spectrum



Respiration

Plot 0

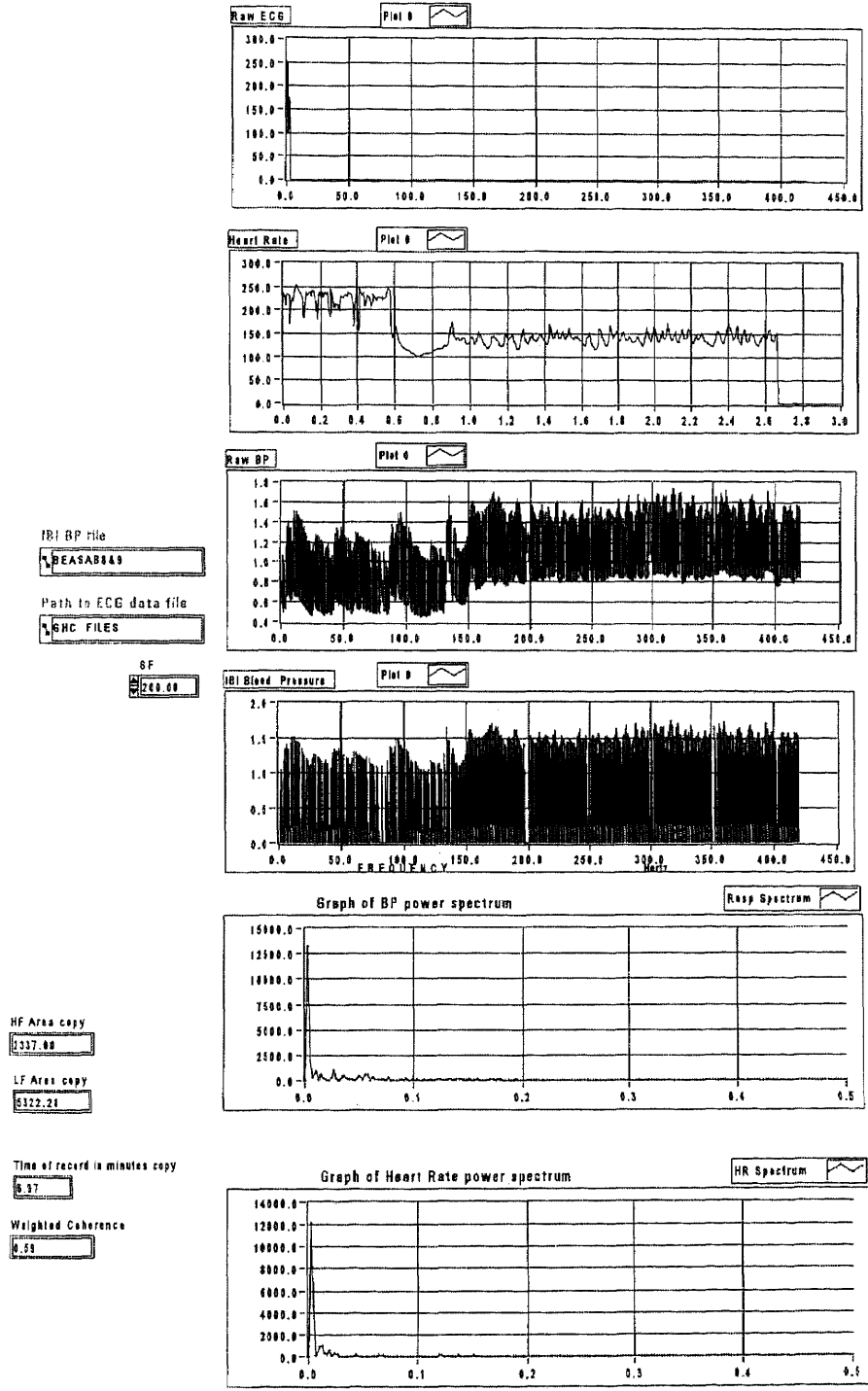


APPENDIX F

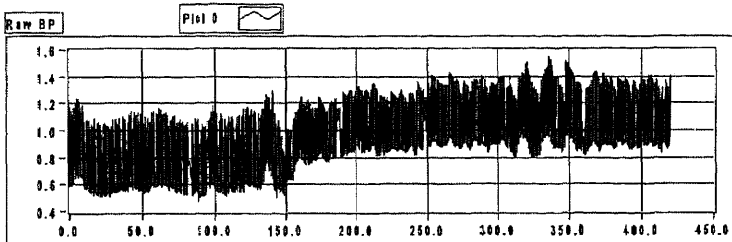
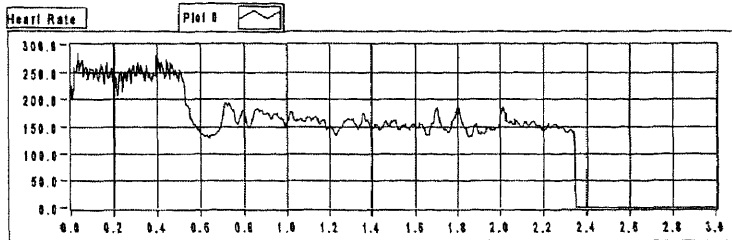
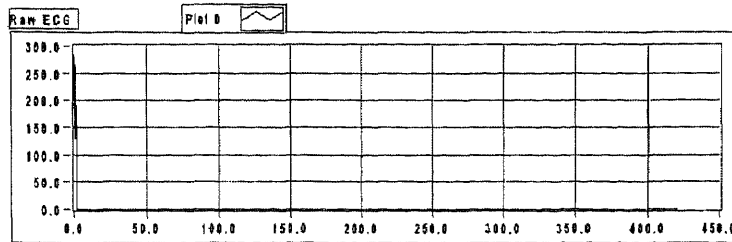
RESULTS OF HEART RATE VARIABILITY ANALYSIS

Power Spectrum Curves Utilizing BP Signal

(Subject: GHC-BS)



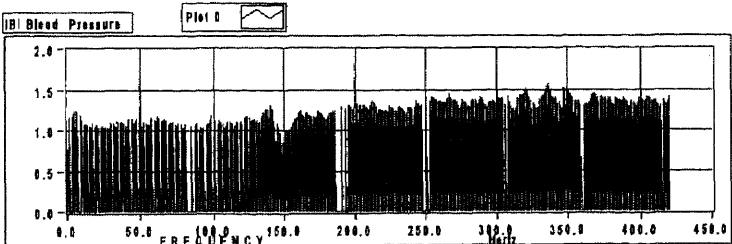
(Subject: GHC-JR)



IBI BP file

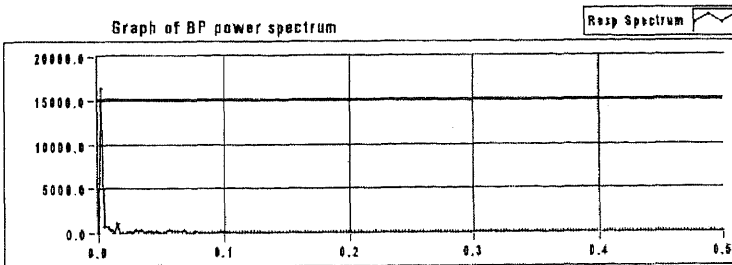
 Path to ECG data file

SF



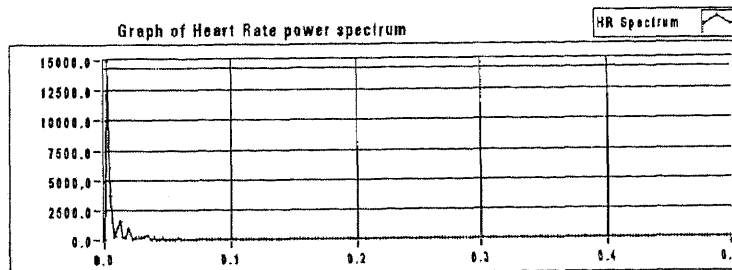
HF Area copy

 LF Area copy

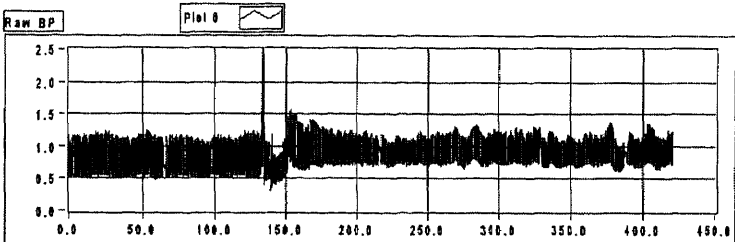
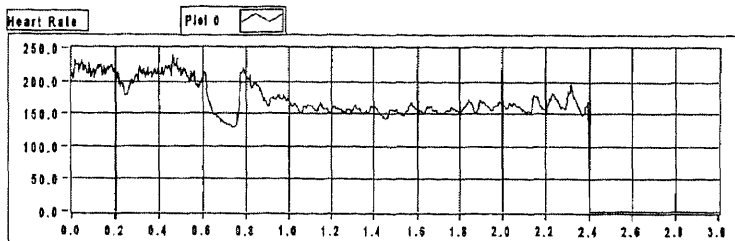
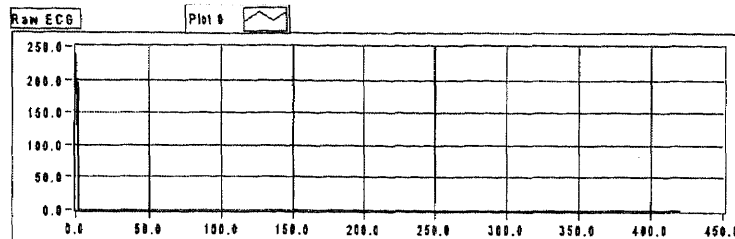


Time of record in minutes copy

Weighted Coherence



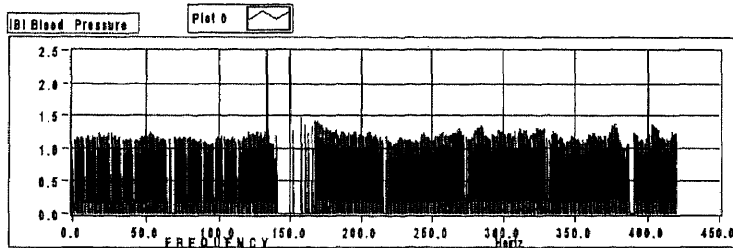
(Subject: GHC-LL)



IBI BP file

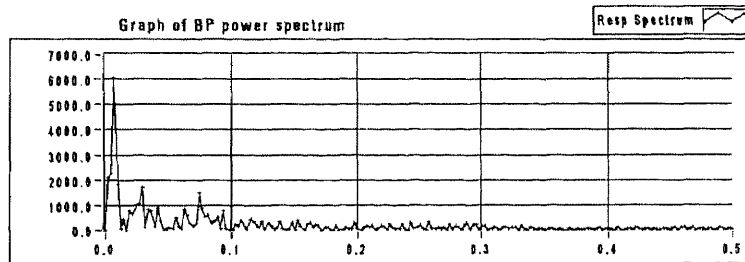
Path to ECG data file

SF



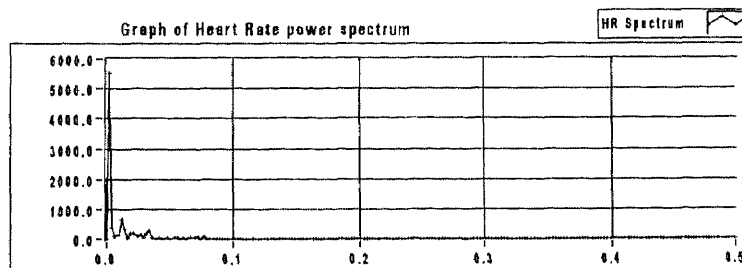
HF Area copy

LF Area copy

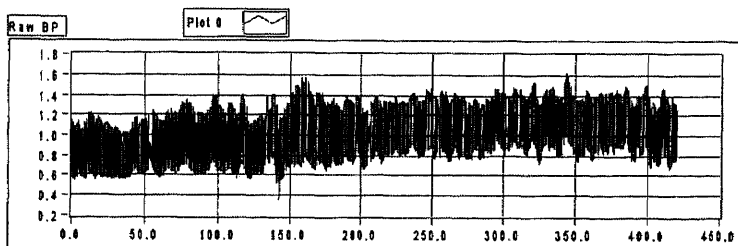
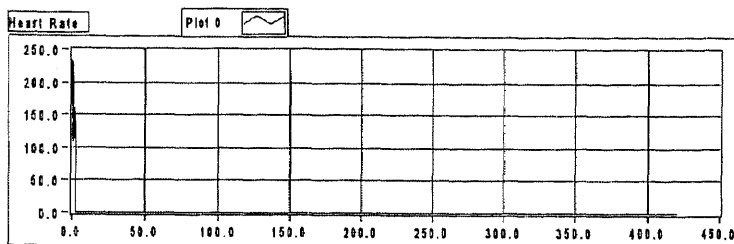
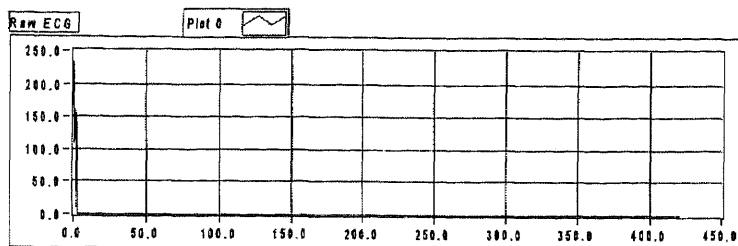


Time of record in minutes copy

Weighted Coherence



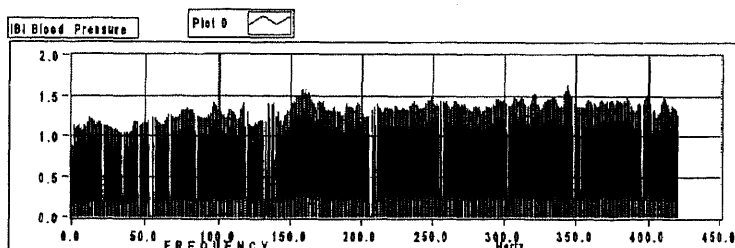
(Subject: GCF-AY)



IBI BP file

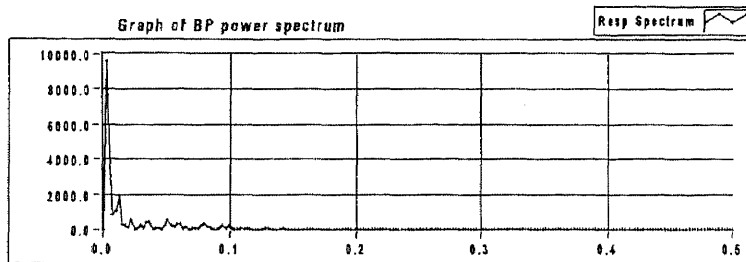
 Path to ECG data file

SF



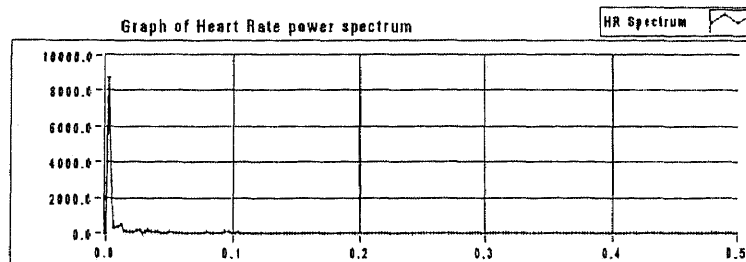
HF Area copy

LF Area copy

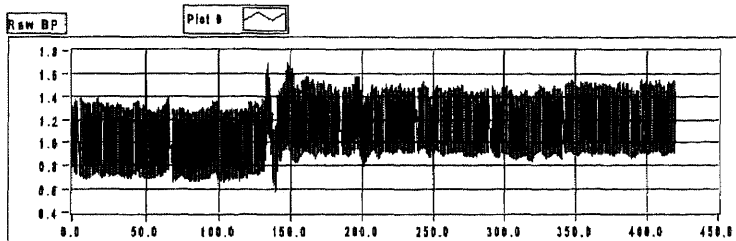
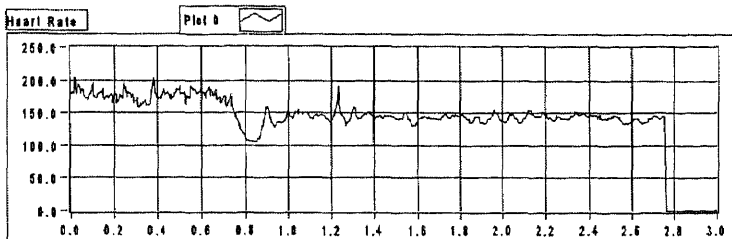
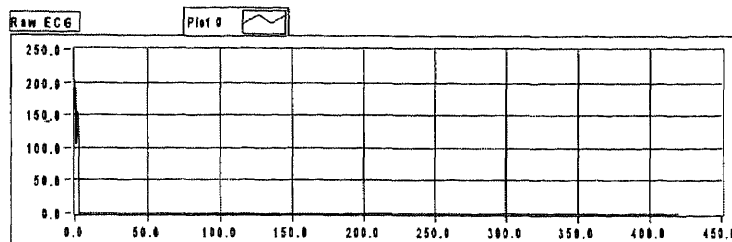


Time of record in minutes copy

Weighted Coherence



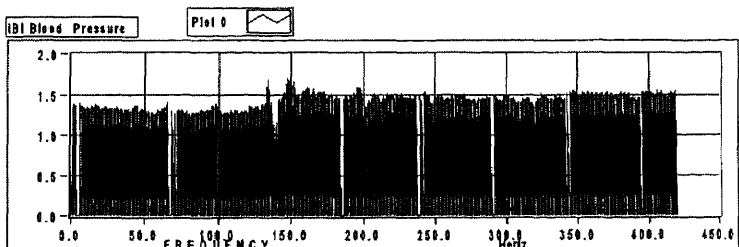
(Subject: GCF-JB)



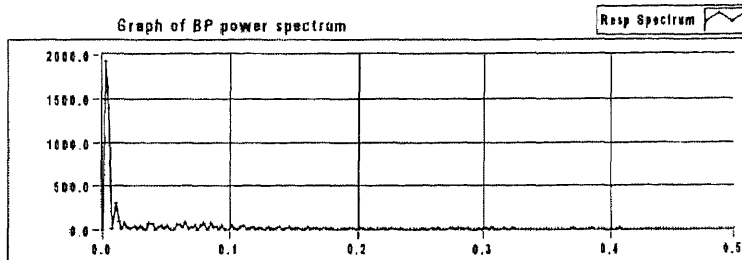
IBI BP file
%GIBAB&S

Path to ECG data file
%GCF FILES

SF
200.00



Graph of BP power spectrum



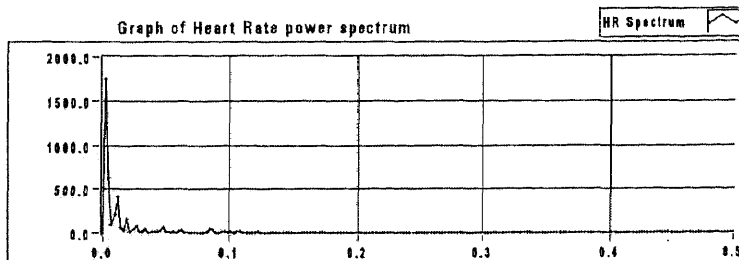
HF Area copy
752.58

LF Area copy
1151.58

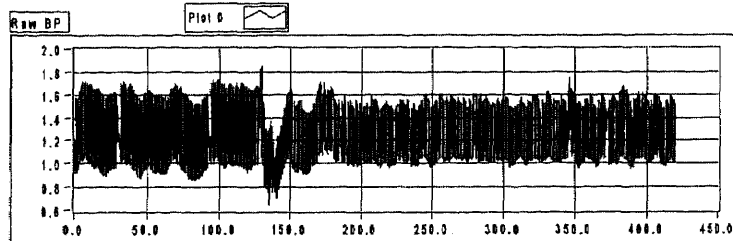
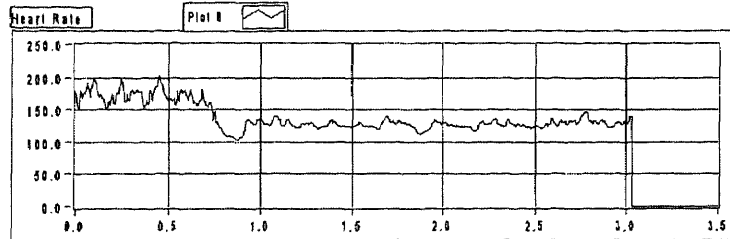
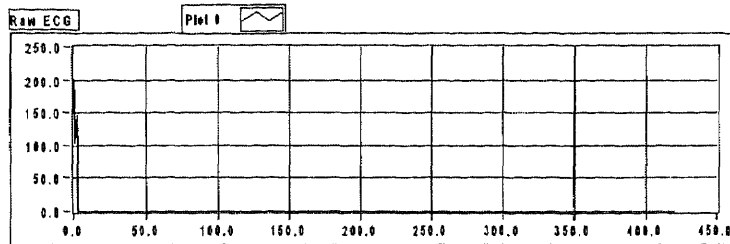
Time of record in minutes copy
8.97

Weighted Coherence
0.14

Graph of Heart Rate power spectrum



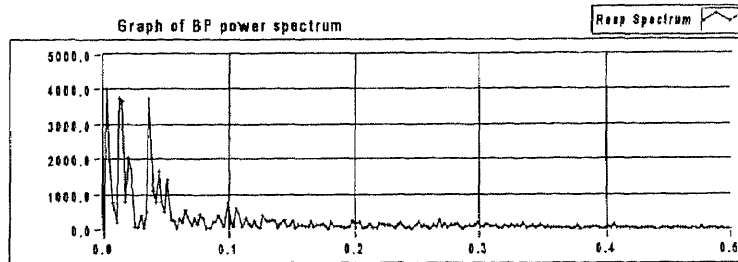
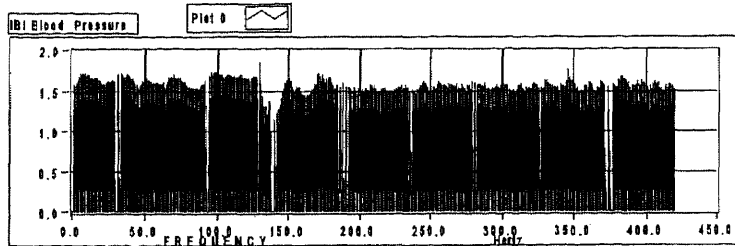
(Subject: GCF-JA)



IBI BP file

 Path to ECG data file

SF

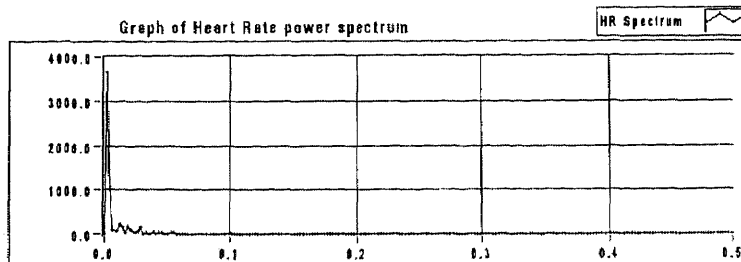


HF Area copy

 LF Area copy

Time of record in minutes copy

Weighted Coherence



REFERENCES

- [1] G. A. Thibodeau and K. T. Patton, *Anthony's Textbook of Anatomy & Physiology*, 14th ed. St. Louis, MO: Mosby-Year Book, Inc., 1994.
- [2] J. G. Creager, *Human Anatomy and Physiology*. Belmont, CA: Wadsworth Inc., 1983.
- [3] E. N. Marieb, *Human Anatomy and Physiology*, 3rd ed. New York: The Benjamin/Cummings Publishing Company, Inc., 1995.
- [4] J. G. Webster, *Medical Instrumentation: Application and Design*, 3rd ed. New York: John Wiley & Sons, Inc., 1998.
- [5] Z. Ori, G. Monir, J. Weiss, X. Sayhouni, and D. H. Singer, "Heart rate variability: frequency domain analysis," *Cardiology Clinics*, vol. 10, pp. 499-533, 1992.
- [6] Task Force of the European Society of Cardiology and the North American Society of Pacing and Electrophysiology, "Heart rate variability: standards of measurement, physiological interpretation, and clinical use," *Circulation*, vol. 93, pp. 1043-1065, 1996.
- [7] M. V. Hojgaard, N. H. Holstein-Rathlou, E. Agner, and J. K. Kanters, "Dynamics of spectral components of heart rate variability during changes in autonomic balance," *American Journal of Physiology*, vol. 275, pp. H213-H219, 1998.
- [8] S. Reisman, EE 667 Lecture Handout, ts. *New Jersey Institute of Technology*, Fall 1998.
- [9] S. Shin, W. N. Tapp, S. Reisman, and B. H. Natelson, "Assessment of Autonomic Regulation by the Method of Complex Demodulation," *IEEE Transactions in Biomedical Engineering*, vol. 36, pp. 274-283, 1983.
- [10] F. C. Mish, *Webster's Ninth New Collegiate Dictionary*. Springfield, MA: Merriam-Webster Inc., 1989.
- [11] K. Fukuda, S. E. Straus, I. Hickie, M. C. Sharpe, J. G. Dobbins, A. Komaroff, and the International Chronic Fatigue Syndrome Study Group, "The chronic fatigue syndrome: a comprehensive approach to its definition and study," *Annals of Internal Medicine*, vol. 121, pp. 953-959, 1994.
- [12] S. S. Jain and J. A. DeLisa, "Chronic fatigue syndrome: a literature review for a psychiatric perspective," *American Journal of Physical Medicine & Rehabilitation*, vol. 77, pp. 160-167, 1998.

- [13] R. W. Haley, "Is Gulf War syndrome due to stress? The evidence reexamined," *American Journal of Epidemiology*, vol. 146, pp. 695-703, 1997.
- [14] M. V. Kamath and E. L. Fallen, "Power Spectral Analysis of Heart Rate Variability: A Noninvasive Signature of Cardiac Autonomic Function." *Clinical Reviews in Biomedical Engineering*, vol. 21, pp. 245-311, 1993.
- [15] M. Zullo, "Using heart rate variability to measure the effects of manual medicine on autonomic activity," *MS Thesis in Biomedical Engineering, Biomedical Engineering Committee, New Jersey Institute of Technology*, October 1997.
- [16] E. L. Fallen, M. V. Kamath, and D. N. Ghista, "Power spectrum of heart rate variability: a non-invasive test of integrated neurocardiac function," *Clinical and Investigative Medicine*, vol. 11, pp. 331-340, 1988.
- [17] D. Laude, F. Weise, A. Girard, and J.L. Elghozi, "Spectral analysis of systolic blood pressure and heart rate oscillations related to respiration," *Clinical and Experimental Pharmacology and Physiology*, vol. 22, pp. 352-357, 1995.
- [18] C. O'Bara, "Signal processing techniques in heart rate and systolic arterial blood pressure variability studies," *MS Thesis in Biomedical Engineering, Biomedical Engineering Committee, New Jersey Institute of Technology*, January 1996.
- [19] D. L. Jones, J. S. Touvannas, P. Lander, and D. E. Albert, "Advanced time-frequency methods for signal-averaged ECG analysis," *Journal of Electrocardiology*, vol. 25 supplement, pp. 188-194, 1992.
- [20] S. Dagli, "Effect of postural tilt on the autonomic nervous system in Gulf War veterans," *MS Thesis in Biomedical Engineering, Biomedical Engineering Committee, New Jersey Institute of Technology*, May 1999.
- [21] X. Tang, B. Dworkin, S. Dworkin, and S. Reisman, "Time frequency analysis of heart rate variability in rat sleep/wakefulness cycles," *Proceedings of the IEEE 25th Annual Northeast Bioengineering Conference*, pp. 78-80, 1999.
- [22] A. Peckerman, J. J. Lamanca, S. L. Smith, G. Lange, L. Tiersky, C. Pollet, L. Korn, N. Fiedler, J. E. Ottenweller, and B. H. Natelson, "Cardiovascular stress responses and their relation to symptoms and putative causes of fatiguing illness in Gulf War veterans," submitted manuscript, 1998.
- [23] L. K. Wells, *The LabVIEW Student Edition User's Guide*. Englewood Cliffs, NJ: Prentice-Hall, Inc., 1995.

- [24] S. Carrasco, R. Gonzalez, J. Jimenez, R. Roman, V. Medina, and J. Azpiroz, "Comparison of the heart rate variability parameters obtained from the electrocardiogram and the blood pressure wave," *Journal of Medical Engineering & Technology*, vol. 22, pp. 195-205, 1998.
- [25] A. S. M. Koeleman, H. H. Ros, and T. J. van den Akker, "Beat-to-beat interval measurement in the electrocardiogram," *Medical & Biological Engineering & Computing*, vol. 23, pp. 213-219, 1985.
- [26] J.O. Fortrat, C. Formet, J. Frutoso, and C. Gharib, "Even slight movements disturb analysis of cardiovascular dynamics," *American Journal of Physiology*, vol. 277, pp. H261-H267, 1999.
- [27] V. Novak, P. Novak, T. L. Opfer-Gehriking, and P. A. Low, "Postural tachycardia syndrome: time frequency mapping," *Journal of the Autonomic Nervous System*, vol. 61, pp. 313-320, 1996.
- [28] V. Novak, P. Novak, T. L. Opfer-Gehriking, P. C. O'Brien, and P. A. Low, "Clinical and laboratory indices that enhance the diagnosis of postural tachycardia syndrome," *Mayo Clinic Proceedings*, vol. 73, pp. 1141-1150, 1998.
- [29] H.E. Klugh, *Statistics: The Essentials for Research*. New York: John Wiley & Sons, Inc., 1970.
- [30] G. A. Kimble, *How to Use (and misuse) Statistics*. Englewood Cliffs, NJ: Prentice-Hall, Inc., 1978.
- [31] R. Schondorf and R. Freeman, "The importance of orthostatic intolerance in the chronic fatigue syndrome," *The American Journal of the Medical Sciences*, vol. 317, pp. 117-123, 1999.
- [32] R. Freeman and A. L. Komaroff, "Does the chronic fatigue syndrome involve the autonomic nervous system?" *American Journal of Medicine*, vol. 102, pp. 357-364, 1997.
- [33] A. Yataco, H. Talo, P. Rowe, D. A. Kass, R. D. Berger, and H. Calkins, "Comparison of heart rate variability in patients with chronic fatigue syndrome and controls," *Clinical Autonomic Research*, vol. 7, pp. 293-297, 1997.
- [34] J.L. Elghozi, D. Laude, and A. Girard, "Effects of respiration on blood pressure and heart rate variability in humans," *Clinical and Experimental Pharmacology and Physiology*, vol. 18, pp. 735-742, 1991.
- [35] F. De Lorenzo, J. Hargreaves, and V. V. Kakkar, "Possible relationship between chronic fatigue and postural tachycardia syndromes," *Clinical Autonomic Research*, vol. 6, pp. 263-264, 1996.

- [36] J. E. Sanderson, L. Y. C. Yeung, D. T. K. Yeung, R. L.C. Kay, B. Tomlinson, J. A. J. H. Crichley, K. S. Woo, and L. Bernard, "Impact of changes in respiratory frequency and posture on power spectral analysis of heart rate and systolic blood pressure variability in normal subjects and patients with heart failure," *Clinical Science*, vol. 91, pp. 35-43, 1996.
- [37] V. Novak, P. Novak, J. De Champlain, A. R. Le Blanc, R. Martin, and R. Nadeau, "Influence of respiration on heart rate and blood pressure fluctuations," *Journal of Applied Physiology*, vol. 74, pp. 617-626, 1993.
- [38] S. Omboni, G. Parati, M. Di Rienzo, W. Wieling, and G. Mancia, "Blood pressure and heart rate variability in autonomic disorders: a critical review," *Clinical Autonomic Research*, vol. 6, pp. 171-182, 1996.